CHAPTER IV

RESULTS AND DISCUSSION

In this work we studied the copolymerization of alkyl (meth)acrylate-divinylbenzene by suspension technique. Monomers used in this study are methyl methacrylate, butyl methacrylate, lauryl methacrylate, dodecyl acrylate and stearyl acrylate.

4.1 Methyl methacrylate-divinylbenzene copolymer

The appropriate condition for the synthesis of methyl methacrylate-divinylbenzene copolymer was obtained by varying the polymerization parameters, such as the initiator concentration, suspending concentration, monomer phase ratio, agitation rate, crosslinking concentration, diluent ratio, reaction temperature, and time. The effects of each parameter, which response to properties of these copolymer beads were shown below.

4.1.1 Effect of crosslinking agent concentration

The effects of the crosslinking agent concentration on the conversion, average particle size, particle size distribution and swelling properties were investigated by varying the crosslinking agent concentration of 0, 0.025, 0.5, 1.0 and 1.5 wt % based on the monomer phase. The other parameters were kept constant as follows:

Monomer phase ratio	0.14
- Methyl methacrylate-divinylbenzene ratio	95 wt %
- Initiator concentration	0.5 wt %
Aqueous phase	0.86
- Suspending agent concentration	0.2 wt %
- Reaction temperature	70°C
- Reaction time	20 hours
- Agitation rate	140 rpm

- Toluene: heptane (100:0) 100 wt %

The unit of any chemicals is % weight based on the monomer phase. The resultant copolymer beads were confirmed by IR spectrum as shown in Figure 4.1.

The characterization of methyl methacrylate-divinylbenzene copolymer beads was performed by the FTIR transmission spectroscopy. Figures 4.1 and 4.7 (a) show the characteristic peaks of methyl methacrylate monomer at 2956, 1725, 1630, 1445, 1325, 1305, 1199, 1164, 1017, 941 and 818 cm^{-1}. The peak at 2956 cm^{-1} is due to the C-H stretching of aliphatic, the peak at 1725 cm^{-1} is due to the C=O stretching, the conjugated C=C, the peak at 1630 cm^{-1} caused by the C=C stretching, the peak at 1445 cm^{-1} is due to the deformation of CH_2 and CH_3, the peaks at 1325 and 1305 cm^{-1} caused by the CH_3 bending, the peaks at 1199 and 1164 cm^{-1} are due to the C-O stretching of ester functional group, the peaks at 1017 and 941 cm^{-1} are due to the C-H out of plane deformation, and 818 cm^{-1} caused by CH_2 rocking at n = 1. Figures 4.3 - 4.6 and 4.1 (b-e) show the FTIR spectra of poly[(methyl methacrylate)-co-divinylbenzene] at various crosslinking agent concentrations of 0.025, 0.5, 1.0 and 1.5, respectively. The peak at 1630 cm^{-1} in Figure 4.1 was disappeared because the conversion of monomer to its corresponding polymer (a double bond to a single bond) which is a proof of polymerization. It is noticeable that in all of the system including methyl methacrylate, the peak at 1630 cm^{-1} was still slightly appeared due to the most termination reaction of methyl methacrylate is disproportionation which the C=C is still remained in the system. Figures 4.2 and 4.7 (f) show the characteristic peaks of divinylbenzene at 2959-3081 cm^{-1}, due to the C-H stretching of aromatic group and C-H stretching of vinyl groups, the peak at 1628 cm^{-1} caused by the C=C from Ph-C=C, the peak at 1592 - 1402 cm^{-1} caused by the C=C stretching of aromatic skeletal, the peaks at 985 and 906 cm^{-1} are due to the C-H out of plane deformation from $RCH=CH_2$ and 800 cm^{-1} is due to the *para* substituted C-H out of plane deformation. The copolymer in Figures 4.1(b-e) does not show the peak characteristics of crosslinking agent divinylbenzene because divinylbenzene concentration added into the system is too low, thus no effect on the FTIR spectrum.

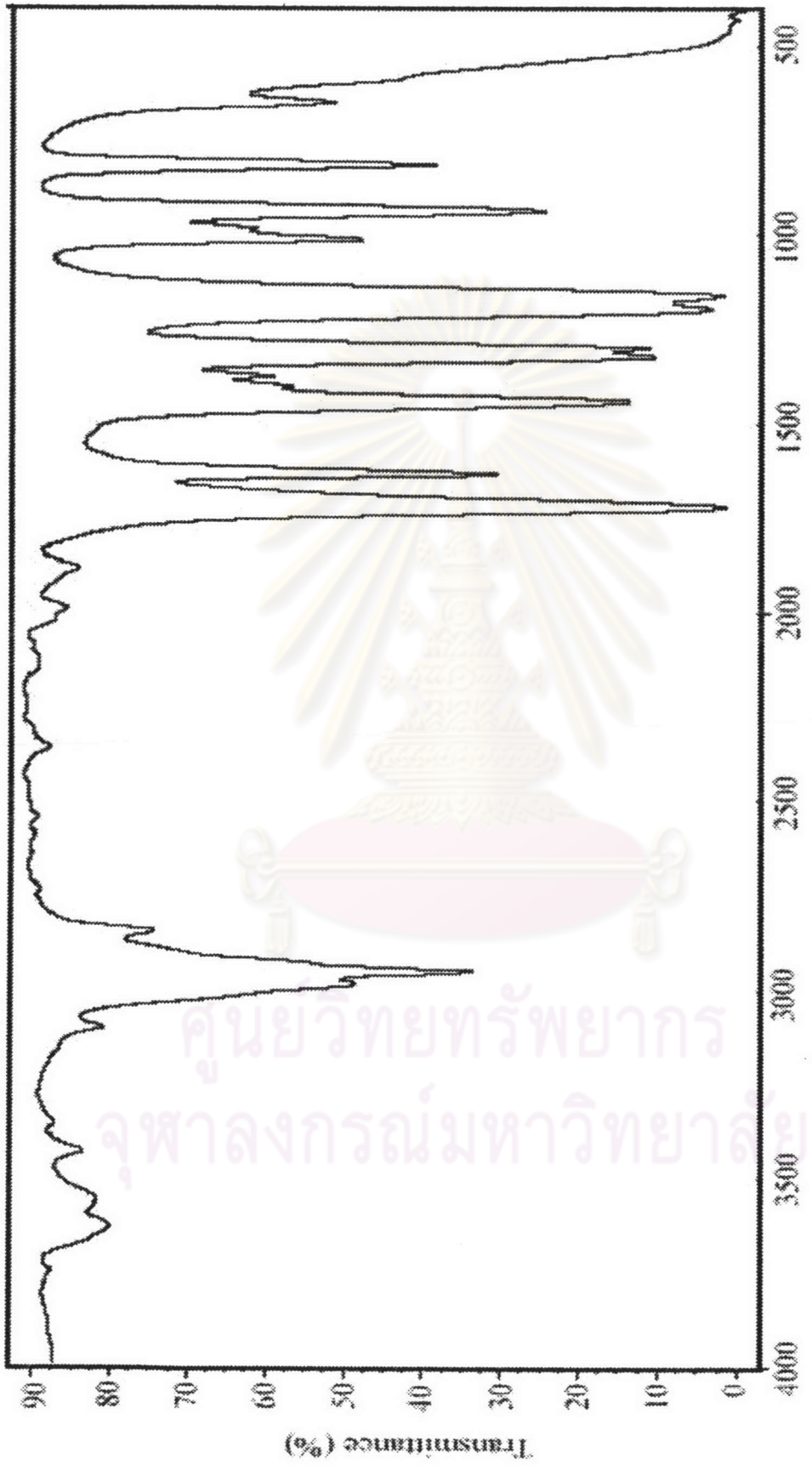

Figure 4.1 FTIR spectrum of methyl methacrylate monomer.

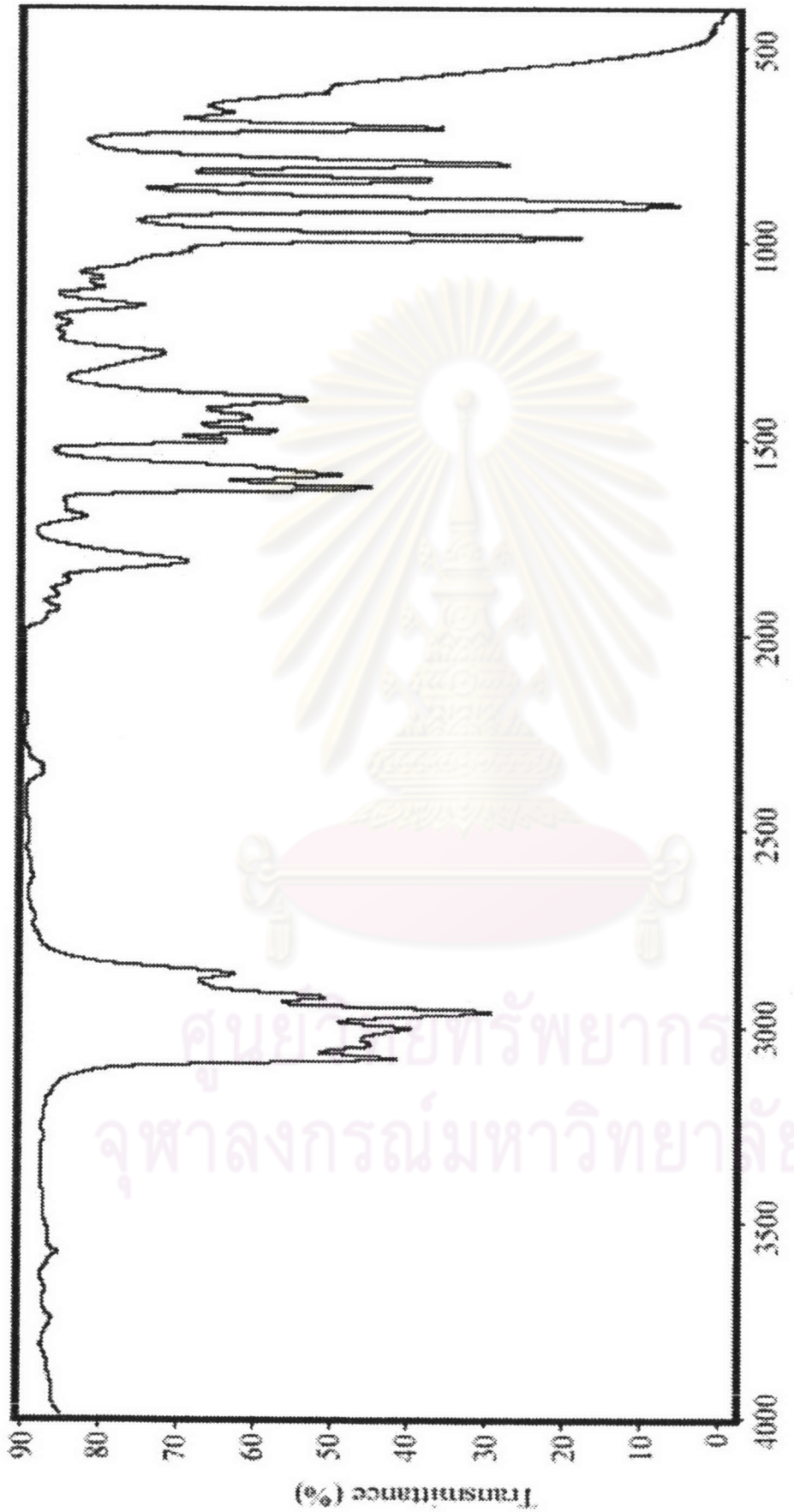

Figure 4.2 FTIR spectrum of divinylbenzene monomer.

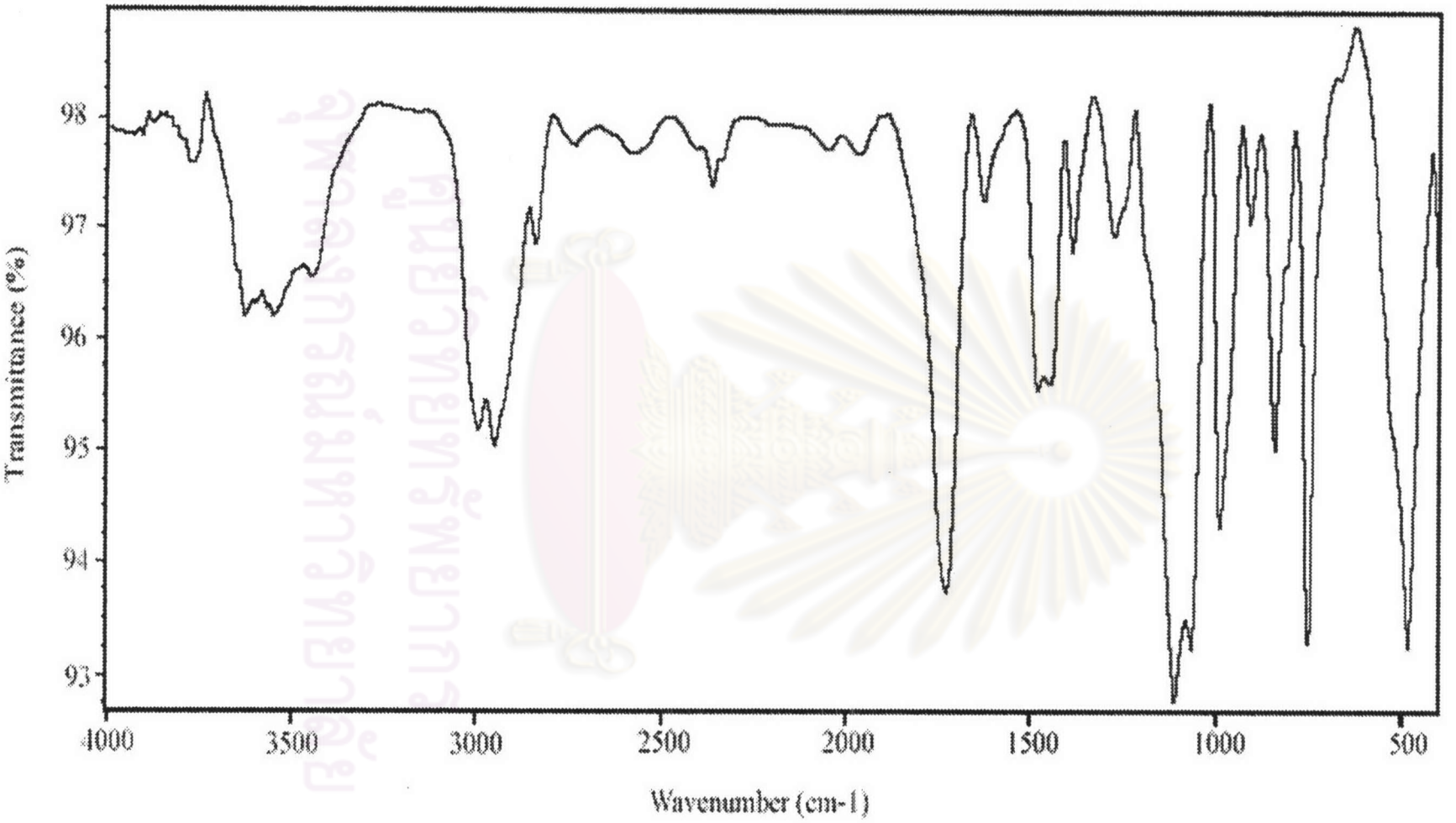

Figure 4.3 FTIR spectrum of poly(methyl methacrylate-co-divinylbenzene) at the concentration of crosslinking agent is 0.025% wt based on the monomer phase.

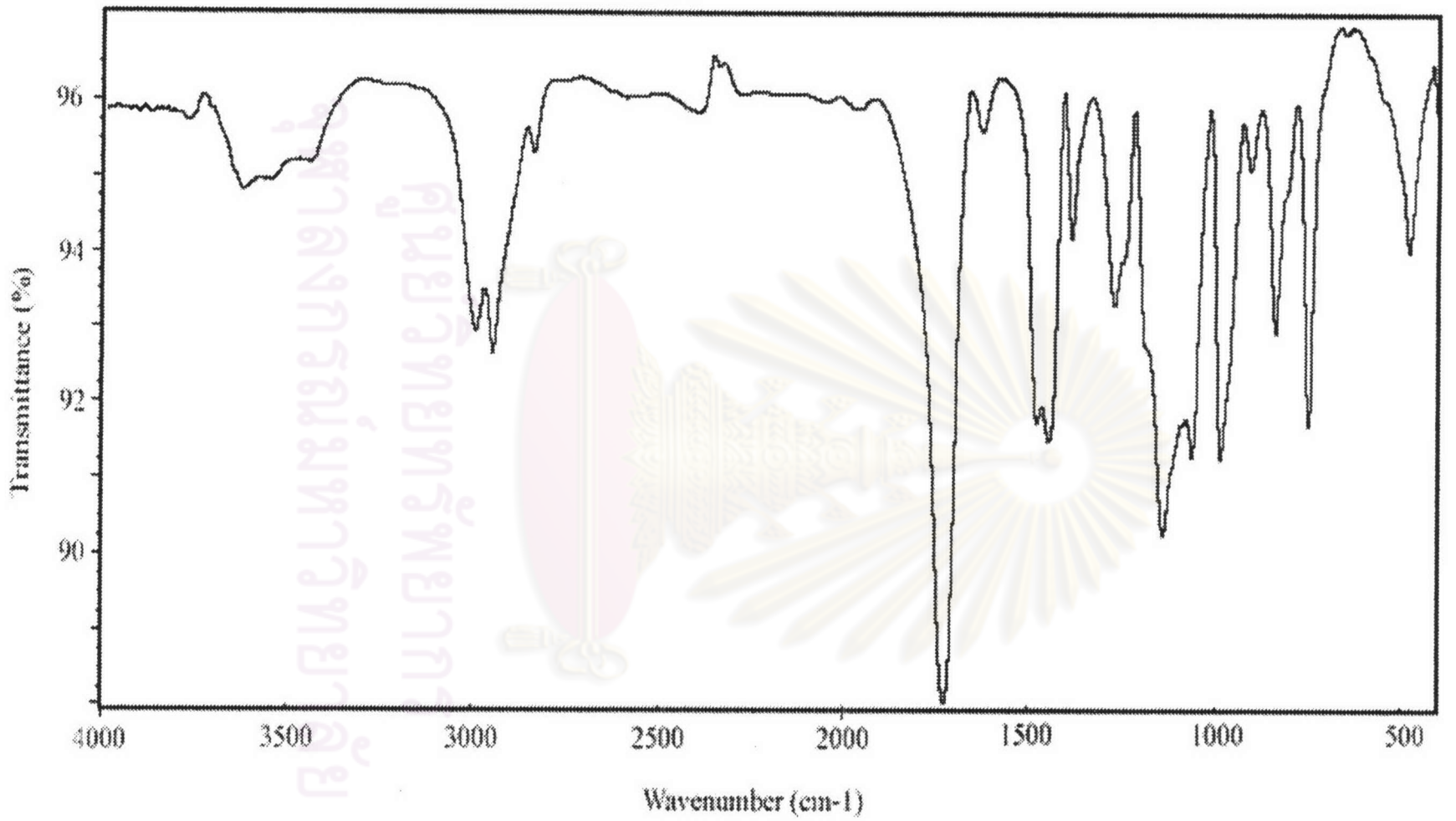

Figure 4.4 FTIR spectrum of poly(methyl methacrylate-co-divinylbenzene) at the concentration of crosslinking agent is 0.5% wt based on the monomer phase.

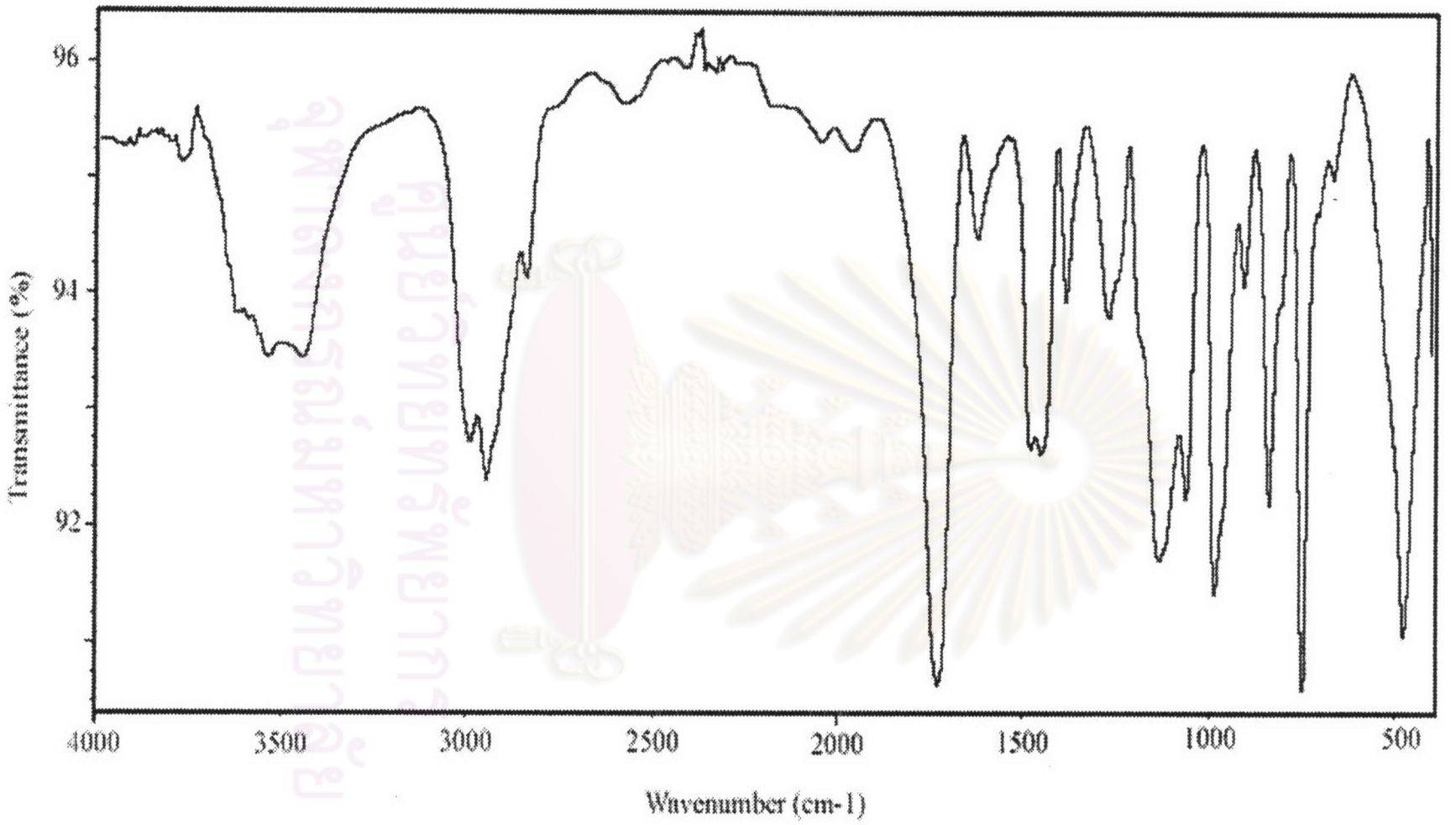

Figure 4.5 FTIR spectrum of poly(methyl methacrylate-co-divinylbenzene) at the concentration of crosslinking agent is 1.0% wt based on the monomer phase.

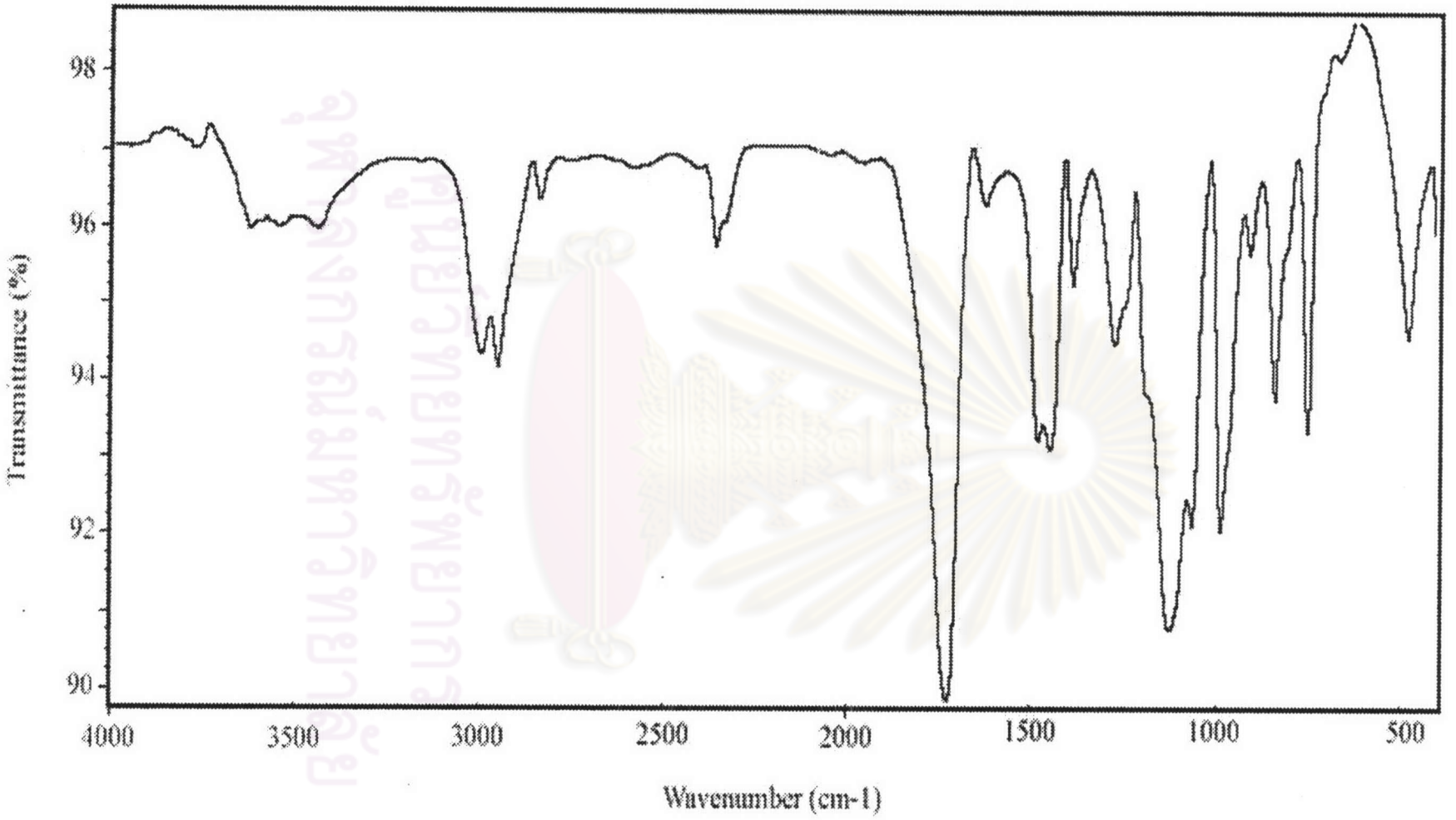

Figure 4.6 FTIR spectrum of poly(methyl methacrylate-co-divinylbenzene) at the concentration of crosslinking agent is 1.5 % wt based on the monomer phase.

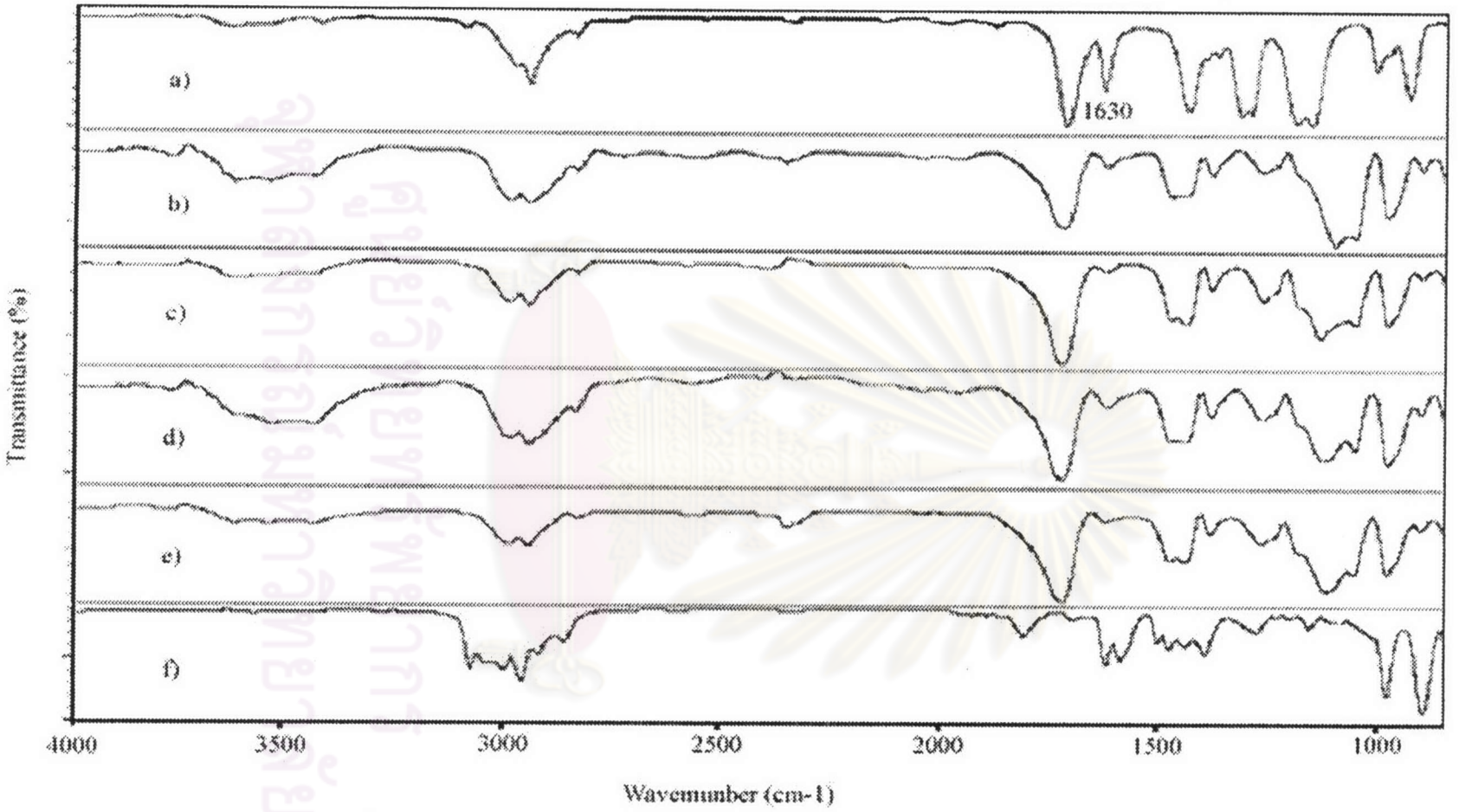

Figure 4.7 FTIR spectrum of poly[(methyl methacrylate)-co-divinylbenzene] beads prepared by suspension copolymerization at various crosslinking agent concentrations; a) 0% or 100%, b) 0.025%, c) 0.5%, d) 1.0%, e) 1.5% based on the monomer phase, and f) divinylbenzene monomer.

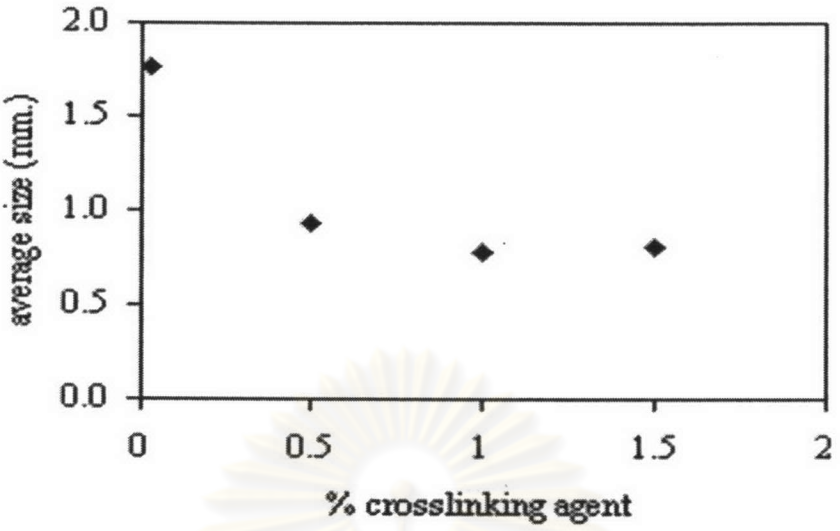

Figure 4.8 The average particle size of in relation to the crosslinking agent concentration.

Table 4.1 Effect of the Crosslinking Agent Concentration on Bead Properties

Parameter	Run			
	C025	C05	C10	C15
DVB concentration, wt %	0.25	0.5	1	1.5
% Yield	89	88	94	98
Bead size distribution, wt %				
<0.42 mm	0.20	2.80	6.88	6.47
0.42-0.59 mm	0.57	9.69	11.51	9.37
0.59-0.84 mm	0.68	3.48	0.61	4.90
0.84-2.0 mm	6.45	8.05	8.66	6.96
>2.0 mm	17.14(fused)	2.10	0.22	1.11
Average bead size, mm	1.77	0.93	0.78	0.80
$\overline{Mc}$	128300	18600	11300	7600
Crosslinking density	1.1	7.3	12.1	17.9
Swelling ratio in toluene (by				
volume)	20.5	15.1	8.5	7.4
(by weight)	15.4	10.5	5.8	5.3
Bead density, kg m^{-3}	1101	1166	1190	1042

Toluene was used as a diluent. M_0 = 136300.

Table 4.1 shows the overall conversion, the average particle size, particle size distribution, average molecular weight between crosslink ($\overline{M_c}$), crosslinking density, swelling ratio and density in relation to divinylbenzene content, as a crosslinking agent.

It is found that the overall conversion increased with increasing DVB concentration. Figure 4.8 shows the average particle size decreased when increasing the crosslinking agent concentration and the shape of particles was sphere and unchanged. Figure 4.9 shows the particle size distribution charts which were affected by crosslinking agent concentration. when the crosslinking agent concentration was low the particle size distribution favored for the large particles. At 0.025 % crosslinking agent concentration, some larger particles were fused because the crosslinking agent concentration was too low to produce enough crosslinking sites to maintain the dimension of the beads. Thus, this amount of the crosslinking agent is not sufficient to help the bead formation [19]. Figure 4.10 shows the effect of the crosslinking agent concentration on toluene absorbency and crosslinking density. It was found that the toluene absorbency decreased with increasing DVB content but crosslinking density increased when increased crosslinking concentration. Generally, the swelling behavior is affected by three factors, which are rubber elasticity, affinity to the solution, and crosslinking density [12]. Toluene absorbency decreased with increase in the amount of DVB due to the restricted relaxation of the polymeric chain. An increase in the amount of the crosslinking agent forms a denser network of the copolymer and reduces the $\overline{M_c}$, the average molecular weight between crosslinks. Generally, the higher $\overline{M_c}$ decreases the swelling ratio [12], which is shown in Table 4.1

From Figure 4.11, the copolymer beads are harder and dense, when increased the DVB content, leading to the decrease in shrinkage of the copolymer bead surface. The bead surfaces become smoother when higher concentrations of the crosslinking agent were copolymerized [Fig. 4.11 (a)-(d)]. The shrinkage of the copolymer bead surfaces in Fig 4.11 (a)-(d) occurred because of the low crosslinking density resulting from a low DVB content. When the copolymers were being swollen by a good solvent during solvent extraction, an imbalance tension arose between the bead interior and outer surface surrounded by extracting solvent. The removal of the uncrosslinked

copolymer beads caused the weak, expanded network of the bead outer surface to shrink and this shrinkage of some areas of the surface was enhanced as a result of the cohesive forces when the solvated polymer chains approached each other due to loss of the solvent.

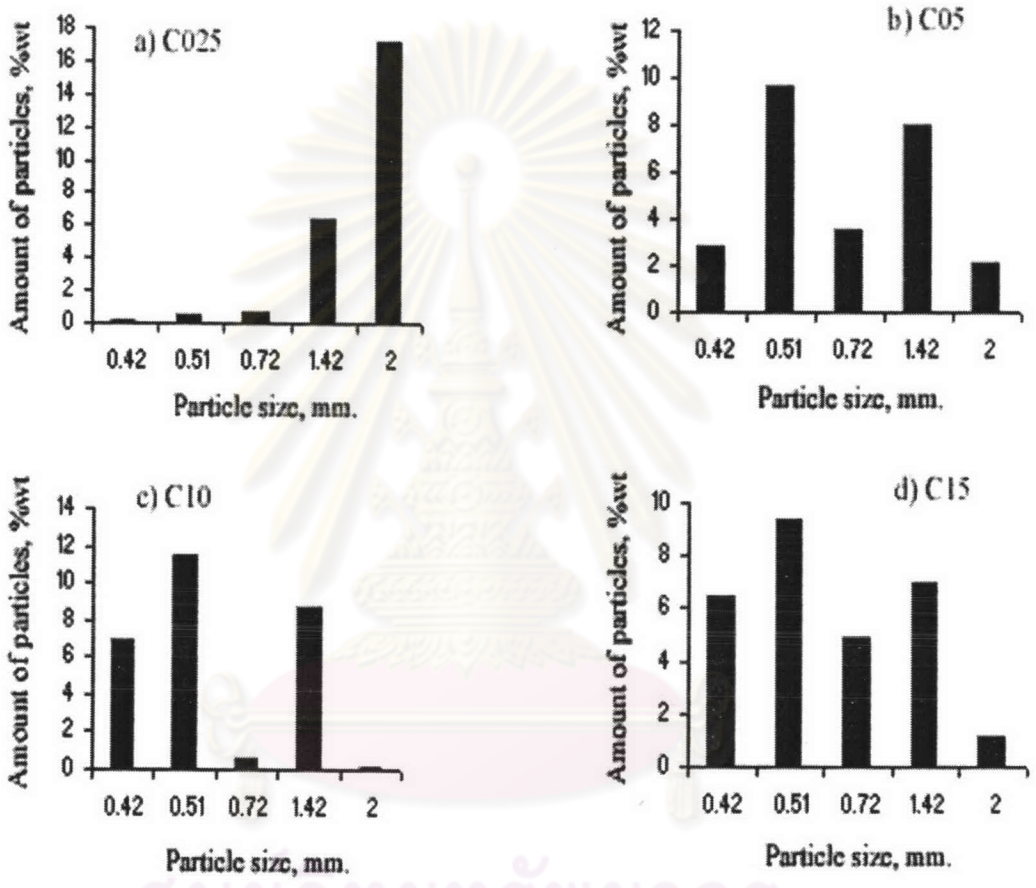

Figure 4.9 Effect of the crosslinking agent concentration on particle size and size distributions. a) C025, b) C05, c) C10 and d) C15.

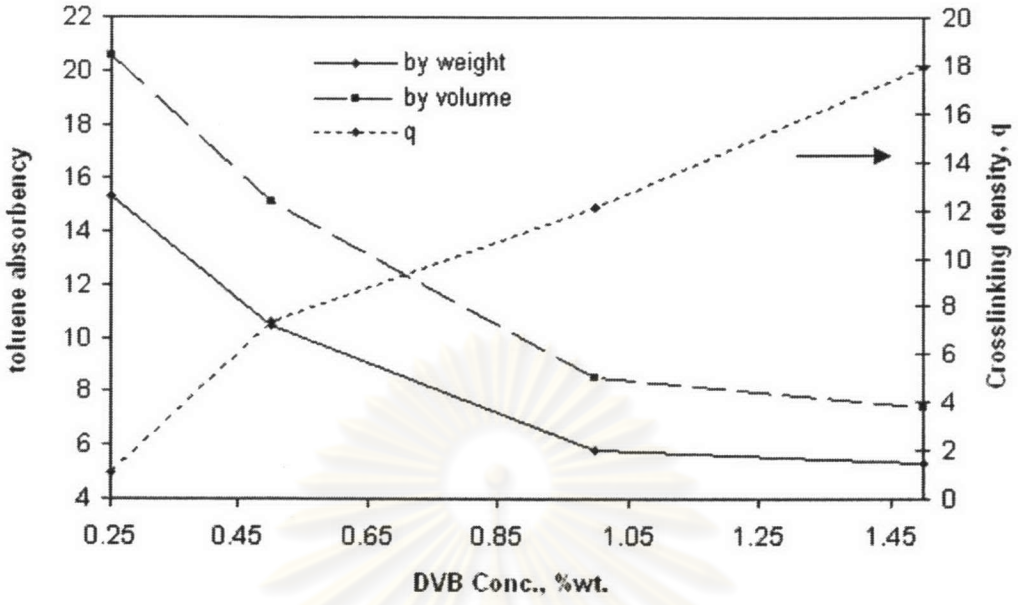

Figure 4.10 Effect of the crosslinking agent concentration on toluene absorbency and crosslinking density.

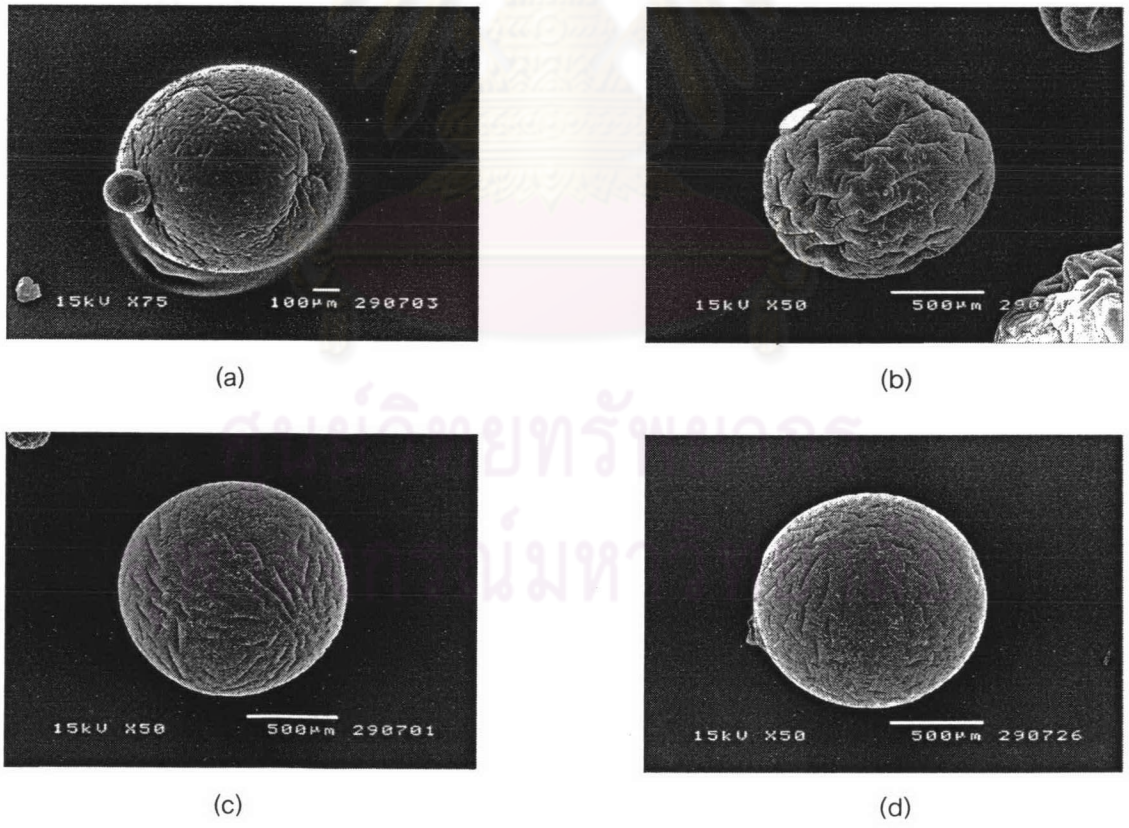

Figure 4.11 SEM photographs of the copolymers prepared at different crosslinking agent concentrations: (a) C025, 0.25%; (b) C05, 0.5%; (c) C10, 1.0% and (d) C15, 1.5% (×50).

Figure 4.12 shows that a higher magnification (500 times) of the surface morphology of MMA-DVB copolymer beads reveals the effect of the crosslinking agent concentration. When the system is copolymerized in the presence of a good diluent (toluene), two kinds of porous structure can be obtained as an expanded load, and a macroporous gel. At a low DVB content, the final structure is an expanded gel [Fig.4.11 (a)], because the chains are fully solvated during the polymerization and they shrink less than those of the corresponding system do in the absence of a solvating diluent. However, the internuclear chains can collapse with the removal of the solvating diluent to make the approaching nuclei become a compact mass. A porous copolymer is obtained when the DVB content is relatively high [Fig. 4.11 (b)-(d)].

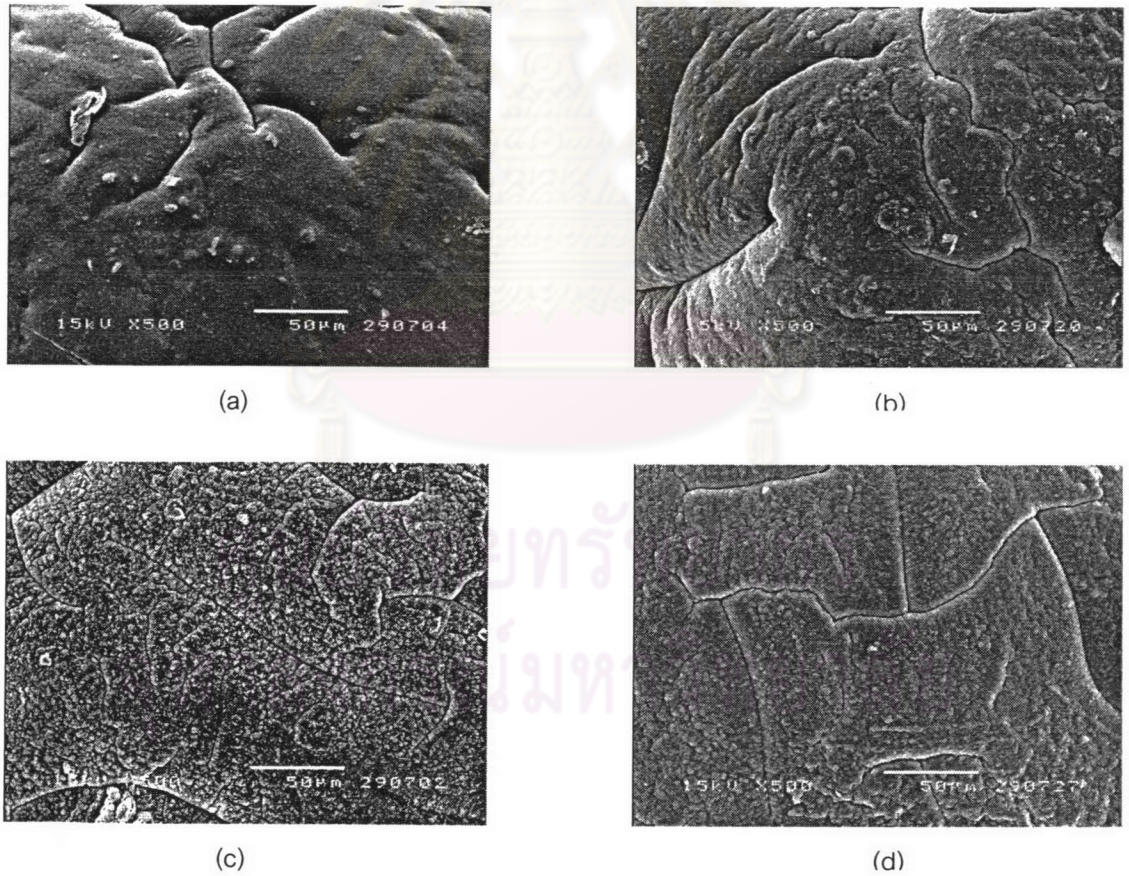

Figure 4.12 SEM photographs of the surface of copolymers prepared at different crosslinking agent concentrations: (a) C025, 0.25%; (b) C05, 0.5%; (c) C10, 1.0%, and (d) C15, 1.5% (×5000).

In this case, the collapse of the internuclear chains occurs before all the solvating diluents have been removed. The porosity is, of course, a result of a removal of the remaining diluent. A bead with a relatively higher crosslinking density caused by the DVB content, as shown in Table 1 and Figure 4.9, results in a greater increase in the elastic-retractile force, which allows more formation of crosslinked microspheres with a porous structure.

4.1.2 Effect of monomer phase weight fraction

The effects of monomer phase weight fraction on the conversion, average particle size, particle size distribution and swelling properties were investigated by varying the monomer phase weight fractions of 0.1, 0.12, 0.14, and 0.16. The other parameters were kept constant as follows:

Monomer phase	
- Methyl methacrylate-divinylbenzene ratio (94:6)	95 %wt
- Initiator concentration	0.5 %wt
- Crosslinking agent concentration	0.1%wt
Aqueous phase	
- Suspending agent concentration	0.2 %wt
- Reaction temperature	70 °C
- Reaction time	5 hours
- Agitation rate	140 rpm
- Toluene: Heptane (100:0)	100 %wt

The unit of any chemical is % weight based on the monomer phase. The resultant copolymer beads were confirmed by IR spectrum as shown in Figure 4.7.

The characterization of methyl methacrylate- divinylbenzene copolymer beads was performed with FTIR transmission spectroscopy. The peak interpretations are the same as those in the previous section. The peak at 1630 cm^{-1} was disappeared due to the conversion of monomer to polymer.

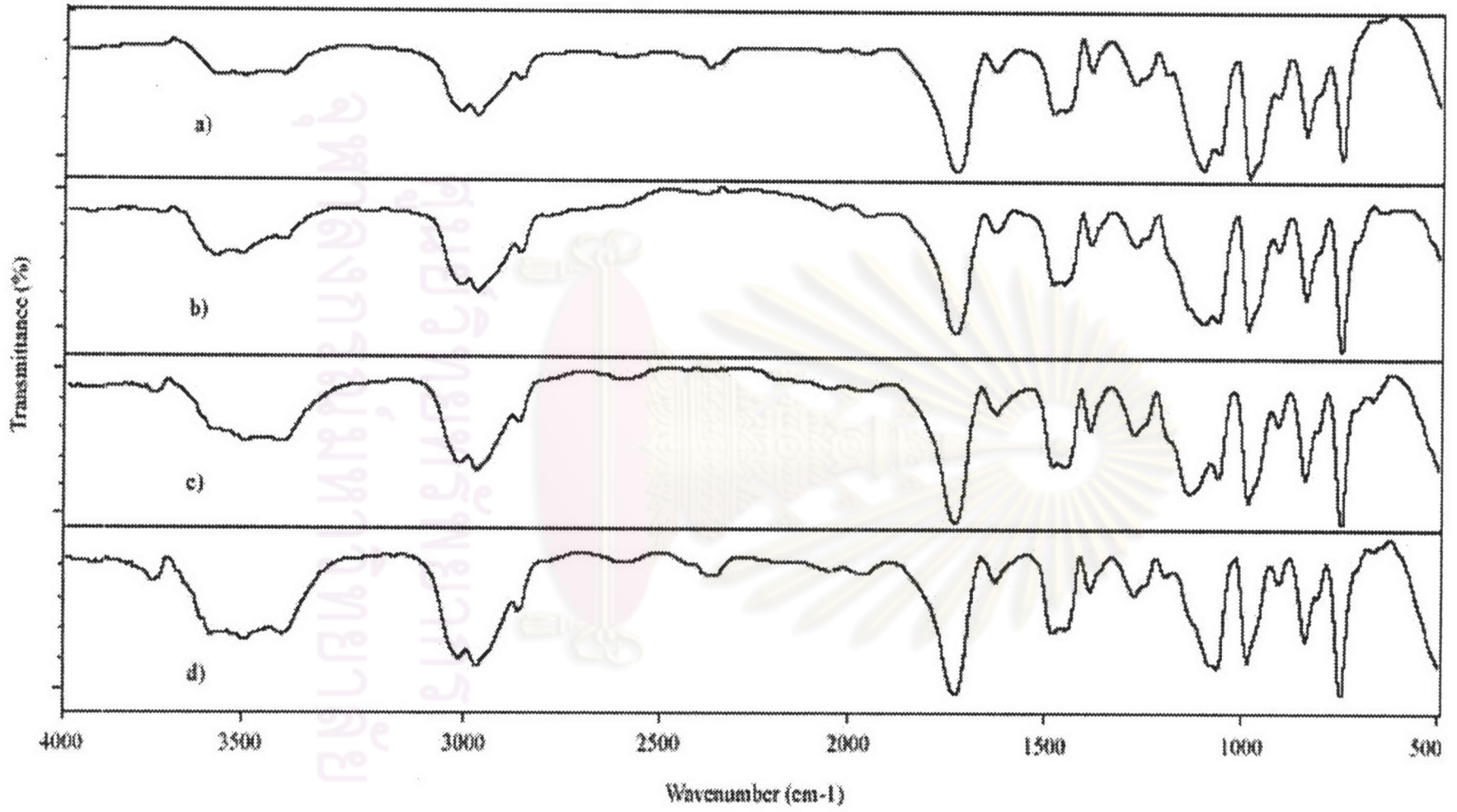

Figure 4.13 FTIR spectra of poly[(methyl methacrylate)-co-divinylbenzene] beads prepared by suspension copolymerization of various monomer phase weight fractions: a) 1.0, b) 1.2 c) 1.4, and d) 1.6.

Table 4.2 shows the overall conversion, the average particle size, particle size distribution, average molecular weight between crosslink ($\overline{M_c}$), crosslinking density, swelling ratio and density in relation to monomer phase weight fraction. It is found that all the overall conversions were higher than 95%. Figure 4.14 shows that the average particle size increased when increased the monomer phase weight fraction and the shape of particles still was sphere and unchanged. Figure 4.15 shows the particle size distribution charts which were affected from the monomer phase weight fraction, when the monomer phase weight fraction was low, it gave a broad distribution of particle size. At M16, it seems to give the monodispersity the particle size but it had some particles fused together. The volume fraction of the monomer phase is usually within the range 0.1-0.5. Polymerization reactions may be performed at the lower monomer volume fractions. At higher volume fractions, the concentration of continuous phase may be insufficient to fill the space between droplets. The coagulation of particle droplets is caused the increase of the monomer ratio inside the vessel; a large number of monomer droplets were generated and distributed throughout the system, while the liquid medium responsible for the heat transfer was reduced. Water is a good medium for removing heat from polymerizing droplets because it has both a high heat capacity and high thermal conductivity. These caused the heat inside the vessel gradually accumulated to the point at which the droplets melt and agglomerate onto the propeller of the mixing shaft [22].

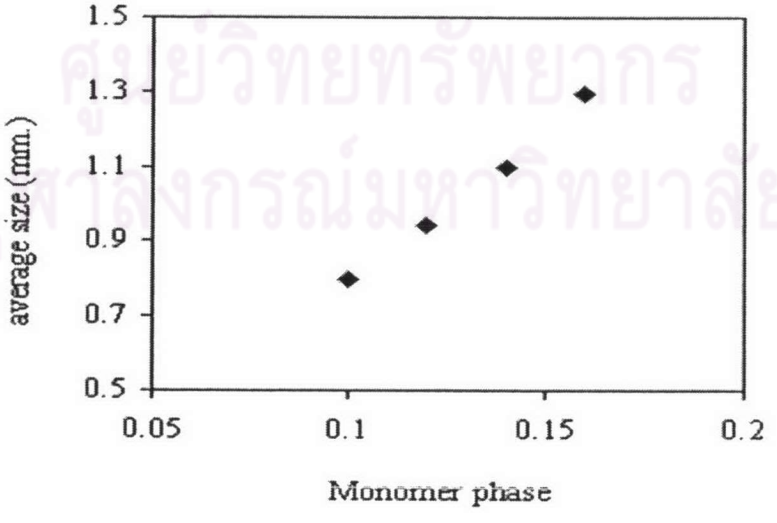

Figure 4.14 The average particle size in relation to the monomer phase weight fraction.

Table 4.2 Effect of the monomer phase weight fraction on Bead Properties

Run	M10	M12	M14	M16
Monomer phase	0.10	0.12	0.14	0.16
% Yield	95	96	100	97
Bead size distribution, wt %				
<0.42 mm	9.05	5.05	1.65	1.12
0.42-0.59 mm	8.36	6.63	6.04	2.34
0.59-0.84 mm	3.18	4.35	4.30	2.15
0.84-2.0 mm	4.41	11.39	17.56	21.28 (partially fused)
>2.0 mm	2.08	0.98	0.78	2.02
Average bead size, mm	0.80	0.94	1.10	1.30
$\overline{Mc}$	10000	11100	11200	20400
Crosslinking density	13.7	12.3	12.1	6.7
Swelling ratio in toluene (by volume)	8.7	8.8	8.5	9.4
(by weight)	6.4	6.5	5.8	6.3
Bead density, kg m^{-3}	1045	1047	1190	1162

Toluene was used a diluent. M_0 = 136300.

Table 4.2 and Figure 4.16 shows that toluene absorbency and crosslinking density were affected by the monomer phase weight fraction, but it was not significantly influenced by the from monomer phase weight fraction. However, it seems that when monomer phase weight fraction increased, the crosslinking density was decreased. However, it is not clear cut to conclude as such,

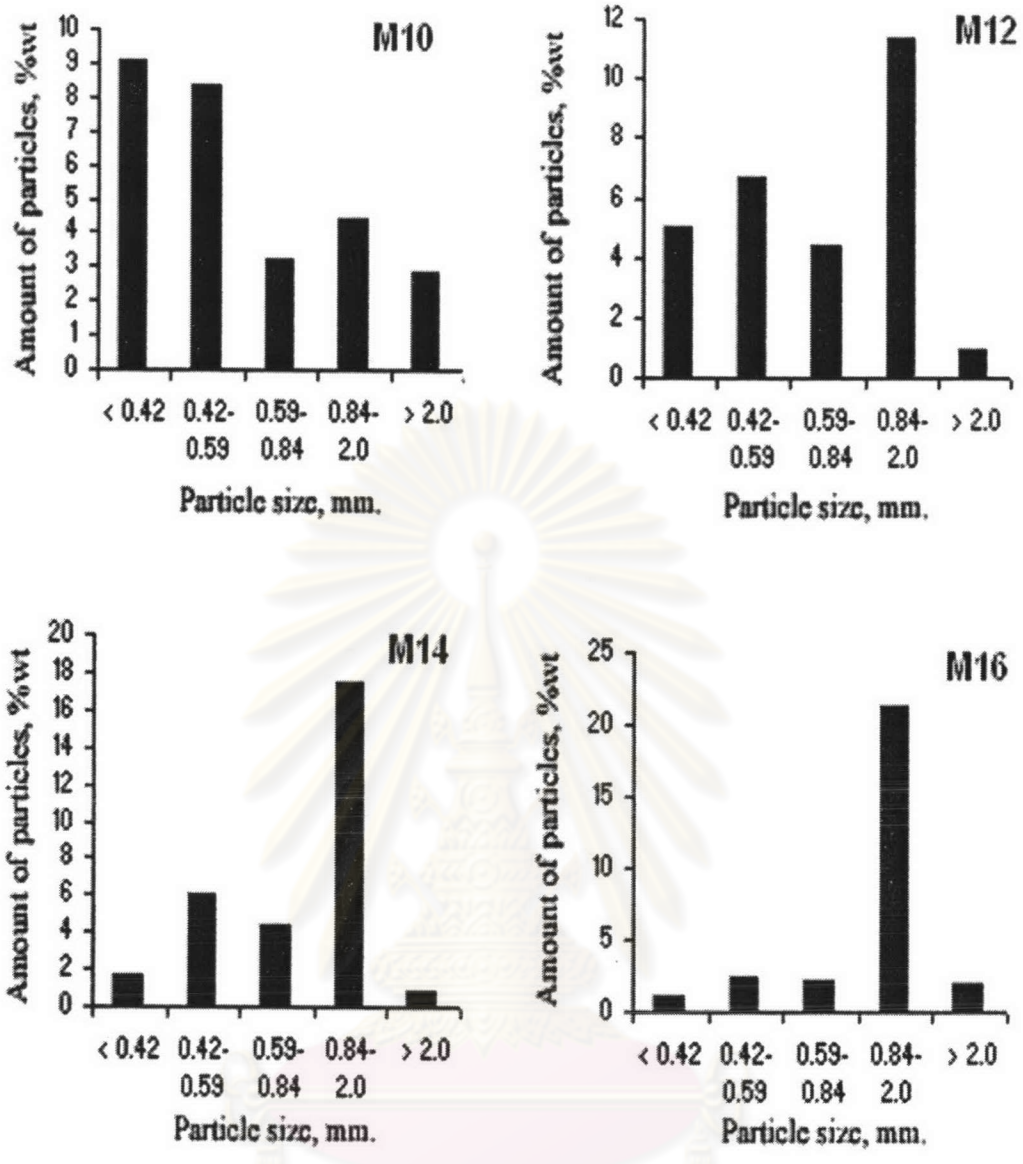

Figure 4.15 Particle size distribution under the effect of the in monomer phase weight fractions. a) 1.0, b) 1.2, c) 1.4, and d) 1.6.

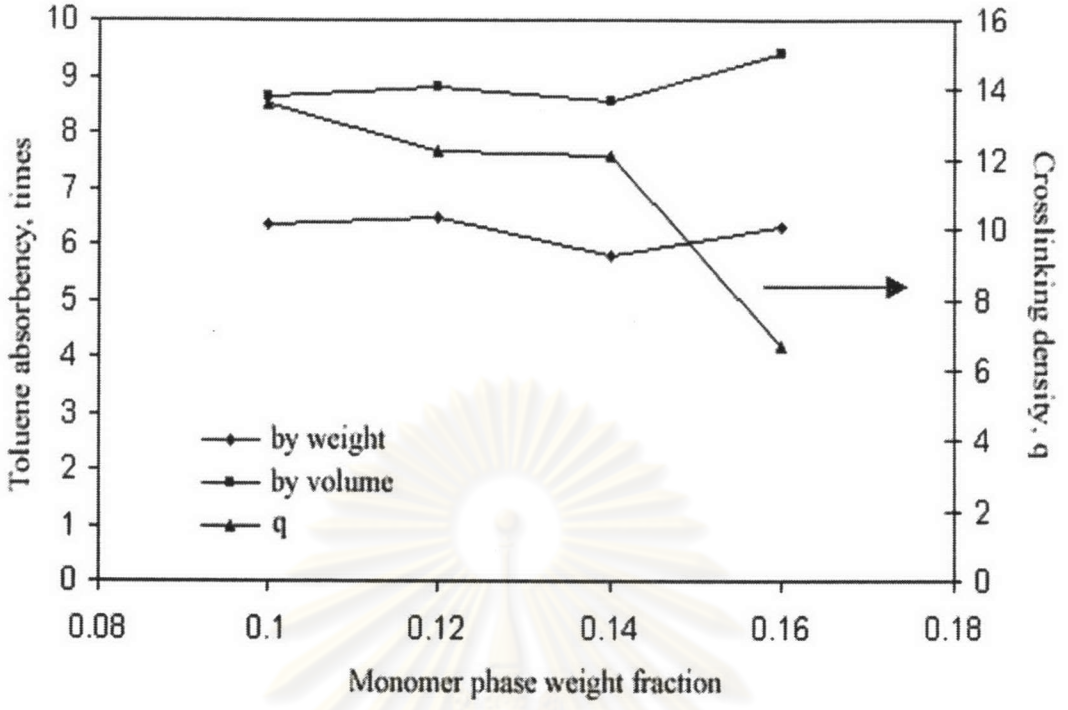

Figure 4.16 Effect of the monomer phase weight fraction on toluene absorbency and crosslinking density.

4.1.3 Effect of suspending agent concentration

The effects of suspending agent concentration on the conversion, average particle size, particle size distribution and swelling properties were investigated by varying the % suspending agent concentrations of 0.1, 0.15, 0.2, and 0.25 %wt based on the monomer phase. The other parameters were kept constant as follows:

Monomer phase (0.14)	
- Methyl methacrylate-Divinylbenzene ratio (94:6)	95 wt %
- Initiator concentration	0.5 wt %
- Crosslinking agent concentration	0.1wt %
Aqueous phase (0.86)	
- Reaction temperature	70 °C
- Reaction time	5 hours
- Agitation rate	140 rpm
- Toluene: Heptane (100:0)	100 wt %

The unit of any chemical is % weight based on monomer phase. The resultant copolymer beads were confirmed by IR spectrum as shown Figure 4.17.

The characterization of methyl methacrylate-co-divinylbenzene copolymer beads was performed with FTIR transmission spectroscopy. The peak interpretations are the same as those in the previous section. The peak at 1630 cm^{-3} is due to C=C stretching. This peak was disappeared because the conversion of monomer to polymer.

Suspension polymerization takes place in the organic droplets and each droplet acts as a small bulk polymerization reactor. Suspension polymerization kinetics consists of three stages. In the first one, the viscosity of the organic phase is low, the drop size is small, and the particle size distribution is relatively narrow, depending on agitation and the nature of suspending agent. In this stage, the suspension is quite stable, the drop population dynamic is fast, and the assumption of a quasi-steady state is valid. In the second state, which starts around 20-35% conversion, the droplets become high viscous and viscoelastic, and the breakage and coalescence rates decrease; however, the breakage rate decreases faster, so that the average droplet size increases. Moreover, if the coalescence rate dominates or if this stage lasts too long, a broadening of particle size distribution or even an agglomeration will occur. At even higher conversions, the mobility of the polymer chains within the droplets diminishes due to entanglements which result in a reduction of the termination rate; this is called the Trommsdorff or gel effect. This effect also causes an increase in the overall rate of reaction. In the third stage, the conversions are even higher and the particles are quite solid. The monomer molecules start to have diffusion problems and the propagation rate decreases.

At low concentrations, water-soluble protective colloids act in two ways. First, they decrease the interfacial tension between the monomer droplets and the aqueous phase to promote the dispersion and to reduce droplet size. Second, they are adsorbed at the surface of the monomer droplet to produce a thin layer that prevents coalescence when a collision occurs. The protective mechanism is due to the repulsion force that two polymer-covered surfaces feel when their segments begin to overlap as a result of the segments between the surfaces [23].

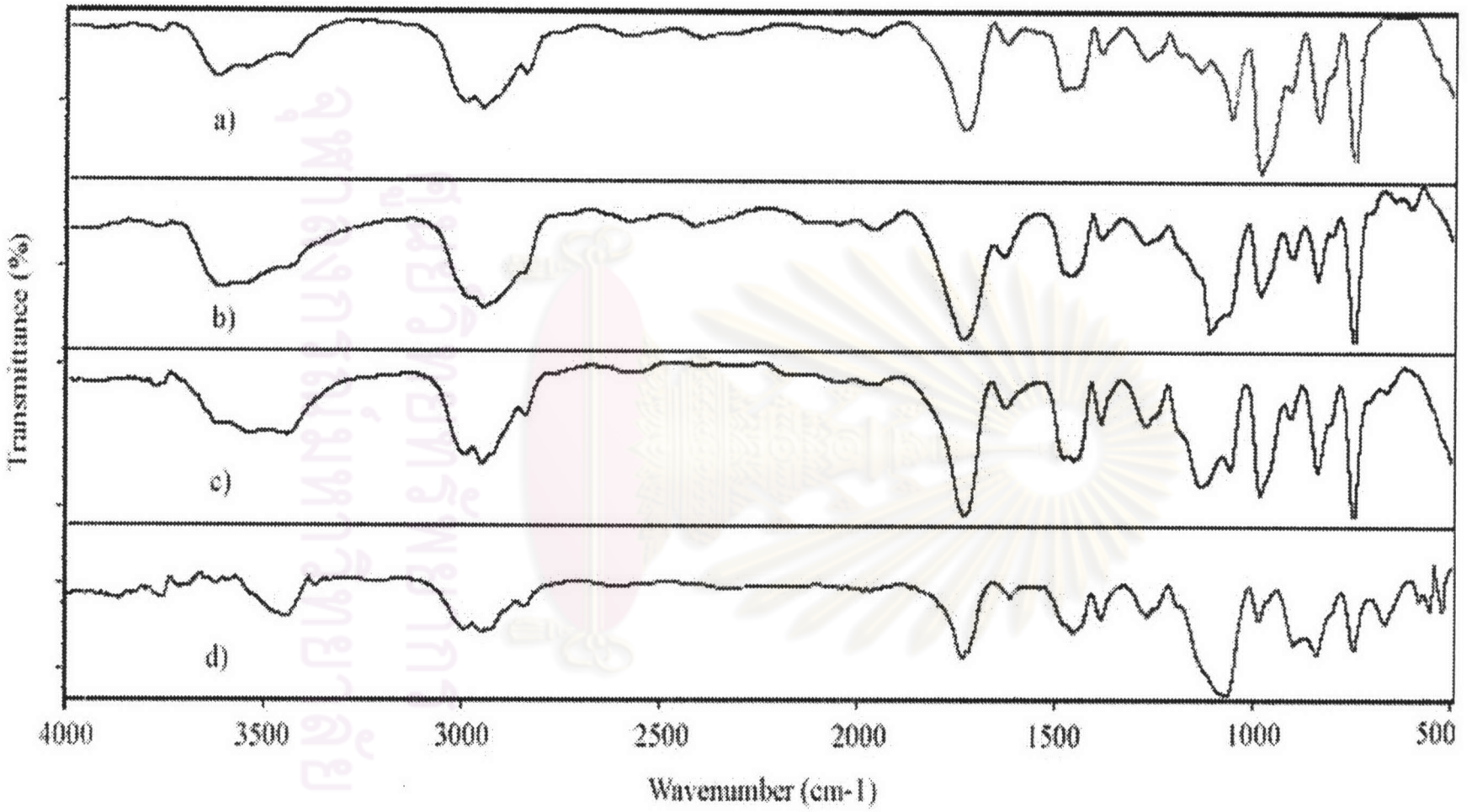

Figure 4.17 FTIR spectra of poly[(methyl methacrylate)-co-divinylbenzene] beads prepared by suspension copolymerization various suspending agent concentrations: a) S03, b) S045 c) S06, and d) S075.

Table 4.3 Effect of the suspending agent concentration on bead properties

Parameter	Run			
	S30	S45	S60	S75
Suspending agent concentration	0.10	0.15	0.20	0.25
% Yield	100	96	100	93
Bead size distribution, wt %				
<0.42 mm	1.83	3.70	1.66	4.42
0.42-0.59 mm	4.47	6.27	6.04	5.18
0.59-0.84 mm	1.75	3.62	4.30	2.70
0.84-2.0 mm	17.44	13.88	17.56	12.45
>2.0 mm	4.45	1.19	0.78	2.59
Average bead size, mm	1.27	1.03	1.10	1.07
$\overline{Mc}$	10600	11600	11200	16500
Crosslinking density	12.8	11.7	12.1	8.3
Swelling ratio in toluene (by volume)	9.04	8.86	8.54	9.16
(by weight)	5.86	6.09	5.79	6.46
Bead density, kg m^{-3}	1094	1119	1190	1094

Toluene was used as a diluent. M_0 = 136200.

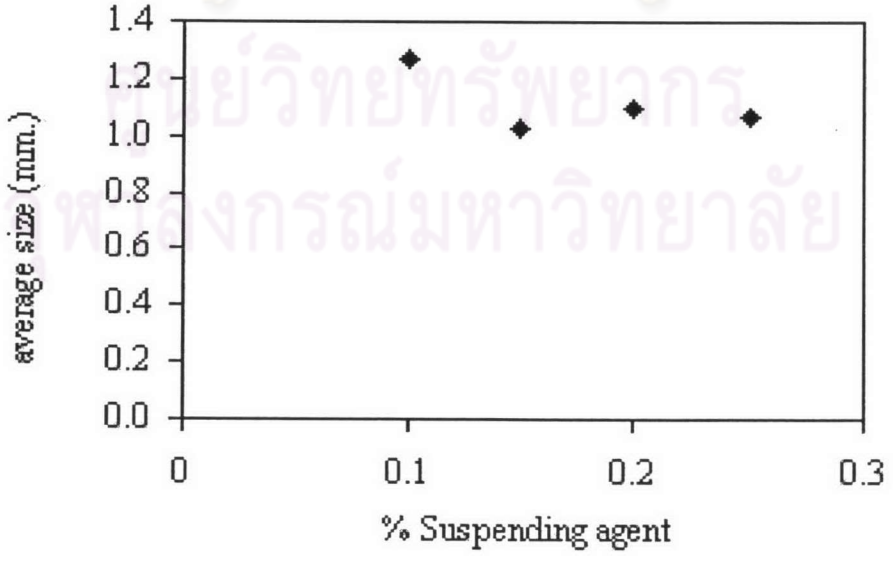

Figure 4.18 The average particle size in relation to suspending agent concentration.

Table 4.2 shows the overall conversion, the average particle size, particle size distribution, average molecular weight of the crosslink ($\overline{M_c}$), crosslinking density, swelling ratio and density in relation to poly(vinyl alcohol) concentration as the suspending agent. It is found that the overall conversion in all batches was higher than 90%. Figure 4.18 shows that the average particle size decreased in the early range and approached a steady state. The shape of the particles was spherical in all of the batches. Figure 4.19 shows the particle size distribution histograms, which were affected by suspending agent content. It seems that the particle size distribution is polydispersity with a decreasing manner when concentration of the suspending agent was increased. Figure 4.20 shows the effect of the suspending agent concentration on toluene absorbency and crosslinking density. It was found that the toluene absorbency does not effected by the concentration of suspending agent. The bead copolymers synthesized from all condition could absorb the toluene solvent about 9 times by volume and 6 times by weight.

In order to prevent coagulation during suspension polymerization, especially during the second stage when particles become sticky, suspending agents or stabilizers are added to the reaction system. Suspending agent covers the surface of the droplets, the amount of dispersing powder depends upon the desired droplet size. In the system where all factors are kept constant, the average particle size should be affected by surface of the entire droplet in the system. When the suspending agent content decreased, the average particle size increases because the suspending agent tries to cover the entire surface of whole droplet. The increasing droplet size is the result of a decrease in the entire surface of whole droplet. In the early stage show in Figure 4.18, the average particle size decreased when increased the suspending agent concentration. However, the average particle size was later nearly constant. The particle size distribution was polydispersity when the suspending agent concentration was further increased as shown in Figure 4.20.

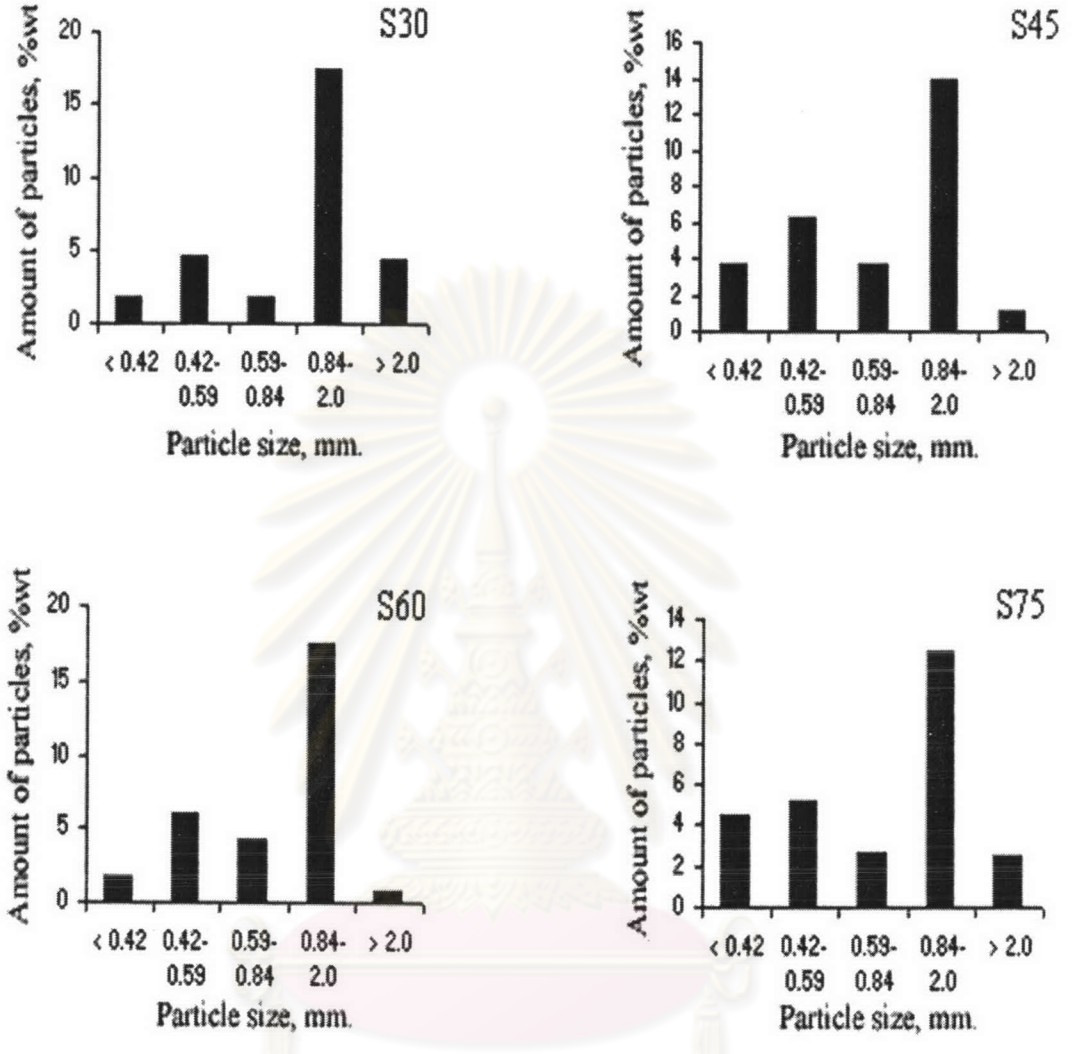

Figure 4.19 Effect of the suspending agent concentration on particle size and particle size distribution: a) S30, b) S45, c) S60 and d) S75.

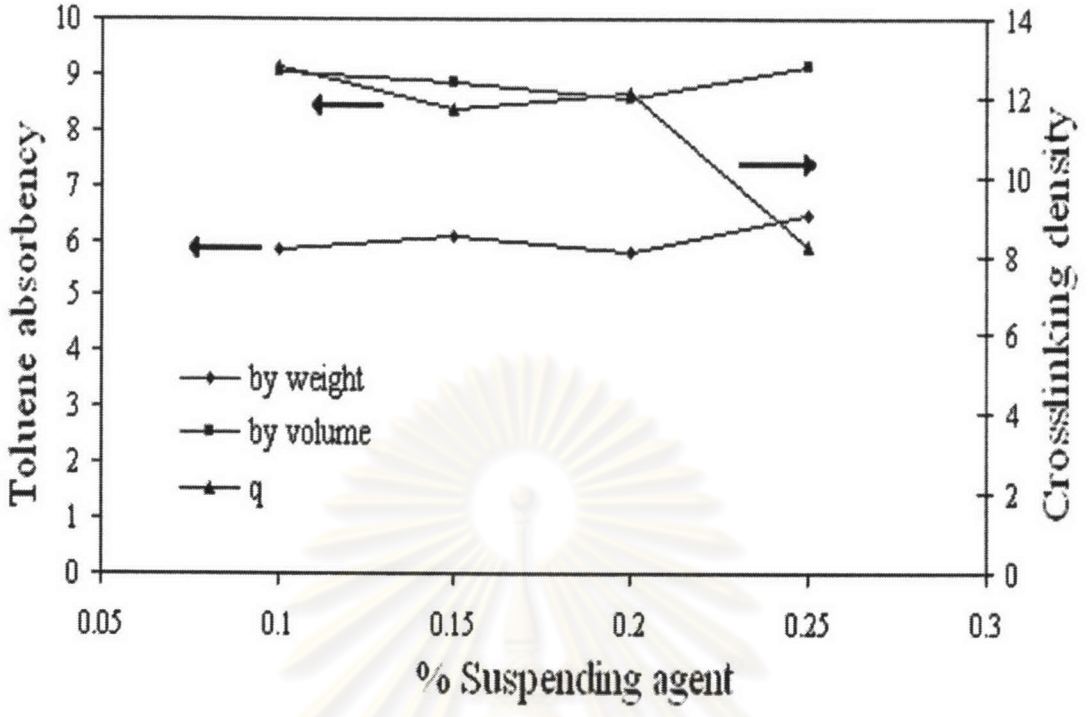

Figure 4.20 Effect of the suspending agent concentration on toluene absorbency and crosslinking density.

4.1.4 Effect of initiator concentration

The effects of initiator concentration on conversion, average particle size, particle size distribution and swelling properties were investigated with the % initiator concentrations of 0.125, 0.25, 0.5, and 1.0 wt % based on the monomer phase. The other parameters were kept constant as follows:

Monomer phase (0.14)	
- Methyl methacrylate-to-divinylbenzene ratio (94:6)	95 wt %
- Crosslinking agent concentration	0.1wt %
Aqueous phase (0.86)	
- Reaction temperature	70 °C
- Reaction time	5 hours
- Agitation rate	140 rpm
- Toluene: Heptane (100:0)	100 wt%

(The unit of any chemicals is used by weight % based on the monomer phase.) The resultant copolymer beads were confirmed by IR spectrum as shown in Figure 4.21.

The characterization of methyl methacrylate-co-divinylbenzene copolymer beads are performed by the FTIR transmission spectroscopy. The peak interpretations are the same as those in the previous section. The peak at 1630 cm^{-3} was disappeared due to the conversion of monomer to polymer.

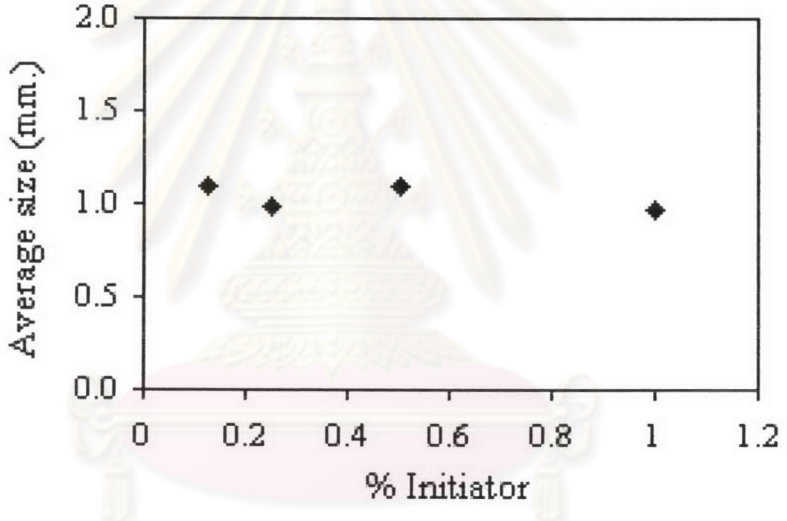

Figure 4.21 The average particle size in relation to initiator concentration.

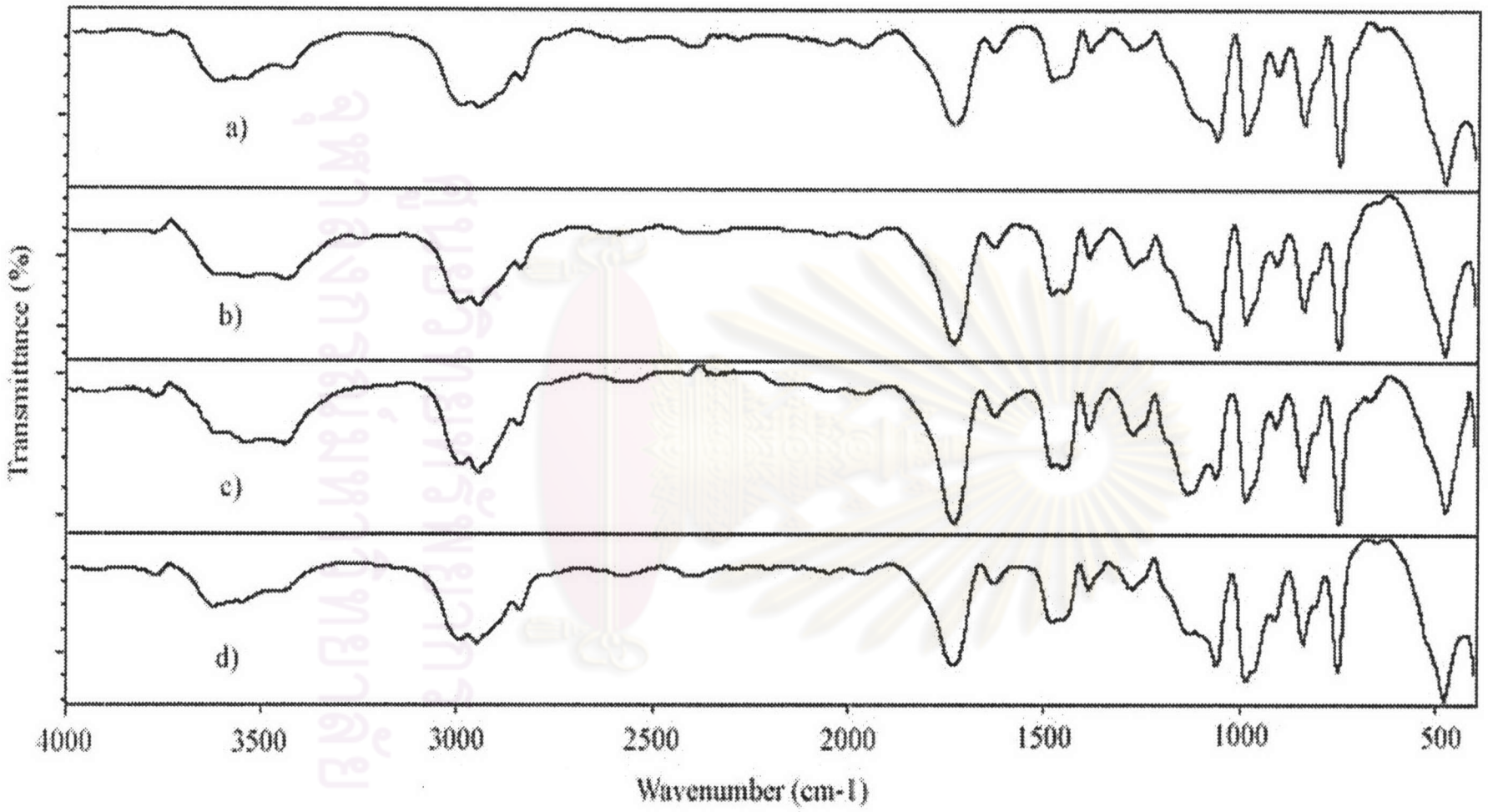

Figure 4.22 FTIR spectra of poly[(methyl methacrylate)-co-divinylbenzene] beads prepared by suspension copolymerization at various initiator concentrations: a) I03, b) I07 c) I15, and d) I30.

Table 4.4 Effect of the initiator concentration on bead properties

Parameter	Runs			
	I03	I07	I15	I30
Initiator concentration	1.0	0.25	0.5	0.125
% Yield	100	87	100	86
Bead size distribution, wt %				
<0.42 mm	4.75	3.25	1.65	2.87
0.42-0.59 mm	6.92	4.45	6.04	4.05
0.59-0.84 mm	4.49	4.67	4.30	4.01
0.84-2.0 mm	12.84	9.50	17.56	12.91
>2.0 mm	1.23	1.14	0.78	1.87
Average bead size, mm	0.97	0.99	1.10	1.10
$\overline{Mc}$	27900	12700	11200	7600
Crosslinking density	4.91	10.8	12.1	7.9
Swelling ratio in toluene (by				
volume)	9.8	8.8	8.5	8.2
(by weight)	7.0	7.6	5.8	6.0
Bead density, kg m^{-3}	1096	1024	1190	1048

Toluene was used a diluent. M_0 = 136300.

Table 4.4 shows the overall conversion, the average particle size, particle size distribution, average molecular weight between crosslink ($\overline{M_c}$), crosslinking density, swelling ratio and density in relation to benzyl peroxide as an initiator. It was found that the conversion increased when the initiator concentration increased. It is well known that in radical chain polymerization the initiator efficiency and conversion will be are control by the initiator concentration. The increasing initiator concentration in the free radical polymerization increases the polymerization rate of the reaction. From Figure 4.22, the average particle size in this study was slightly decreased when increased the concentration of initiator. The particle size polydispersity of distribution (Figure 4.24) was not affected by the initiator concentration. Table 4.4 and Figure 4.23 show the toluene absorbency and the average molecular weight of the crosslink decreased when increased the initiator content. However, the crosslinking density was

increased because the kinetic chain length decreased. The kinetic chain length is inversely dependent on the radical concentration or the polymerization rate.

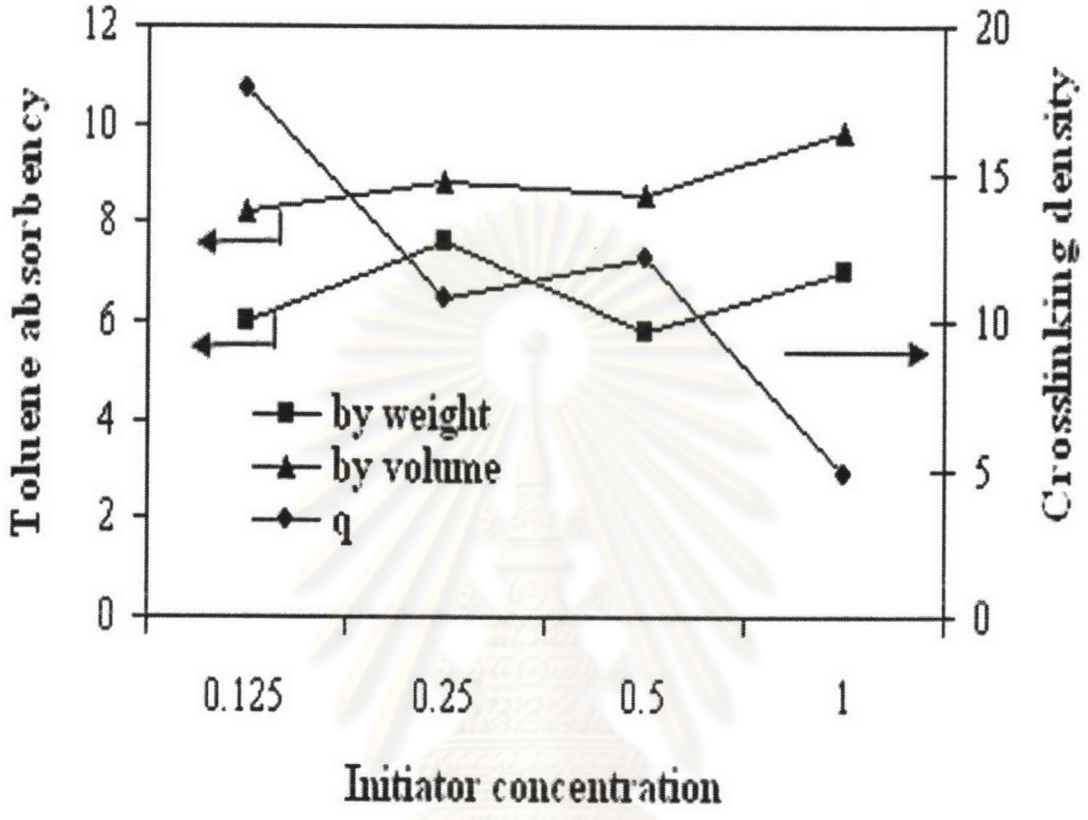

Figure 4.23 Effect of the initiator concentration on toluene absorbency and crosslinking density.

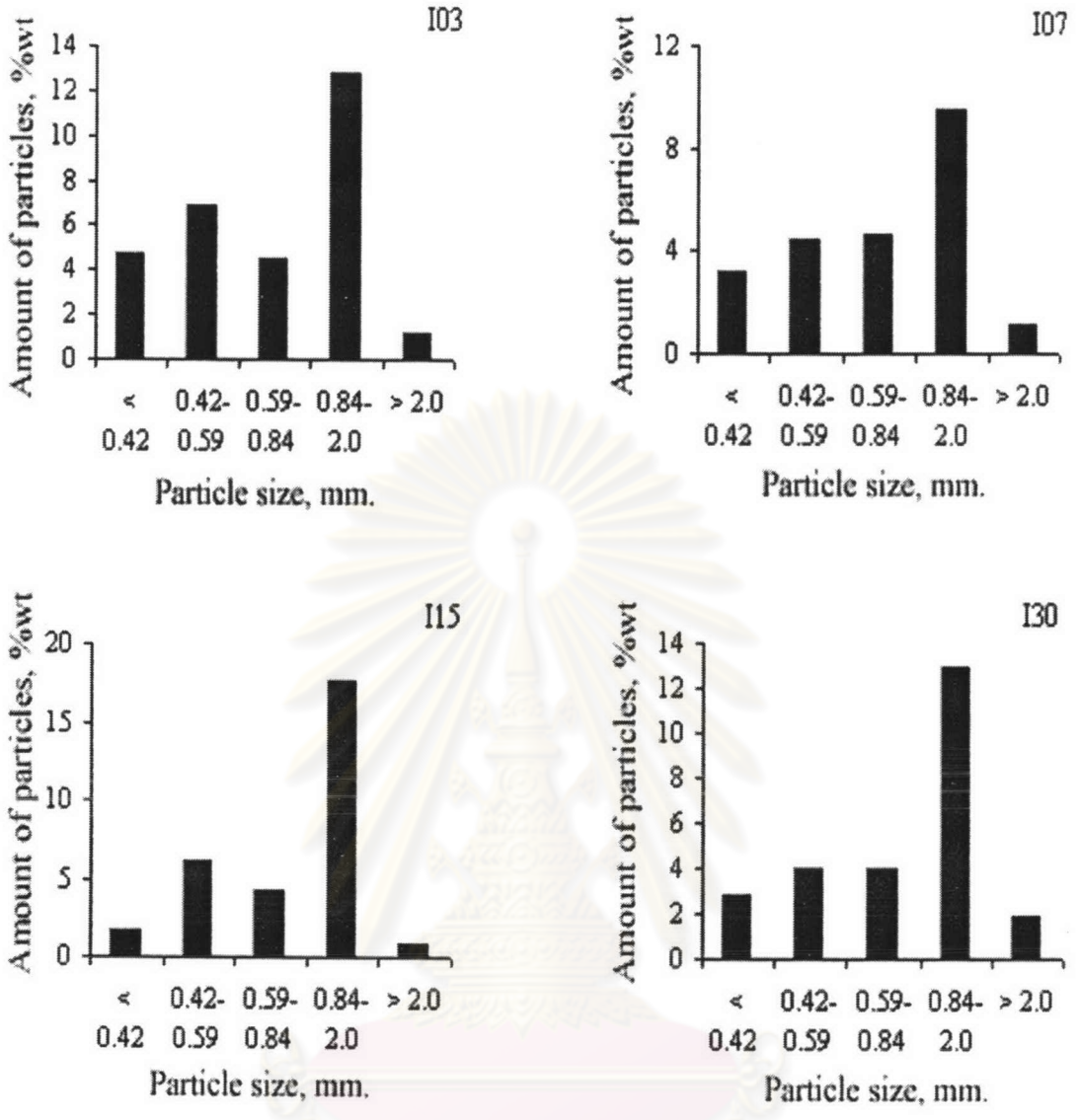

Figure 4.24 Effect of the initiation concentration on particle size and distribution of a) I03, b) I07, c) I15, and d) I30.

The crosslinking density increased because DVB is consumed more readily than is methyl methacrylate to form radicals, since DVB has a higher reactivity than methyl methacrylate.[24] Also, the increasing BPO content produced the increasing crosslinking sites in the polymer network, the copolymer beads are then less flexible leading to the decrease in the swelling ratio.

4.1.5 Effect of the impeller speed

The effects of the impeller speed on the conversion, average particle size, particle size distribution and swelling properties were investigated. The impeller speeds of 120, 130, 140, and 150 rpm were used in the experiment. The other parameters were kept constant as follows:

Monomer phase (0.14)	
- Methyl methacrylate: Divinylbenzene ratio (94:6)	95 wt %
- Initiator concentration	0.5 wt %
- Crosslinking agent concentration	0.1wt %
Aqueous phase (0.86)	
- Reaction temperature	70 °C
- Reaction time	5 hours
- Toluene: Heptane (100:0)	100 wt %

(The unit of any chemicals is % weight based on monomer phase.) The resultant copolymer beads were confirmed by IR spectrum as shown in Figure 4.25.

The characterization of methyl methacrylate-co-divinylbenzene copolymer beads are performed by the FTIR transmission spectroscopy. The peak interpretations are the same as those in the previous section. The peak at 1630 cm^{-1} was disappeared due to the conversion of monomer to polymer.

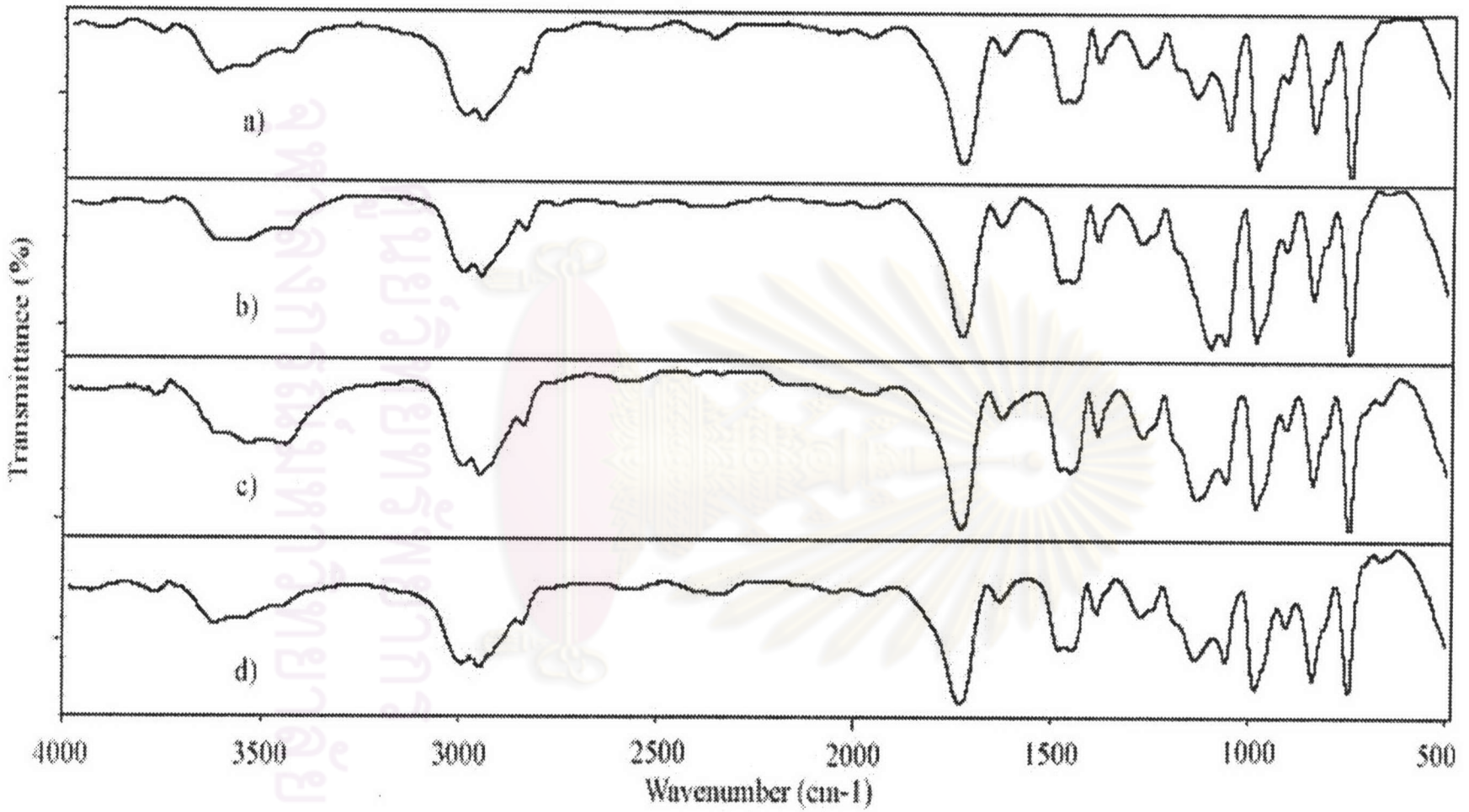

Figure 4.25 FTIR spectra of poly[(methyl methacrylate)-co-divinylbenzene] beads prepared by suspension copolymerization with various impeller speeds: a) 120 rpm, b) 130 rpm c) 140 rpm, and d) 150 rpm.

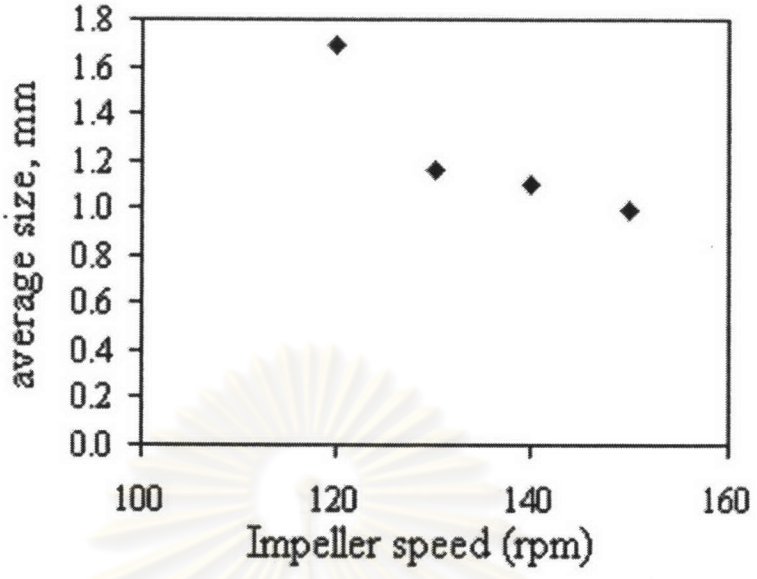

Figure 4.26 The average particle size in relation to the impeller speed.

Table 4.5 shows the overall conversion, the average particle size, particle size distribution, average molecular weight between crosslink ($\overline{M_c}$), crosslinking density, swelling ratio and density in relation to the impeller speed. It was found the over all conversion in all reactors was higher than 90 %. Figure 4.26 shows that the average particle size was smaller when increased the impeller speed. When increasing the impeller speed to 130 rpm and higher, the average size of copolymer particles slightly decreased. Figure 4.27 shows the particle size distribution polydispersity

In suspension polymerization, monomer is suspended as liquid droplets in a continuous water phase by agitation. The monomer particles are subject to coalescence, their reverse dispersion into smaller particles being possible. The polymerization conditions, especially the stirring rate, influence the average particle size and distribution at this point and finally also the properties of the polymer suspension. The stage of medium conversion is characterized by increased stickiness of the polymer particles and their greater tendency to coalesce. The coalescence of these particles is irreversible: neither addition of extra stabilizer nor more vigorous stirring leading to dispersion of the associates. As the reaction reaches higher conversions, the polymer particles lose their stickiness and are no longer vulnerable to coalescence. An increase in the intensity of stirring usually leads to a decrease of the

average size of the polymer particles due to the increasing of the shear force at any droplet. When concentrations of the stabilizer used are such that the surface coverage is above the oil suspension shows no tendency towards coalescence when the stirring speed is much reduced. [25]

Table 4.5 Effect of the Impeller speed on Bead Properties

Parameter	Run			
	R12	R13	R14	R15
Impeller speed (rpm)	120	130	140	150
% Yield	98	94	100	96
Bead size distribution, wt %				
<0.42 mm	0.38	1.40	1.65	3.31
0.42-0.59 mm	0.50	3.81	6.04	7.21
0.59-0.84 mm	0.50	4.32	4.30	4.44
0.84-2.0 mm	12.10	16.18	17.56	12.71
>2.0 mm	15.32	1.46	0.78	1.01
Average bead size, mm	1.69	1.16	1.10	0.99
$\overline{Mc}$	11700	10600	11200	12900
Crosslinking density	11.7	12.8	12.1	10.6
Swelling ratio in toluene (by				
volume)	8.8	8.8	8.5	8.9
(by weight)	5.9	6.3	5.8	6.4
Bead density, kg m^{-3}	1149	1072	1190	1081

Toluene was used as a diluent. M_0 = 136300.

The toluene absorbency and crosslinking density of copolymer beads were investigate as shown in Figure 4.28. It was found that the impeller speed had no great influence on both the toluene absorbency and crosslinking density. However, the toluene absorbency values slightly vary.

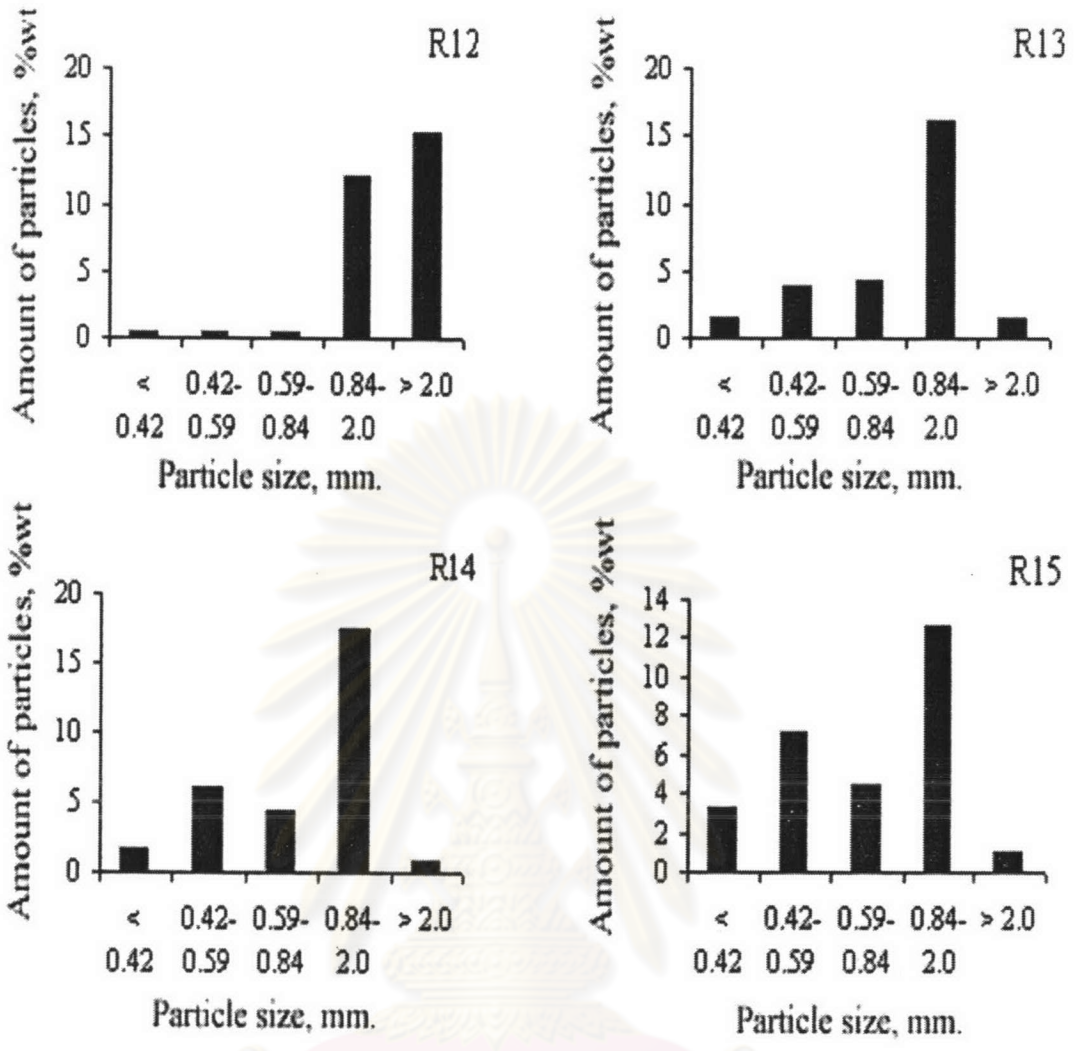

Figure 4.27 Effect of the impeller speed on particle size and distribution on of the polymer: a) 120 rpm, b) 130 rpm, c) 140 rpm, and d) 150 rpm.

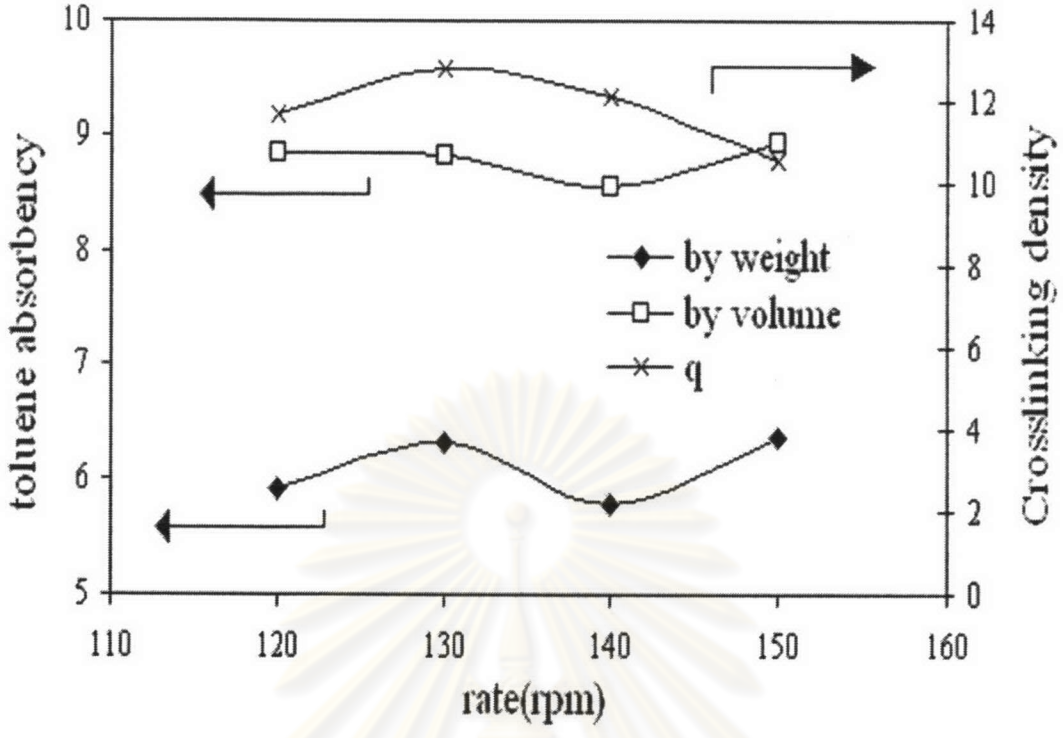

Figure 4.28 Effect of the impeller speed on toluene absorbency and crosslinking density.

The particle size of copolymer bead was not affected on the toluene absorbency. When the agitation rate increased, the average particle size was decreased, it did not effect on the toluene absorbency.

4.1.6 Effect of the reaction time

The effects of the reaction time on the conversion, average particle size, particle size distribution and swelling properties were investigated. The reactor times were 3.5, 5.0, 6.5, and 8.0 hours respectively, while the other parameters were kept constant as follows:

Monomer phase (0.14)	
- Methyl methacrylate: Divinylbenzene ratio (94:6)	95 wt %
- Initiator concentration	0.5 wt %
- Crosslinking agent concentration	0.1wt %
Aqueous phase (0.86)	
- Reaction temperature	70 °C
- Agitation rate	140 rpm

- Toluene: Heptane (100:0) 100 wt%

(The unit of any chemicals is % weight based on monomer phase.) The resultant copolymer beads were confirmed by IR spectrum as shown in Figure 4.29.

The characterization of methyl methacrylate- divinylbenzene copolymer beads was performed with FTIR transmission spectroscopy. The peak interpretations are the same as those in the previous section. The peak at 1630 cm^{-1} was disappeared due to the conversion of monomer to polymer.

Table 4.6 shows the overall conversion, the average particle size, particle size distribution, average molecular weight between crosslink ($\overline{M_c}$), crosslinking density, swelling ratio and density in relation to the reaction time. It was found that the overall conversion increased when increased the reaction time. Figure 4.29 shows that the average particle size increased when increased the reaction time. At the reaction time of 3.5 hours, the conversion was 57 % and some polymer particles were clustered and sticky. The suspension polymerization system usually consists of three stages as describe in the previous section. In the second stage where the conversion of 20-35% get start, the droplets become highly viscous and viscoelastic, and the breakage and coalescence rates decrease; however, the breakage rate decreases faster, so that the average droplet size increases. Moreover, if the coalescence rate dominates or if this stage lasts too long, a broadening of the particle size distribution or even an agglomeration will occur. [23] It was shown in the Figure 4.30 that the particle size distribution was not affected by the reaction time.

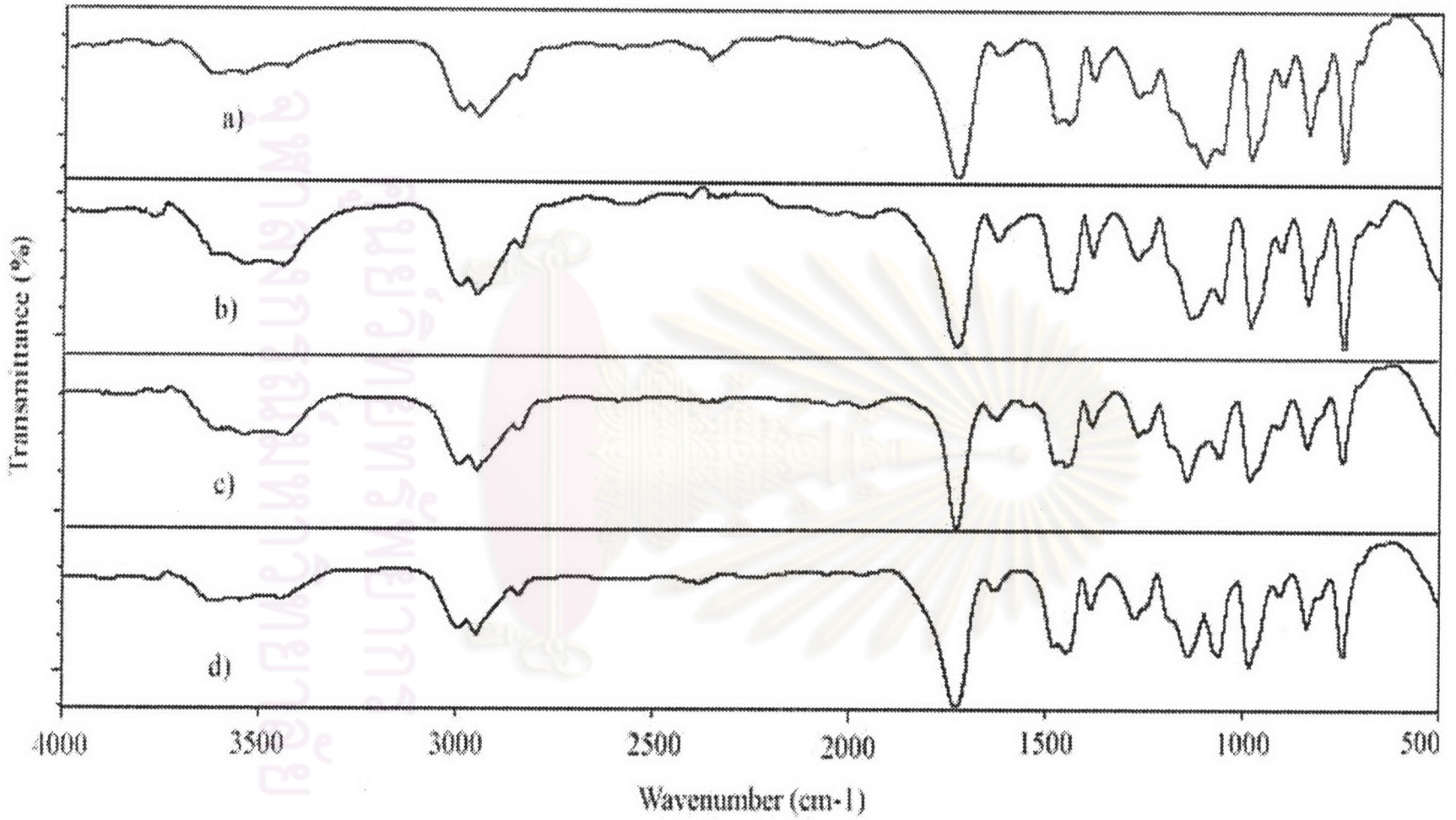

Figure 4.29 FTIR spectra of poly[(methyl methacrylate)-co-divinylbenzene] beads prepared by suspension copolymerization by various reaction times: a) 3.5 h, b) 5.0 h c) 6.5 h, and d) 8.0 h.

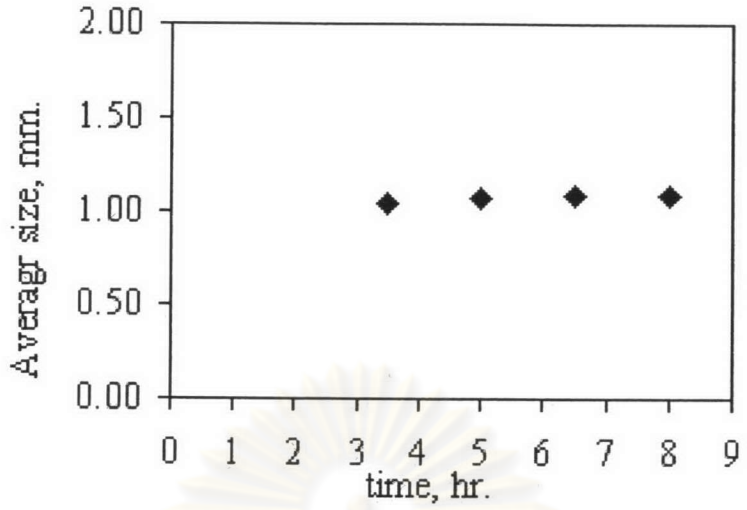

Figure 4.30 The average particle size in relation to the reaction time.

Table 4.6 Effect of the Reaction time on Bead Properties

Parameter	Reaction time, hr			
	t35	t50	t65	t80
Reaction time	3.5	5.0	6.5	8.0
% Yield	57	94	99	99
Bead size distribution, wt %				
<0.42 mm	0.51	1.64	0.68	1.07
0.42-0.59 mm	1.95	6.04	4.17	7.72
0.59-0.84 mm	2.06	5.34	5.87	3.42
0.84-2.0 mm	4.79	16.51	10.35	9.68
>2.0 mm	0.24	0.79	1.08	0.67
Average bead size, mm	1.04	1.07	1.06	0.85
$\overline{Mc}$	34500	11200	5500	7100
Crosslinking density	3.9	12.1	24.9	19.1
Swelling ratio in toluene				
(by volume)	9.3	8.5	7.0	7.3
(by weight)	6.7	5.8	4.6	5.1
Bead density, kg m^{-3}	1079	1190	1.114	1072

Toluene was used a diluent. M_0 = 136300.

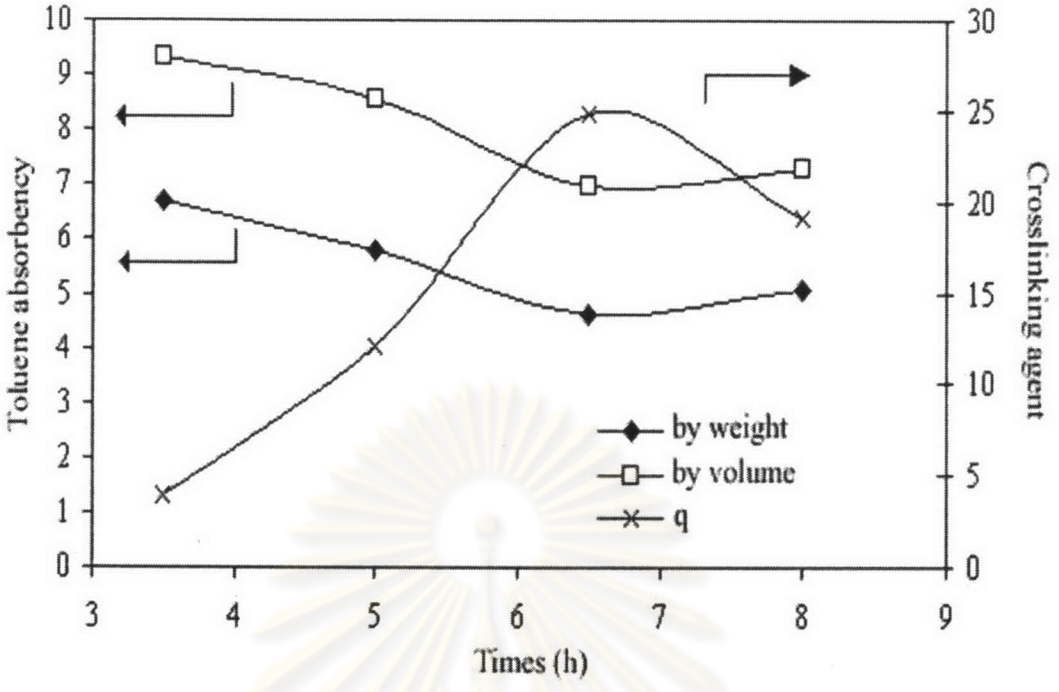

Figure 4.31 Effect of the reaction time on toluene absorbency and crosslinking density.

Figure 4.31 shows the effect of reaction time on the toluene absorbency and crosslinking density. It was found that the toluene absorbency decreased when increased in the reaction time and the crosslinking density increased when increased the reaction time. The higher conversion or longer reaction time, the polymer chains are more entangled and the second double bond or vinyl group of DVB was consume as the crosslinking sites. When increasing the crosslinking sites, chain mobility inside the beads is restricted, it causes decreases in the swelling ratio. [26]

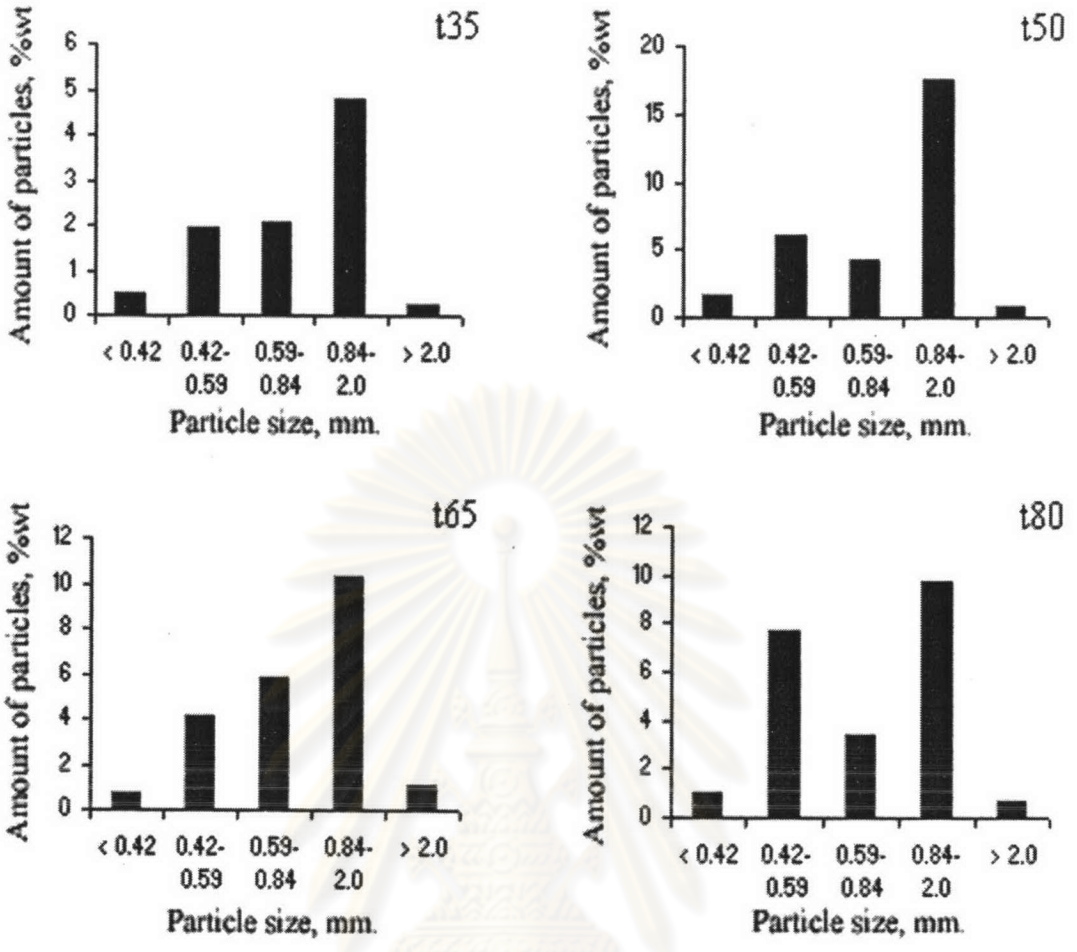

Figure 4.32 Effect of the reaction time on particle size and particle size distribution: a) 3.5 h, b) 5.0 h, c) 6.5 h, and d) 8.0 h.

4.1.7 Effect of the reaction temperature

The effects of the reaction temperature on the conversion, average particle size, particle size distribution and swelling properties were investigated. The reaction temperatures of 60, 70, and 80°C were used, which the other parameters were kept constant as follows:

Monomer phase (0.14)	
- Methyl methacrylate-Divinylbenzene ratio (94:6)	95 wt %
- Initiator concentration	0.5 wt %
- Crosslinking agent concentration	0.1wt %

Aqueous phase (0.86)

- Reaction time 5 hours
- Agitation rate 140 rpm
- Toluene: Heptane (100:0) 100 wt%

(The unit of any chemical is % weight based on monomer phase.) The resultant copolymer beads were confirmed by IR spectrum as shown in Figure 4.27.

The characterization of methyl methacrylate- divinylbenzene copolymer beads was performed with FTIR transmission spectroscopy. The peak interpretations are the same as those in the previous section. The peak at 1630 cm^{-1} was disappeared due to the conversion of monomer to polymer.

Table 4.7 Effect of the Reaction Temperature on Bead Properties

Parameter	Run		
	T60	T70	T80
Reaction temperature	60	70	80
% Yield	71	94	100
Bead size distribution, wt %			
<0.42 mm	3.99	6.88	3.81
0.42-0.59 mm	6.26	11.51	6.44
0.59-0.84 mm	5.06	0.61	3.24
0.84-2.0 mm	5.14	8.66	13.51
>2.0 mm	0.47	0.22	0.21
Average bead size, mm	0.80	0.78	0.98
$\overline{Mc}$	6600	11200	7700
Crosslinking density	20.7	12.1	17.6
Swelling ratio in toluene (by volume)	7.2	8.5	7.4
(by weight)	5.4	5.8	4.8
Bead density, kg m^{-3}	995	1190	1153

Toluene was used a diluent. M_0 = 136300.

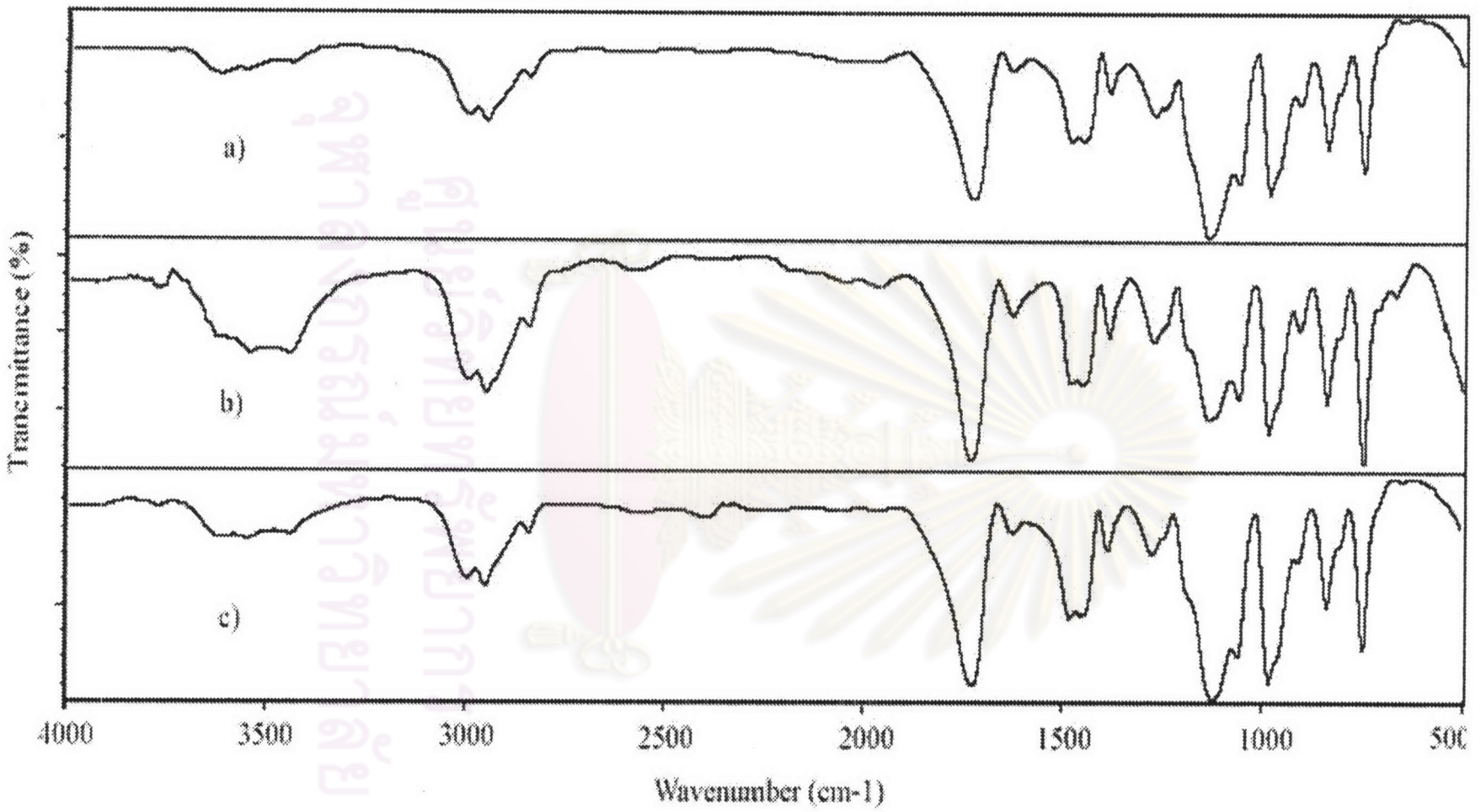

Figure 4.33 FTIR spectra of poly[(methyl methacrylate)-co-divinylbenzene] beads prepared by suspension copolymerization at various reaction temperature, a) 60°C, b)70°C, and c) 80°C.

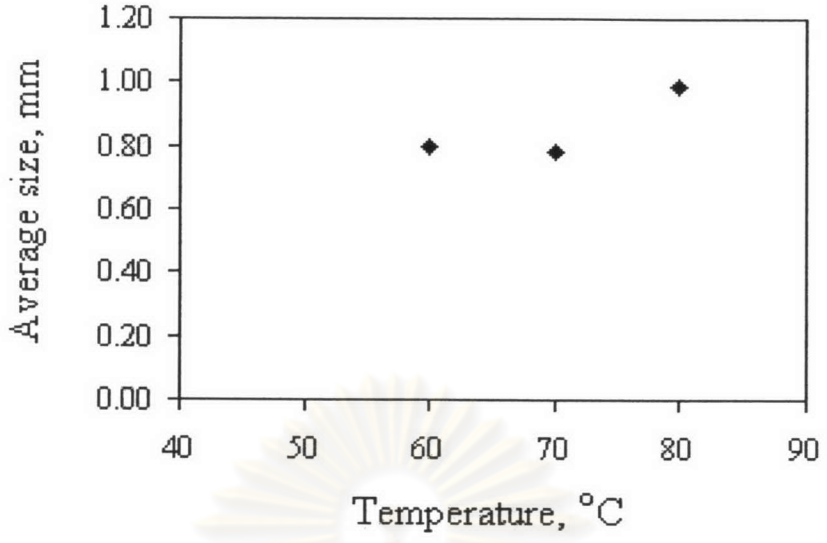

Figure 4.34 The average particle size in relation to the reaction temperature.

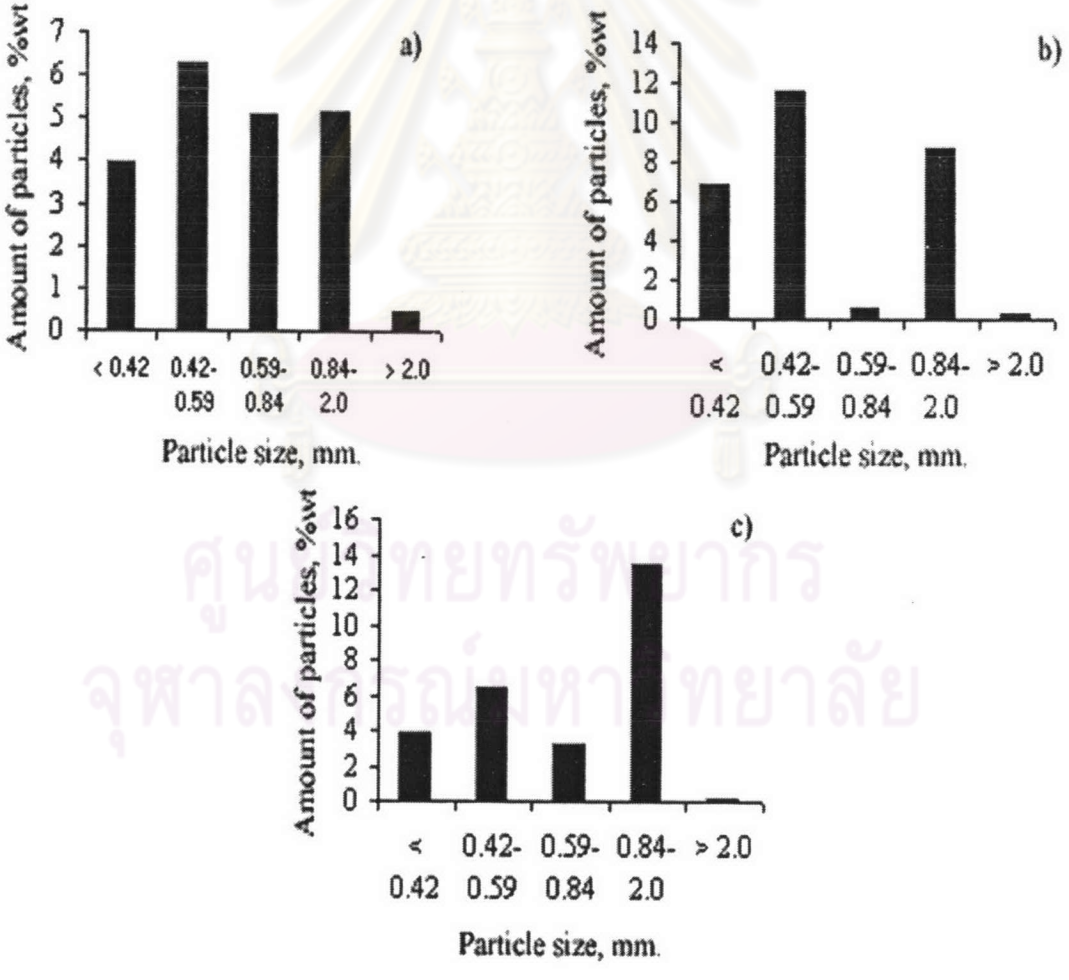

Figure 4.35 Effect of reaction temperature on particle size and distribution at: a) 60°C, b) 70°C, and c) 80°C.

Table 4.7 shows the overall conversion, the average particle size, particle size distribution, average molecular weight between crosslink ($\overline{M_c}$), crosslinking density, swelling ratio and density in relation to the reaction time. The overall conversion increased when increased the reaction temperature because increasing the decomposition rate of the initiator to produce a large amount of free radicals that can initiate to give many polymer radicals. It results in an increased overall conversion. Figure 4.33 shows that the average particle size increased when increased the reaction temperature. As mention in the description in previous section as that, in the second stage if it is at a high conversion the coalescence rate dominates, the average particle size was increased and a broadening of the particle size distribution occurred. Figure 4.34 shows the dependence of polymer particle size and distribution reaction temperature. Figure 4.35 shows the toluene absorbency and crosslinking density which were affected by the polymerization temperature. It was found that the toluene absorbency increased from the polymerization temperature at 60°C to 70°C and then decreased at 80°C. At the low temperature for the polymerization, a low conversion and low molecular weight of the polymer were obtained. The DVB monomer has a higher reactivity than MMA monomer, so that it has many crosslinking for copolymerization to result in a higher crosslinking density and lower toluene absorbency. For a high temperature polymerization, low molecular weight of polymer because the high when increased polymerization temperature results in the enhanced rate of the reaction: the rates of initiation, propagation, and termination. All of these three factors except the rate of termination increase the rate of polymerization. However, a further increase in the polymerization temperature reduces the molecular weight of the polymer, due to increases in the rates of termination and chain transfer to increase in the longer number of the polymer chains. It is similar to the case of low temperature polymerization to result in the higher crosslinking density and the lower toluene absorbency.

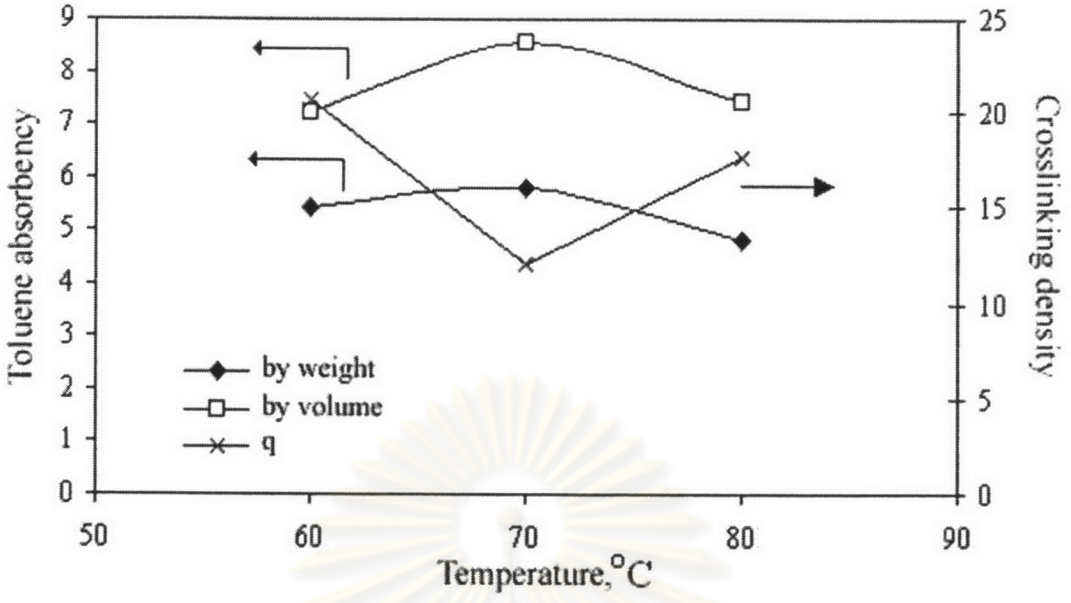

Figure 4.36 Effect of the reaction temperature on toluene absorbency and crosslinking density.

4.1.8 Effect of the diluent composition

The effects of the diluent composition on the conversion, average particle size, particle size distribution and swelling properties were investigated by varying the diluent composition of 0, 20, 40, 60, and 80 wt % based on the monomer phase. The good and poor solvents are toluene and heptane, respectively. The other parameters were kept constant as follows:

Monomer phase (0.14)	
- Methyl methacrylate-Divinylbenzene ratio (94:6)	95 wt %
- Initiator concentration	0.5 wt %
- Crosslinking agent concentration	0.1wt %
Aqueous phase (0.86)	
- Suspending agent concentration	0.2 wt %
- Reaction temperature	70 °C
- Reaction time	5 hours
- Agitation rate	140 rpm

(The unit of any chemical is %weight based on monomer phase.) The resultant copolymer beads were confirmed by IR spectrum as shown in Figure 4.37.

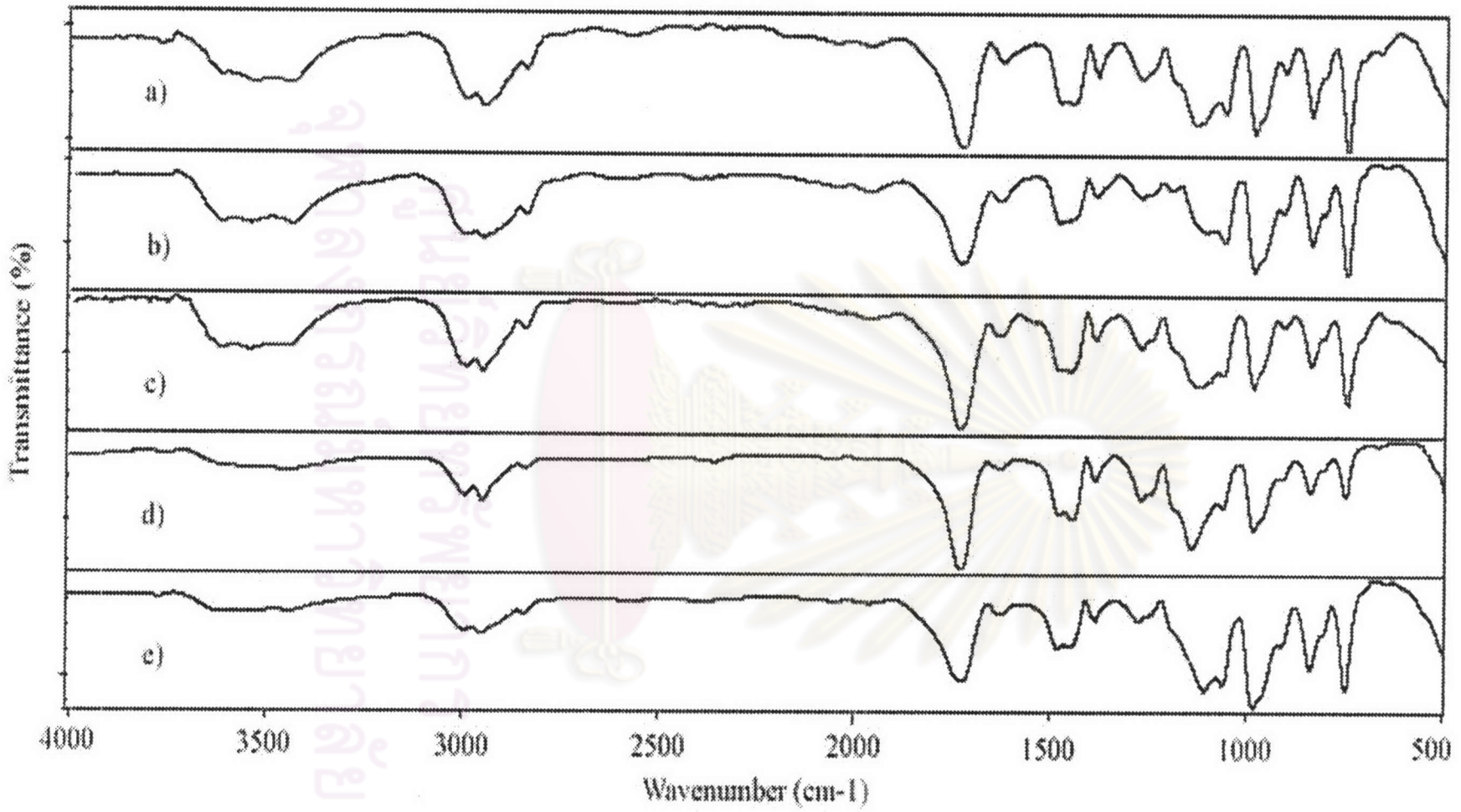

Figure 4.37 FTIR spectra of poly[(methyl methacrylate)-co-divinylbenzene] beads prepared by suspension copolymerization at various diluent compositions: a) 0% heptane, b) 20% heptane, c) 40% heptane, d) 60% heptane, and e) 80% heptane.

The characterization of methyl methacrylate- divinylbenzene copolymer beads was performed with FTIR transmission spectroscopy. The peak interpretations are the same as those in the previous section. The peak at 1630 cm^{-1} was disappeared due to the conversion of monomer to polymer.

Table 4.8 Effect of the Diluent Composition on Bead Properties

Parameter	Run				
	H00	H20	H40	H60	H80
Diluent composition	0	20	40	60	80
% Yield	94	98	100	100	96
Bead size distribution, %wt					
<0.42 mm	1.64	0.88	0.28	0.03	1.70
0.42-0.59 mm	6.04	1.85	0.59	0.19	0.18
0.59-0.84 mm	5.34	1.81	1.09	0.42	0.09
0.84-2.0 mm	16.51	23.14	20.53	16.29	0.92
>2.0 mm	0.79	1.15	8.63	12.45	25.86
Average bead size, mm	1.07	1.31	1.53	1.65	1.88
$\overline{Mc}$	11200	5700	2100	1500	36
Crosslinking density	12.1	24.0	63.6	88.9	3823.0
Swelling ratio in toluene (by					
volume)	8.5	7.0	6.3	5.9	2.7
(by weight)	5.8	4.7	4.8	4.9	5.1
Bead density, kg m^{-3}	1190	1110	874	790	317

Toluene was used a diluent. M_0 = 136300.

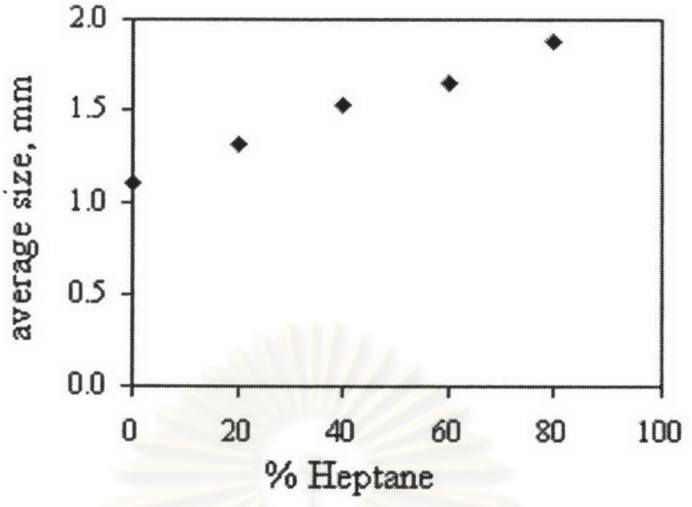

Figure 4.38 The average particle size in relation to the diluent composition.

Table 4.8 shows the overall conversion, the average particle size, particle size distribution, average molecular weight between crosslink ($\overline{M}_c$), crosslinking density, swelling ratio and bead density in the relation to the heptane composition as a poor solvent. It was found the overall conversion in any batch was higher than 94 %. It shows the diluent composition did not significantly affect the conversion. Figure 3.48 shows the increase in the average particle size when increased the heptane composition but the shape of the bead particles at the heptane content higher than 20 % weight was non spherical. The particle size polydispersity decreased when increased the diluent composition as shown in Figure 4.39. The higher concentration of poor solvent component increases the particle size and decreases the polydispersity of polymer particle size distribution because of the increasing phase separation in the system and coalescence rate in the second state. A diluent is considered a good solvent when $|\delta_1 - \delta_2|$ is smaller than 1.0 $(MPa)^{1/2}$ and poor solvent when $|\delta_1 - \delta_2|$ is larger than 3.0 $(MPa)^{1/2}$, where δ is the solubility parameter, 1 denotes the particular solvent used for the specified substrate or polymer 2. The solubility parameter of the MMA-DVB copolymer (δ_2) is 19.3 $(MPa)^{1/2}$, from the swelling method tested in the present work and 19.0 $(MPa)^{1/2}$ from calculation base on Small method [27], whereas that of toluene (δ_1) is 18.2 $(MPa)^{1/2}$ and heptane is 15.1 $(MPa)^{1/2}$. [27] The difference between the solubility parameters of MMA-DVB copolymer and toluene is 1.1 $(MPa)^{1/2}$. It

shows that the toluene solvent is not a good solvent for MMA-DVB copolymer. However, it is reported in Rabelo's work [6] that the borderline between solvating and nonsolvating diluents is not well defined. Thus, they have classified the diluents for which $|\delta_1 - \delta_2|$ is between 1.0 and 3.0 $(MPa)^{1/2}$ as intermediary solvents, taking also into account for their chemical structure. The solubility parameter theory has been developed for some mixtures of nonpolar substances. Some deviations in its predictions should be expected when the diluent and polymer are polar. The deviation was observed in this work and many other works [14, 15, 20] where toluene was use as a good solvent for the MMA-DVB copolymer. In general, if the diluent is a good solvent, expended network gels or small pores are generally produced; and if the diluent is a poor solvent, the miscibility does not occur spontaneously so that the diluent separates out the polymer phase producing larger pores.

Table 4.9 Solubility parameters of the diluents used with and without the polymerizing monomers

Tol/Hep	Solubility parameter, $(MPa)^{1/2}$	$\|\delta_1 - \delta_2\|$	Surface appearance of the copolymer beads
100/0	18.2 (18.1)	1.1 (1.2)	Expended gel
80/20	17.5 (17.7)	1.8 (1.6)	Heterogeous
60/40	16.8 (17.3)	2.5 (2.0)	Porous
40/60	16.2 (17.0)	3.1 (2.3)	Porous
20/80	15.6 (16.6)	3.7 (2.7)	porous

δ_{PMMA} = 19.0 $(MPa)^{1/2}$ [27], δ_{DVB} = 18.0 $(MPa)^{1/2}$ [19], $\delta_{PMMA/DVB}$ or δ_2 = 19.3 $(MPa)^{1/2}$ [from this work], δ_{MMA} = 19.0 $(MPa)^{1/2}$ [27], $\delta_{toluene}$ = 18.2 $(MPa)^{1/2}$ [27], δ_{hepane} = 15.3 $(MPa)^{1/2}$ [27] are calculated from the group molar attraction constant. [3] The numbers in parentheses are the solubility values with considering the presence of the polymerizing monomers.

From Table 4.9 (in the presence of monomers), the diluent phase is more compatible with its polymerizing beads, because the difference of the solubility

parameters of diluent and copolymer was smaller than that in the absence of monomers. Figure 4.40 and Table 4.8 show that the toluene absorbency by volume decreased when increased the heptane content but the crosslinking density increased when increased the heptane content.

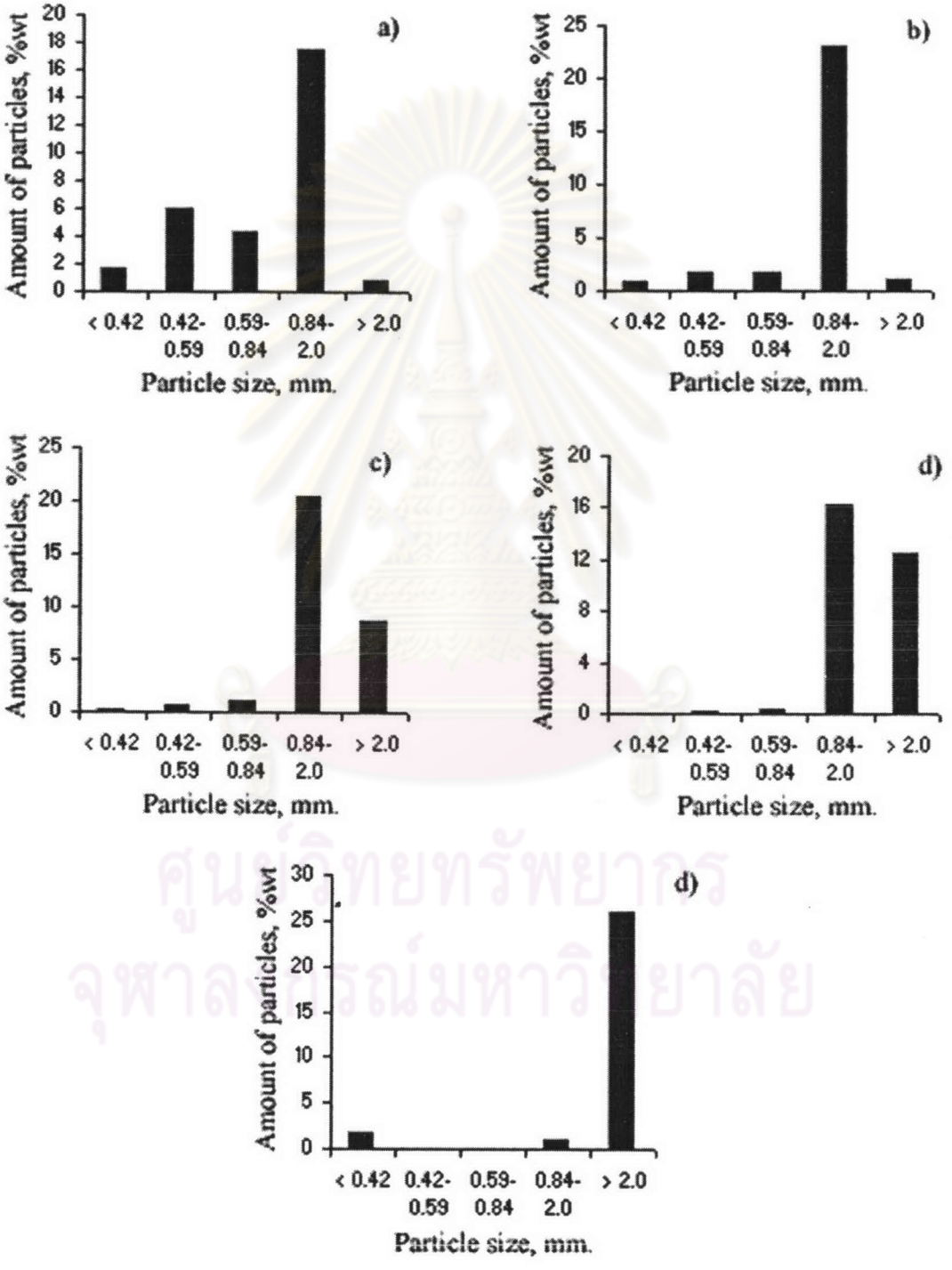

Figure 4.39 Effect of diluent composition on polymer particle size and distribution: a) 0% heptane, b) 20% heptane, c) 40% heptane, d) 60% heptane, and e) 80% heptane.

Each monomer droplet contains a monomer (MMA), a crosslinker (DVB), a mixed solvent (toluene/heptane) and an initiator (BPO). One can postulate that each droplet is composed of an isolated cell in which active polymer radicals are dissolved in the MMA-rich phase and surrounded by a relatively incompatible heptane as a continuous phase. Number of radicals in the droplet increases initially as the polymerization proceeds, the HP-rich phase gradually separated, and finally forming macrodomains. The phase separation allows polystyrene chains to dissolve in a more favorable MMA phase, and the homogeneous bulk copolymerization takes place, and results in a gradual decrease in the average number of radicals in the droplets until the viscosity increase to induce the formation of porous gel. [19] If a good solvent is used only in the system, the gel thus obtained will have a supercoiled (expanded) structure. The expanded gel thus formed collapses during the removal of the diluent after its synthesis and therefore, it is nonporous in the glassy state as shown in the H00(0% heptane) recipe. If a nonsolvent is used in the system, a phase separation may occur in the reaction system before the gel point. This results in the formation of a dispersion of separated (discontinuous) polymer phase in the continuous phase of monomer and diluent. Continuing the polymerization increases the amount of the polymer. As a result, the first phase separated and intramolecularly crosslinked particles (nuclei) agglomerate into larger clusters. Continuing the reaction increases the number of clusters in the reaction system so that the polymer phase becomes continuous, then resulting in a system consisting of two continuous phases. Removal of the diluent from the copolymer produces a macroporous copolymer [28] as illustrated in Figures 4.41-4.42. (20% heptane-80%heptane).

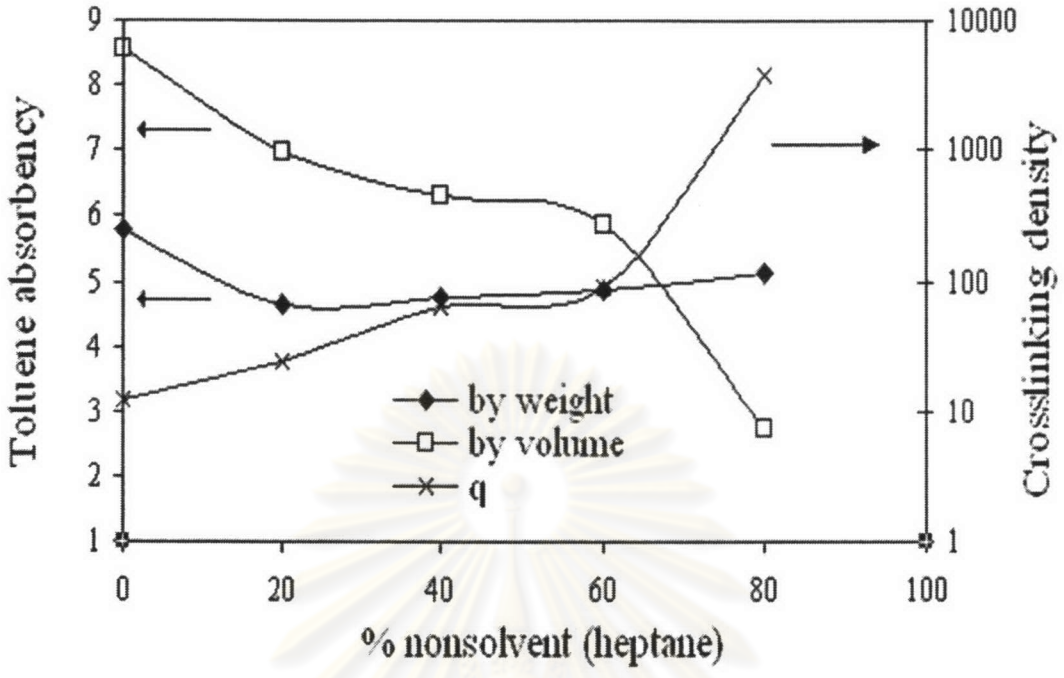

Figure 4.40 Effect of the diluent composition on toluene absorbency and crosslinking density.

Increase in the poor solvent content causes the increasing immiscibility of polymer and the polymer these formed is more porous. Figure 4.41 shows the scanning electron micrographs of the surface morphology of MMA-DVB copolymer beads from the experiments (H00-H80) at the magnification of 50 times.

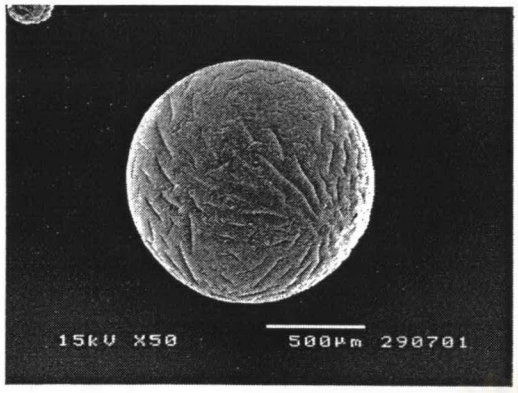

(a)

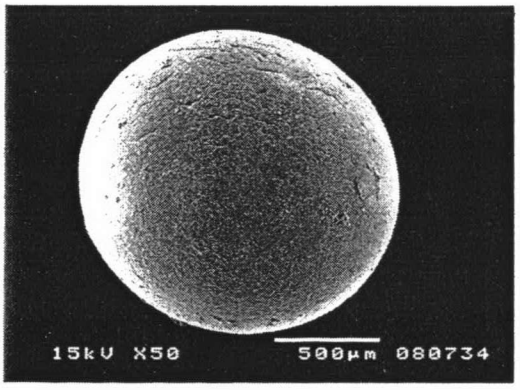

(b)

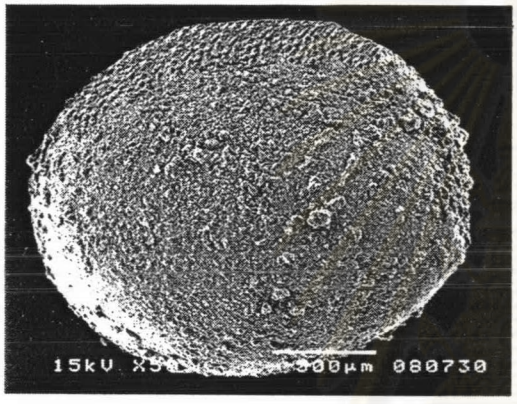

(c)

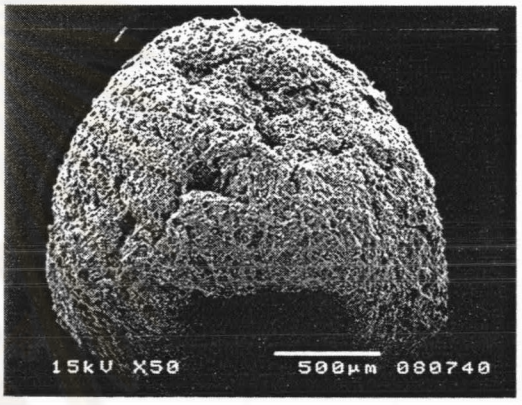

(d)

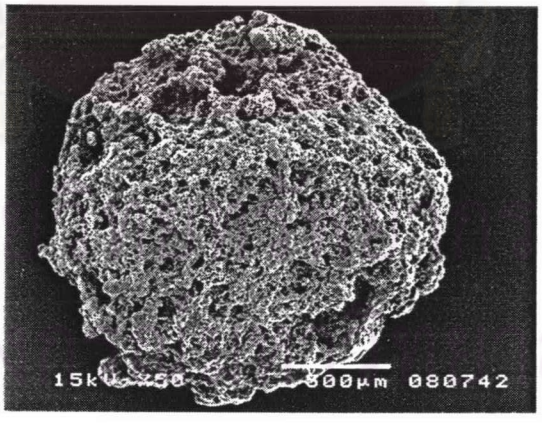

(e)

Figure 4.41 SEM photographs of the copolymers prepared at different toluene/heptane ratios: (a) H00, (b) H20, (c) H40, (d) H60, and (e) H80 (×50).

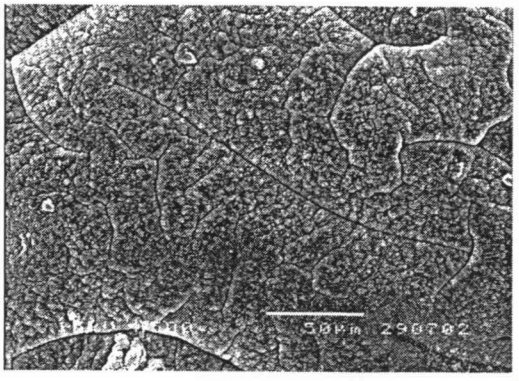

(a)

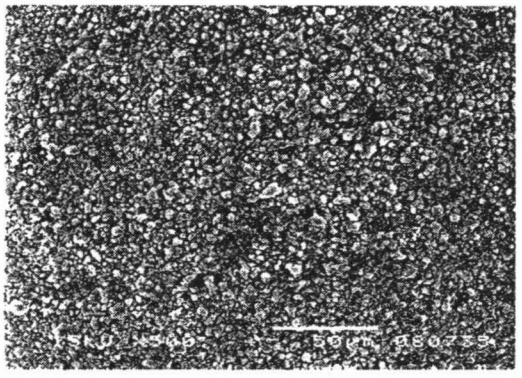

(b)

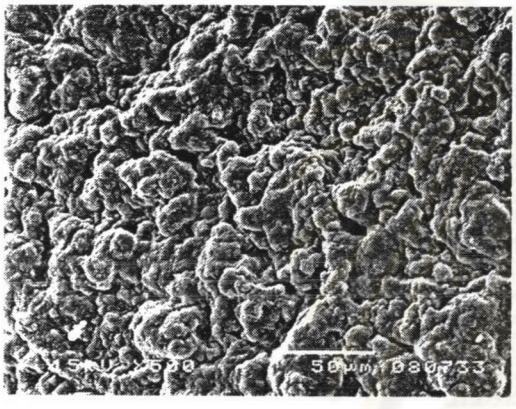

(c)

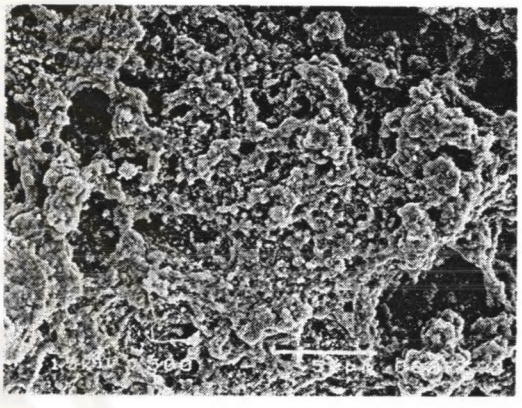

(d)

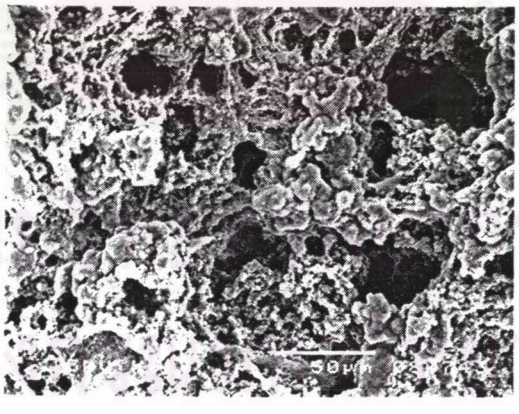

(e)

Figure 4.42 SEM photographs of the copolymers prepared at different toluene/heptane ratios: (a) H00, (b) H20, (c) H40, (d) H60, and (e) H80 (×500).

Figure 4.41 (a) shows the expanded gel with crack on the bead surface obtained when the good solvent (toluene) was used during the course of

polymerization. Figure 4.41 (b) shows the rough surface on the bead and Figures 4.41 (c)-(e) show the higher porous structure with increasing the poor solvent (heptane content). We can confirm the explanation by the scanning electron micrographs of the surface morphology of MMA-DVB copolymer beads from the experiments (H00-H80) at the magnification of 500 times as presented in Figure 4.42. The expanded gel shown in Figure 4.42 (a) was obtain by the low DVB content in toluene when compared with the heterogeous and porous structure shown in Figures 4.42 (b)-(e) for the high content of DVB in toluene. The high crosslinker content results in a permanent porous structure. More interesting thing obtained from this experiment is the toluene absorbency of copolymer beads by weight and volume is not in the same trend. The toluene absorbency by weight (except that of H00) was constant but the toluene absorbency by volume (except that of H00) decreased when the heptane content increased. The toluene absorbency by volume is the polymer fraction included into the swollen gel. It could be said that the toluene absorbency at high poor solvent concentration (heptane) or high crosslinking density from experiment H80 was attributed from the pores in the bead. The solvent uptake can take place in two ways: by filling the pores without affecting the gel regions (no volume change), and by chain displacement in the gel regions, causing bead expansion. The swelling of the heterogeous networks is governed by two separation processes. First, the solvation of network chains is mainly driven by changes in the free energies of mixing and elastic deformation during the expansion of network. The extent of network solvation is determined by the interactions between solvent molecules and network chains. Second, the filling of voids (pores) by the solvent is determined by the total volume of open pores, i.e., by the volume of diluent separated out of the network phase during the polymerization.

4.1.9 Diffusion mechanism of the spherical methyl methacrylate-divinylbenzene copolymer bead

The spherical methyl methacrylate-divinylbenzene copolymer beads were prepares in this experiment by varying the divinylbenzene content at 0.025, 0.5, 1, and 1.5 % weight based on the monomer phase. Therefore, the copolymer beads do not dissolve in the toluene solvent but swell depending on the degree of crosslinking

density. It is well known that the sorption of solvent in glassy polymers generally exhibits swelling behavior ranging from Fickian to Case II extremes, particularly when the experimental temperatures are near or below the glass transition temperature of the polymer. When the thermodynamic compatibility between the solvent and the polymer is favorable, the glass transition temperature is lower than the experimental temperature and the glassy polymer swells to a rubbery state accompanied by a substantial volume expansion. In most cases, a sharp penetrating solvent front separating the glassy phase from the rubbery phase is observed in addition to a volume swelling front at the polymer/solvent boundary. Depending on the relative magnitude of the rate of polymer relaxation in response to the penetrating solvent to the rate of solvent diffusion, the swelling process may be Fickian or non-Fickian. Typically, in a sample of polymer sheet or film, Fickian sorption dominates when the rate of polymer relaxation is fast compared to that of solvent diffusion. This is characterized by square-root time dependence in both the amount diffused and the penetrating front position. On the other hand, Case II transport occurs when the rate of polymer relaxation is slow and rate-limiting. In this case, linear time dependence is observed in both the amount diffused and the penetrating swelling front position. An intermediate situation, often termed non-Fickian or anomalous diffusion, exists whenever the rates of solvent diffusion and polymer relaxation are comparable. [29] Diffusion in polymers is complex and the diffusion rates should lie between liquids and in solids. It depends strongly on the concentration and degree of swelling of polymers.

In the study of solvent diffusion in polymers, different behaviors have been observed. It is known that the diffusion of the solvent is linked to the physical properties of the polymer network and the interaction between the polymer and the solvent itself. The classification according to the solvent diffusion rate and the polymer relaxation rate: Fickian (Case I) and non-Fickian (Case II and anomalous) diffusion. The amount of solvent absorbed per unit area of polymer at time t, M_t, is represented by

$$M_t = kt^n \tag{4.1}$$

where k is a constant and n is a parameter related to the diffusion mechanism, the value of which lies between 0.5 and 1. Equation 4.1 can be used to describe solvent

diffusion behaviors for any polymer-penetrant system whatever the temperature and the penetrant activity. The following equations are used to determine the nature of diffusion of the selected model solvents into P(MMA-DVB) copolymer spherical bead.

$$\frac{M_t}{M_\infty} = kt^n \tag{4.2}$$

where M_t is the amount of solvent diffused in to the spheres at time t and M_∞ is the amount of solvent at equilibrium; k is the constant incorporating characteristic of the macromolecular network system and penetrant; n is the diffusion exponent, which indicates the transport mechanism. This equation is valid for the first 60% of the fractional uptake and is determined by using the equation given below for the sphere.

$$\frac{M_t}{M_\infty} = \frac{\left(r_e^3 - r_i^3\right)}{r_{e,\infty}^3} = kt^n \tag{4.3}$$

where r_e is the external radius, r_i is the inner radius, and $r_{e,\infty}$ is the maximum radius reached at equilibrium. By plotting ln M_t/M_∞ versus ln t graphs, n exponent can be calculated from the slope of the line. The value of n varies with the shape of the material. Table 4.10 shows the relationship between n and the geometer of the system. [18]

Table 4.10 Diffusion exponent and diffusion mechanism [18]

Diffusion type	$n_{\text{thin film}}$	$n_{\text{cyclinder}}$	n_{sphere}
Fickian	0.5	0.45	0.43
Non-Fickian	$0.50 < n < 1.00$	$0.45 < n < 1.00$	$0.43 < n < 1.00$
Case II (Zero order)	1.00	1.00	1.00

The previously discussed model, although adequately describing a major portion of the swelling behavior, fails to give an accurate analysis above M_t/M_∞ =

0.60. To obtain a better model after 60%, we assumed that for long periods the penetrate sorption was mainly dominated by relaxation of the polymer network and that the sorption process of the polymer by relaxation was first-order. Then, the Berens-Hopfenberg differential equation for the relaxation process could be written as follows:

$$\frac{dM_t}{dt} = k_2\left(M_\infty - M_t\right) \tag{4.4}$$

where k_2 is the relaxation rate constant. The integration of Equation 4.4 leads to

$$M_t/M_\infty = 1 - A\exp\left(-k_2 t\right) \tag{4.5}$$

where A is a constant. In this study, the constants A and k_2 were calculated from the slopes and intercepts of the plot of $\ln(1-M_t/M_\infty)$ versus time t at times later than those corresponding to $M_t/M_\infty = 0.60$. [30]

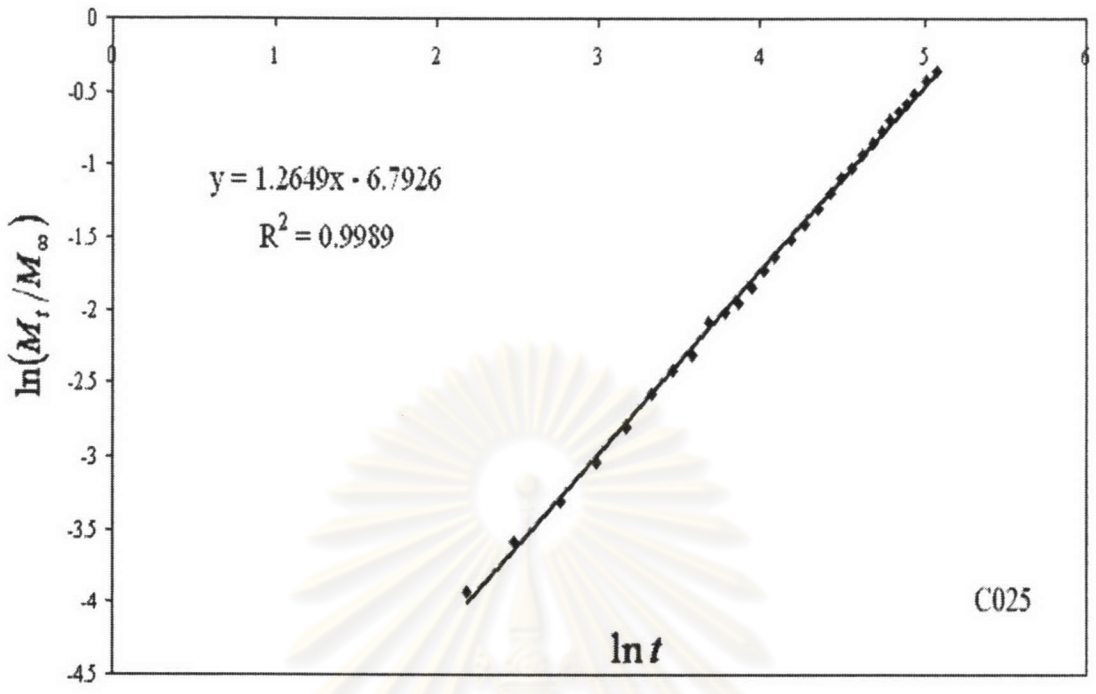

Figure 4.43 Determination of *n* and *k* in Equation 4.3. the graph between $\ln(M_t/M_\infty)$ *versus ln t* of poly(MMA-DVB) at 0.025 % DVB based on the monomer phase.

The *n* and *k* values are the diffusion exponent and the constant characteristic of the network gel, respectively. These values could be calculated from the plot of $\ln(M_t/M_\infty)$ versus *ln t* as shown in Figures 4.43 – 4.46. Table 4.11 shows the *n* and *k* values for all systems calculated from slope and intercept from $\ln(M_t/M_\infty)$ versus *ln t* graphs.

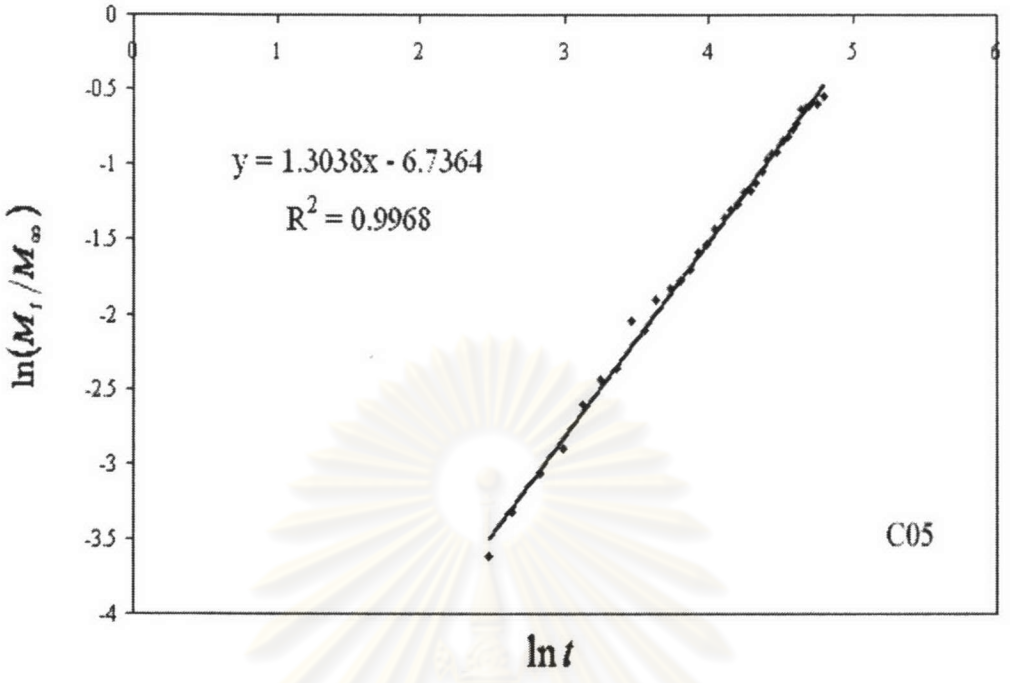

Figure 4.44 Determination of *n* and *k* in Equation 4.3. the graph between $\ln(M_t/M_\infty)$ *versus ln t* of poly(MMA-DVB) at 0.5 % DVB based on the monomer phase.

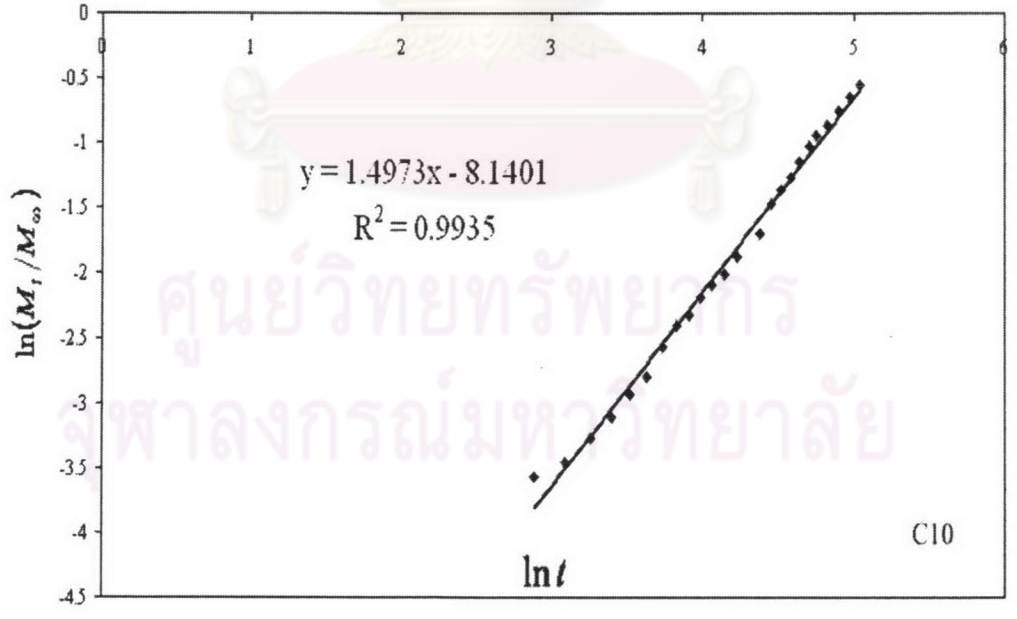

Figure 4.45 Determination of *n* and *k* in Equation 4.3. The graph between $\ln(M_t/M_\infty)$ *versus ln t* of poly(MMA-DVB) at 1.0 % DVB based on the monomer phase.

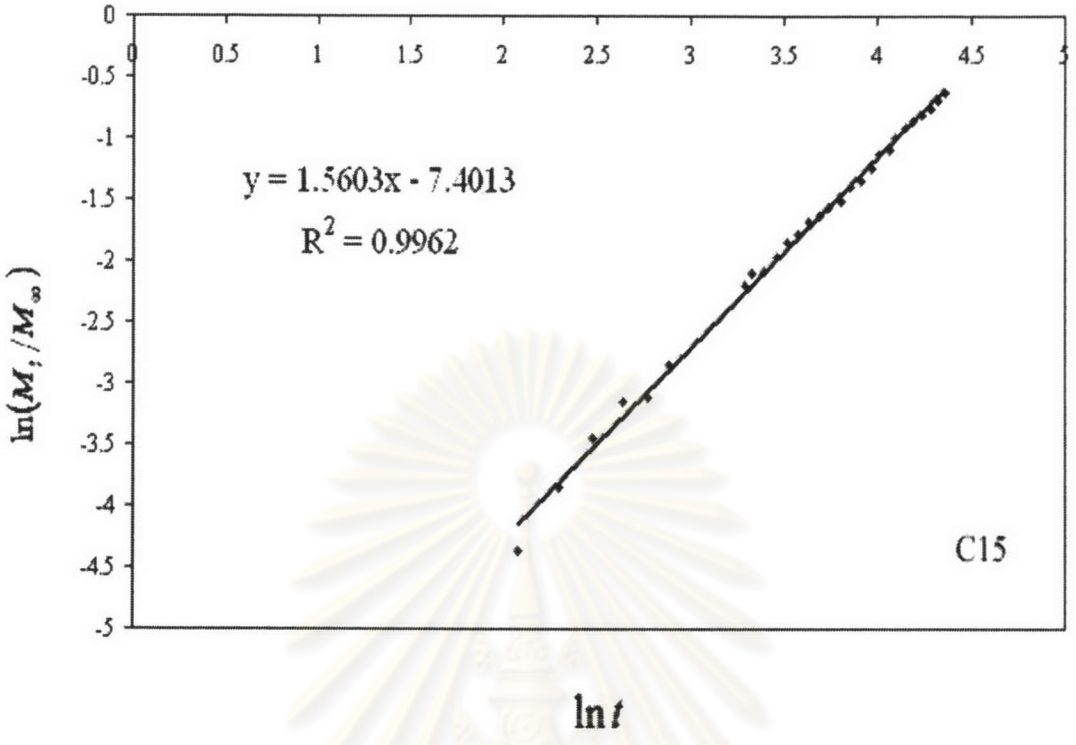

Figure 4.46 Determination of n and k in Equation 4.3. The graph between $\ln(M_t/M_\infty)$ *versus ln t* of poly(MMA-DVB) at 1.5 % DVB based on the monomer phase.

Table 4.11 Parameters n (diffusion exponent) and k (constant characteristic) for poly(MMA-DVB) with various concentrations of the divinylbenzene crosslinking agent.

Run	Diffusion exponent, n	k($\times 10^{-3}$)	R-squared
C025	1.26	1.12	0.9989
C05	1.30	1.19	0.9968
C10	1.50	0.29	0.9935
C15	1.56	0.61	0.9962

The k_2 and A values are the relaxation rate constant and the constant characteristic, respectively. These values could be calculated from the plot of $\ln\left(1-\left(r_e^3 - r_\infty^3/r_{e,\infty}^3\right)\right)$ versus time t as shown in the Figures 4.47 – 4.52. Table 4.12

shows the k_2 and A values for all systems calculated from the slope and the intercept from $\ln\left(1-\left(r_e^3-r_\infty^3/r_{e,\infty}^3\right)\right)$ versus time t graphs.

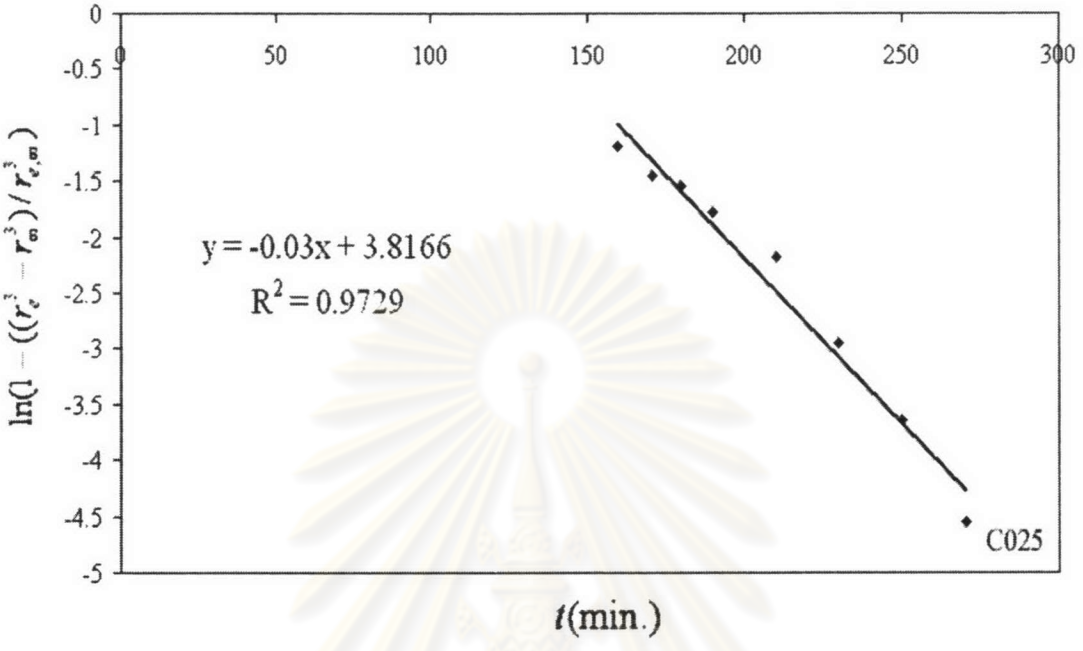

Figure 4.47 Determination of k_2 and A in Equation 4.5. The graph between $\ln\left(1-\left(r_e^3-r_\infty^3/r_{e,\infty}^3\right)\right)$ *versus* time t of poly(MMA-DVB) at 0.025 % DVB based on the monomer phase.

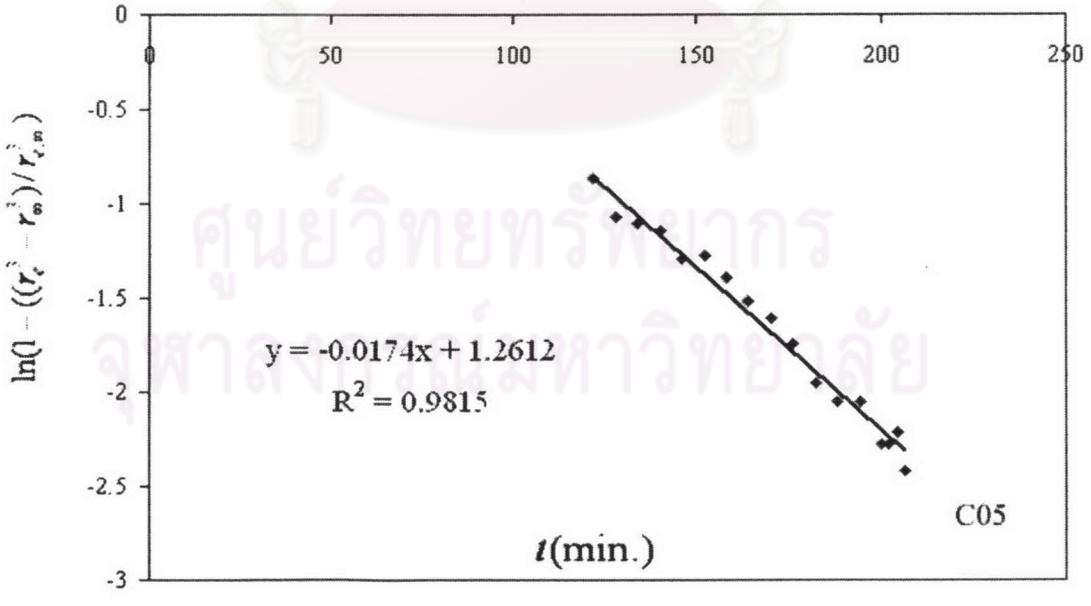

Figure 4.48 Determination of k_2 and A in Equation 4.5. The graph between $\ln\left(1-\left(r_e^3-r_\infty^3/r_{e,\infty}^3\right)\right)$ *versus* time t of poly(MMA-DVB) at 0.5 % DVB based on the monomer phase.

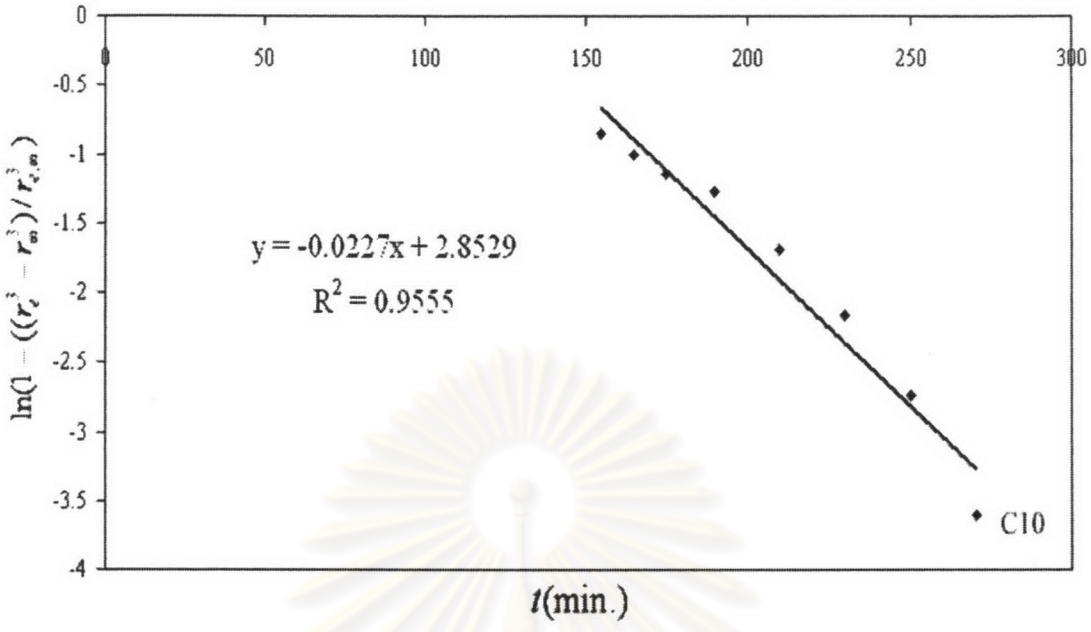

Figure 4.49 Determination of k_2 and A in Equation 4.5. The graph between $\ln\left(1-\left(r_e^3-r_\infty^3/r_{e,\infty}^3\right)\right)$ *versus* time t of poly(MMA-DVB) at 1.0 % DVB based on the monomer phase.

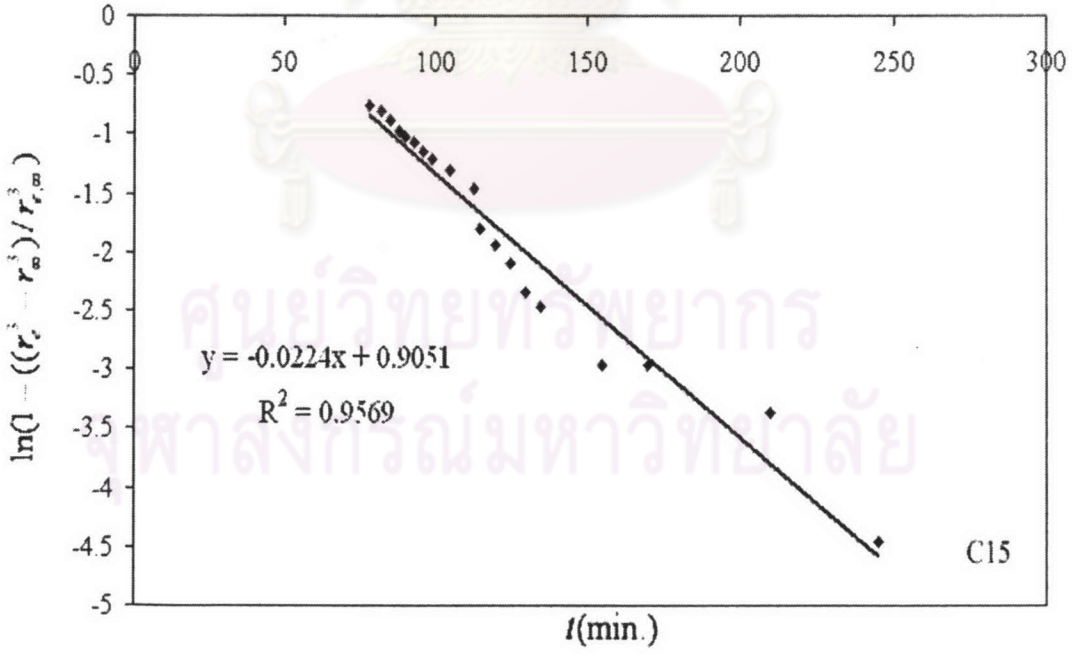

Figure 4.50 Determination of k_2 and A in Equation 4.5. The graph between $\ln\left(1-\left(r_e^3-r_\infty^3/r_{e,\infty}^3\right)\right)$ *versus* time t of poly(MMA-DVB) at 1.5 % DVB based on the monomer phase.

Table 4.12 Parameters k_2 (relaxation rate constant) and A (constant characteristic) for poly(MMA-DVB) with various concentrations of the DVB crosslinking agent.

Run	k_2 (relaxation rate constant)	A (constant characteristic)	R-square
C025	0.03	45.45	0.9729
C05	0.02	3.53	0.9815
C10	0.02	17.34	0.9555
C15	0.02	2.47	0.9569

Table 4.11 shows the value n for the systems containing different amounts of crosslinking agent. The values of n in all systems was close to 1, the variation of the value n in the present experiment could happen from many problems e.g. equipment, the complex processes, the same situation had been happened in many papers. [18, 30] Also, the values of n in all systems were around 1, which indicated that the transport mechanism was the case II type or a relaxation control. The diffusion of toluene solvent into methyl methacrylate-divinylbenzene copolymer spheres is the non-Fickian Case II type. The diffusion exponent was increased when increased the concentration of divinylbenzene crosslinking agent. Table 4.12 shows that the k_2 value (relaxation rate constant) was slightly decreased when increased the concentration of divinylbenzene crosslinking agent.

Non-Fickian diffusion processes are mainly observed in glassy polymer, i.e. when the temperature studied is below T_g. At a specific temperature below T_g, the polymer chains are not sufficiently mobile to permit immediate penetration of the solvent in the polymer core. As mention earlier that two kinds of non-Fickian diffusion were defined: Case II diffusion and anomalous diffusion. The main difference between these two diffusion categories concerns the solvent diffusion rate. In Case II diffusion, the solvent diffusion rate is faster than the polymer relaxation process ($R_{diff} >> R_{relax}$), whereas in anomalous diffusion the solvent diffusion rate and the polymer relaxation are of about the same order of magnitude ($R_{diff} \sim R_{relax}$). In general, Case II diffusion is observed when solvents have high activities. The characteristics of Case II diffusion are the following:

1. A rapid increase in the solvent concentration in the swollen region which leads to a sharp solvent penetration front between the swollen region and the inner polymer core.

2. The solvent concentration is quite constant in the swollen region behind the solvent penetration front.

3. The solvent penetration front is sharp and advances at a constant rate, thus the diffusion distance is directly proportional to time

$$M_t = kt \tag{4.6}$$

4. There is an induction time of Fickian concentration profile, which precedes the solvent penetration front into the glassy polymer core. [31]

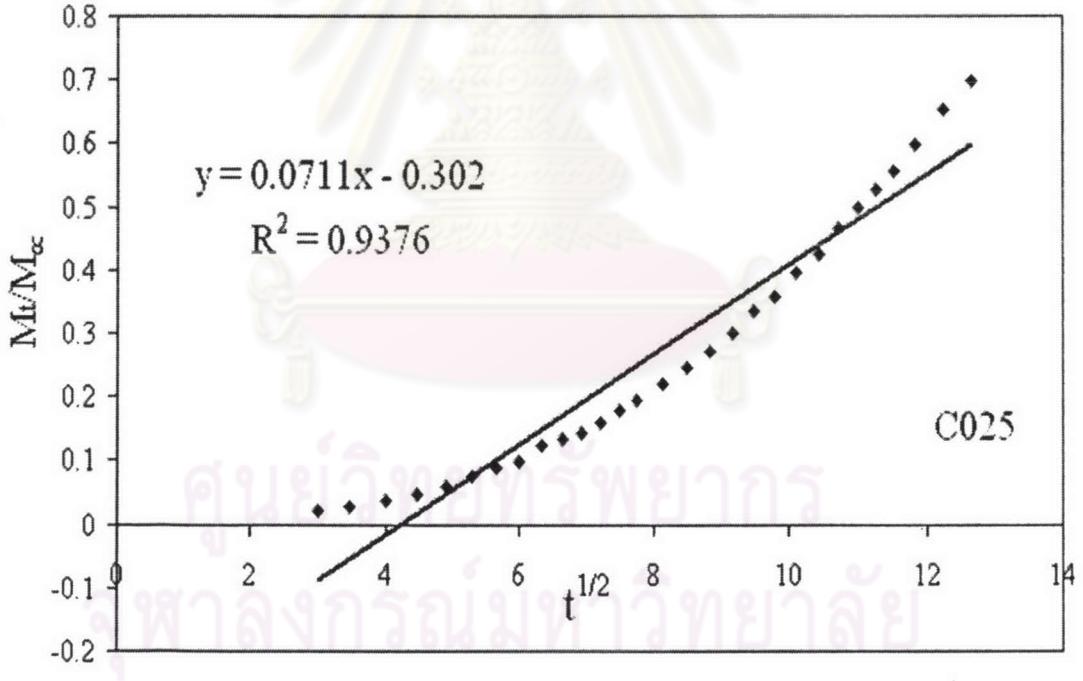

Figure 4.51 Determination of D, diffusion coefficient, in Equation 4.7. The graph between M_t/M_∞ *versus* $t^{1/2}$ of poly(MMA-DVB) at 0.025 % DVB based on the monomer phase.

The diffusion coefficient of the selected solvent for poly(MMA-DVB) spheres was calculated from the following equation by a short-time approximation

$$\frac{M_t}{M_\infty} = 6\left[\frac{Dt}{\pi a^2}\right]^{1/2} - 3\frac{Dt}{a^2} \tag{4.7}$$

where D is the diffusion coefficient, t is the time of diffusion, and a is the radius of the sphere. By ignoring the second term, M_t/M_∞ versus $t^{1/2}$ plot was constructed for the first 60 % of swelling and D values were calculated from the slope of the lines.

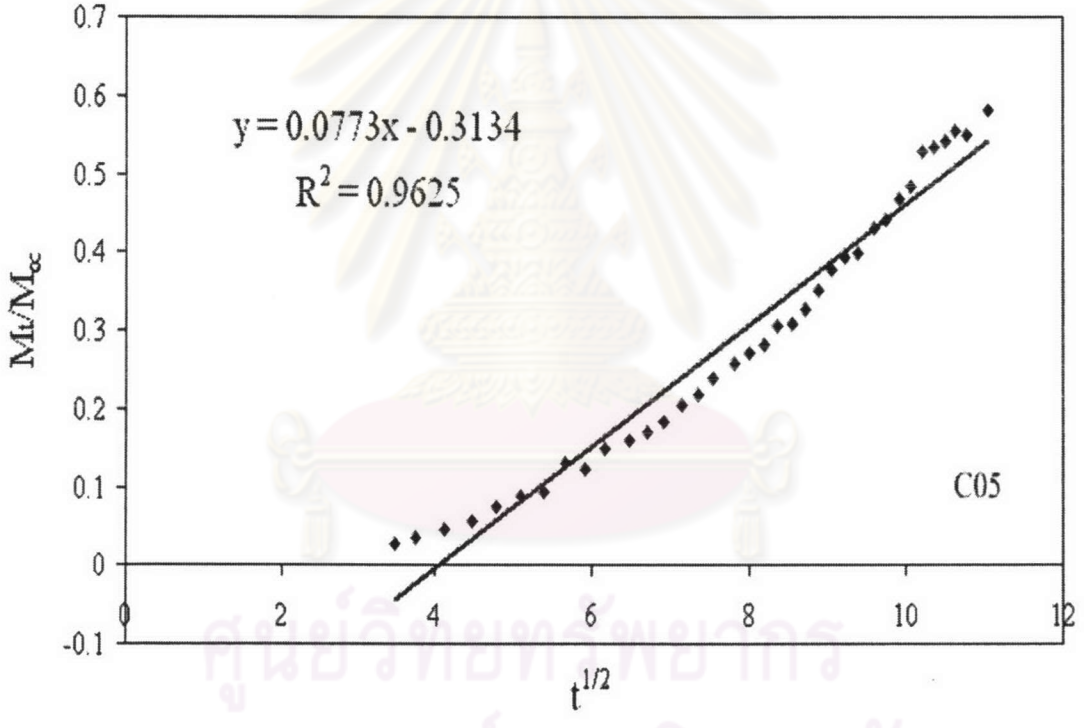

Figure 4.52 Determination of D, diffusion coefficient, in Equation 4.7. The graph between M_t/M_∞ *versus* $t^{1/2}$ of poly(MMA-DVB) at 0.5 % DVB based on the monomer phase.

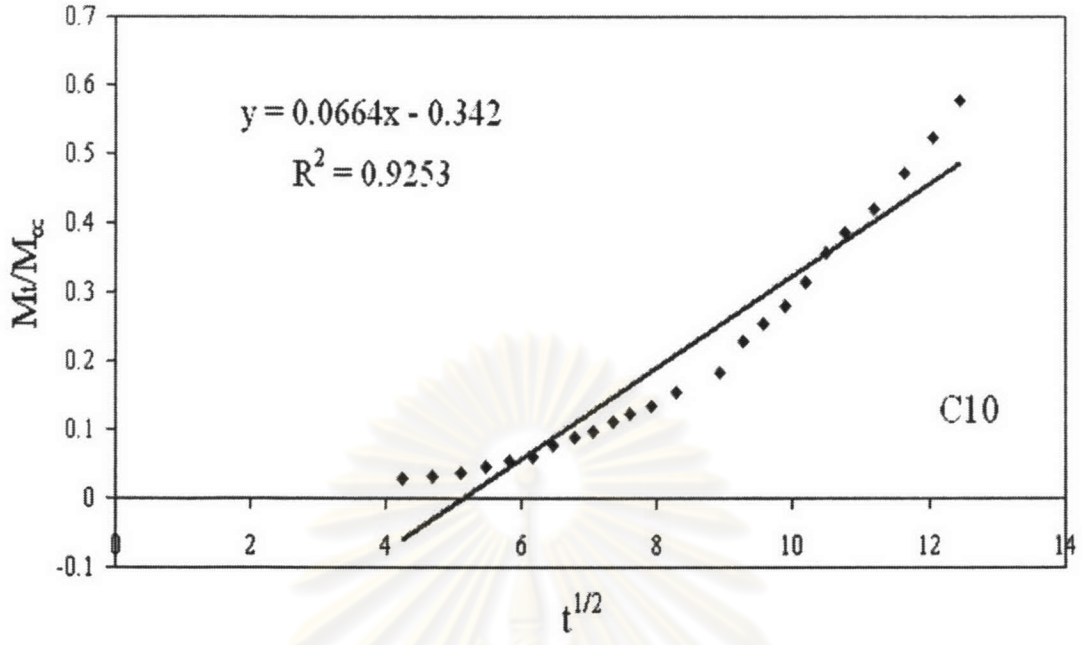

Figure 4.53 Determination of *D*, diffusion coefficient, in e Equation 4.7. The graph between M_t/M_∞ *versus* $t^{1/2}$ of poly(MMA-DVB) at 1.0 % DVB based on the monomer phase.

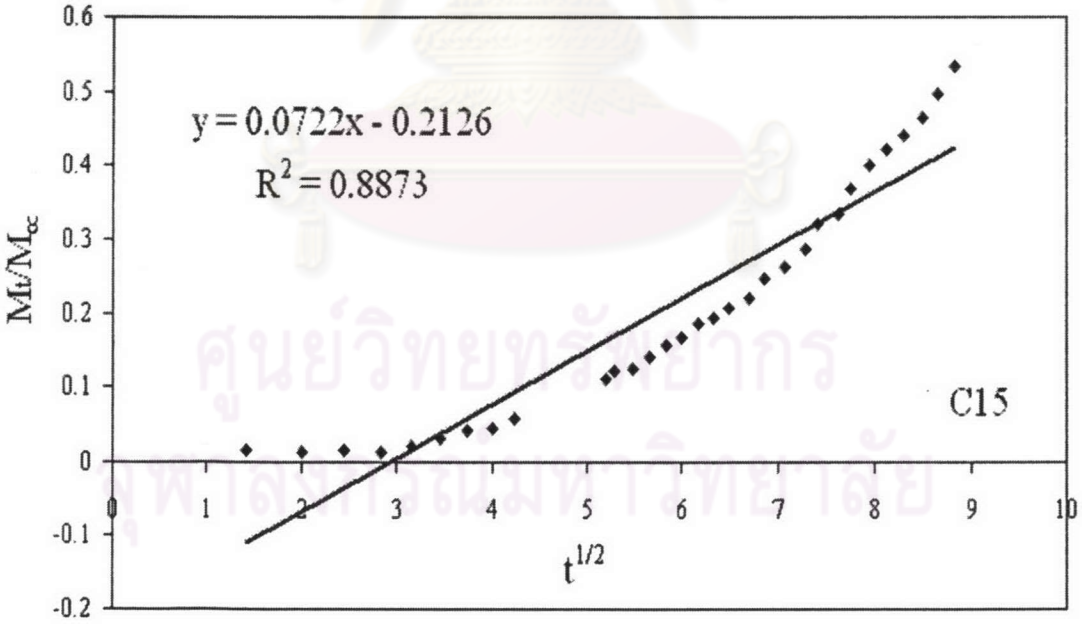

Figure 4.54 Determination of *D*, diffusion coefficient, in Equation 4.7. The graph between M_t/M_∞ *versus* $t^{1/2}$ of poly(MMA-DVB) at 1.5 % DVB based on the monomer phase.

Table 4.13 Variation of D (diffusion coefficient), R-squared, q (crosslinking density), k_2 (the relaxation rate constant), and swelling ratio by volume with the different amounts of crosslinking density by divinylbenzene crosslinker.

Run	D (diffusion coefficient), mm^2/min	R-squared	k_2 (relaxation rate constant)	q (crosslinking density)	swelling ratio by volume
C025	0.11	0.9625	0.03	1.06	20.5
C05	0.10	0.8873	0.02	7.33	15.1
C10	0.11	0.9376	0.02	12.12	8.5
C15	0.10	0.9253	0.02	17.88	7.4

The values of diffusion coefficients were calculated and are shown in Table 4.13 accompanied by R-squared values from Figures 4.51-4.54, q (crosslinking density), k_2 (relaxation rate constant), and swelling ratio by volume. It was found from this table that the diffusion coefficient is almost constant in all systems. It seems that the range of the concentration of crosslinking agent was used in this experiment dose not influence the diffusion coefficient.

4.2 Butyl methacrylate-divinylbenzene copolymer

The synthesis of butyl methacrylate-divinylbenzene copolymer was carried out by varying the polymerization parameters, of crosslinking agent concentration and diluent ratio. The effect of each parameter, which governs the properties of these copolymer beads was shown below.

4.2.1 Effect of crosslinking agent concentration

The effects of the crosslinking agent concentration on the conversion, average particle size, particle size distribution and swelling properties were investigated by varying the crosslinking agent concentrations of 0, 0.5, 1.0 and 2.0 wt % based on the monomer phase. The other parameters were kept constant as follow:

Monomer phase (0.14)	
- Butyl methacrylate-divinylbenzene ratio	95 wt %
- Initiator concentration	0.5 wt %
Aqueous phase (0.86)	
- Suspending agent concentration	0.2 wt %
- Reaction temperature	70°C
- Reaction time	20 hours
- Agitation rate	140 rpm
- Toluene: Heptane (100:0)	100 wt %

(The unit of any chemicals is weight % based on the monomer phase.) The resultant copolymer beads were confirmed by IR spectrum as shown in Figure 4.55.

The characterization of butyl methacrylate- divinylbenzene copolymer beads was performed with FTIR transmission spectroscopy. Figure 4.55 (a) shows the characteristic peaks of butyl methacrylate monomer at 2950, 1715, 1630, 1456, 1400, 1320, 1169, 1018, 939, 817 and 739 cm^{-1}. The peak at 2950 cm^{-1} is due to C-H stretching of aliphatic, the peak at 1715 cm^{-1} is due to C=O stretching conjugated C=C, the peak at 1630 cm^{-1} is for C=C stretching, the peak at 1456 and 1400 cm^{-1} are due to C-H deformation of CH_2 and CH_3, respectively. the peak at 1320 cm^{-1} for the CH_3 bending, the peak at 1169 cm^{-1} is due to the C-O stretching of ester functional group, the peak at 1018 and 939 cm^{-1} is due to the C-H out of plane deformation and 817 cm^{-1} is caused by the CH_2 rocking at $n = 1$, the peak at 739 cm^{-1} is resulted from the CH_2 rocking at $n \geq 4$. Figure 4.55 (b-e) shows the FTIR spectra of poly(butyl methacrylate-co-divinylbenzene) at various crosslinking agent concentrations of 0, 0.5, 1.0 and 2.0 respectively. The peak at 1630 cm^{-1} in Figure 4.49 (b-e) disappeared because the conversion of monomer to polymer from (a double bond to a single bond), which is a proof of polymerization.

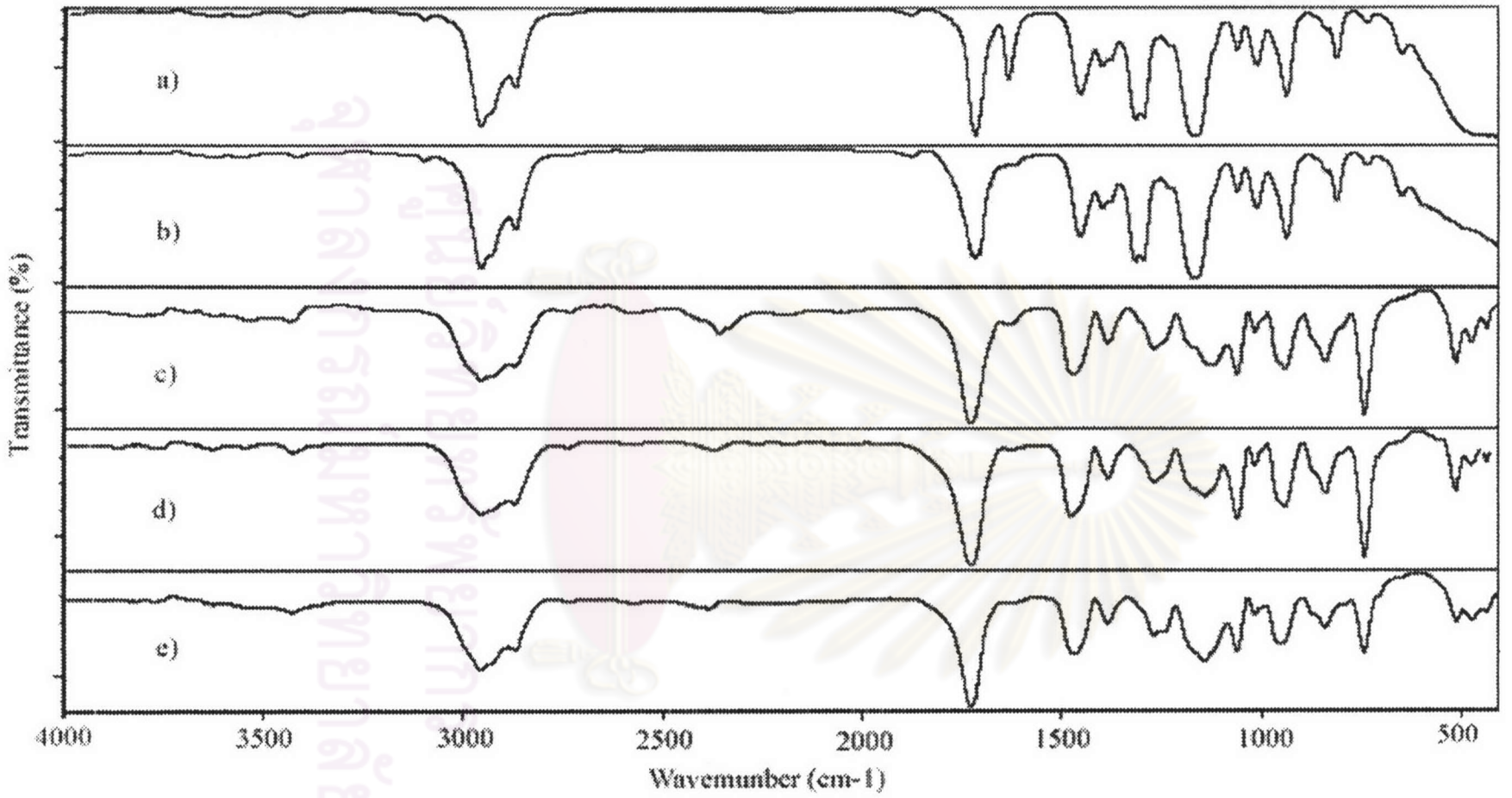

Figure 4.55 FTIR spectra of poly(butyl methacrylate-co-divinylbenzene) beads prepared by suspension copolymerization by various crosslinking agent concentrations: a) butyl methacrylate monomer, b) 0%, c) 0.5%, d) 1.0%, and e) 2.0% crosslinking agent based on the monomer phase.

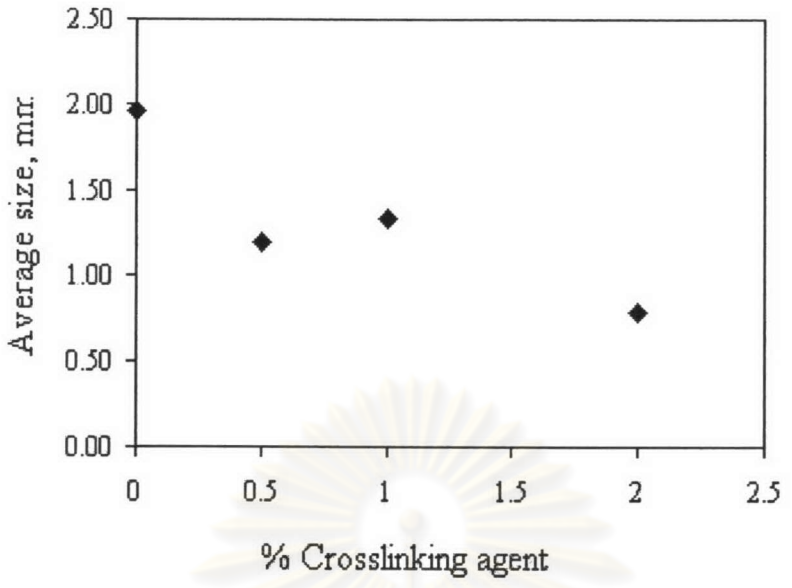

Figure 4.56 The average particle size in relation to the crosslinking agent concentration.

Table 4.14 shows the overall conversion, the average particle size, the particle size distribution, the average molecular weight between crosslink $(\overline{M}_c)$, the crosslinking density, the swelling ratio and bead density in relation to divinylbenzene crosslinking agent content. It shows that the overall conversion was 41 % in the absence of crosslinking agent. The overall conversion in the presence of the crosslinking agent as indicated in C05, C10, and C20 batches were all higher than 98 % conversion of monomer to polymer. Figure 4.56 presents the decreasing average particle size when increasing the concentration of crosslinking agent. The shape of the resultant bead copolymer was not spherical but it looked like a clump, whereas that in the C00 batch gave a spherical bead. Figure 4.57 shows that the particle size distribution was affected by the crosslinking agent concentration. When the crosslinking agent concentration was low, the particle size distribution was referred broad towards large particle size. On the other word, the particle size distribution in the C05 batch is of high polydispersity.

Table 4.14 Effect of the crosslinking agent concentration on bead properties

Parameter	Run			
	BMA C00	BMA C05	BMA C10	BMA C20
DVB concentration, wt %	0	0.5	1.0	2.0
% Yield	41	98	100	98
Bead size distribution, %wt				
<0.42 mm	0	3.17	0.40	5.23
0.42-0.59 mm	0	6.54	3.28	12.18
0.59-0.84 mm	0	2.85	4.31	3.31
0.84-2.0 mm	0.92	8.56	15.66	7.99
>2.0 mm	11.30	7.76	6.35	0.43
Average bead size, mm	1.96	1.19	1.33	0.79
$\overline{Mc}$	186100	3200	870	250
Crosslinking density	1	57	214	741
Swelling ratio in toluene				
(by volume)	soluble	14.8	9.5	6.3
(by weight)	soluble	12.7	7.9	5.1
Bead density, kg m^{-3}	1026	943	936	889

Toluene was used a diluent. M_0 = 186100.

Figure 4.57 shows the effect of crosslinking agent concentration on the toluene absorbency and crosslinking density. It was found that the toluene absorbency decreased with increasing the divinylbenzene content but the crosslinking density increased when increased the crosslinking concentration. The properties of butyl methacrylate- divinylbenzene copolymers are in the same trend with the properties of methyl methacrylate-divinylbenzene copolymers. Similar explanation for the resulting effects could be described as that for methyl methacrylate.

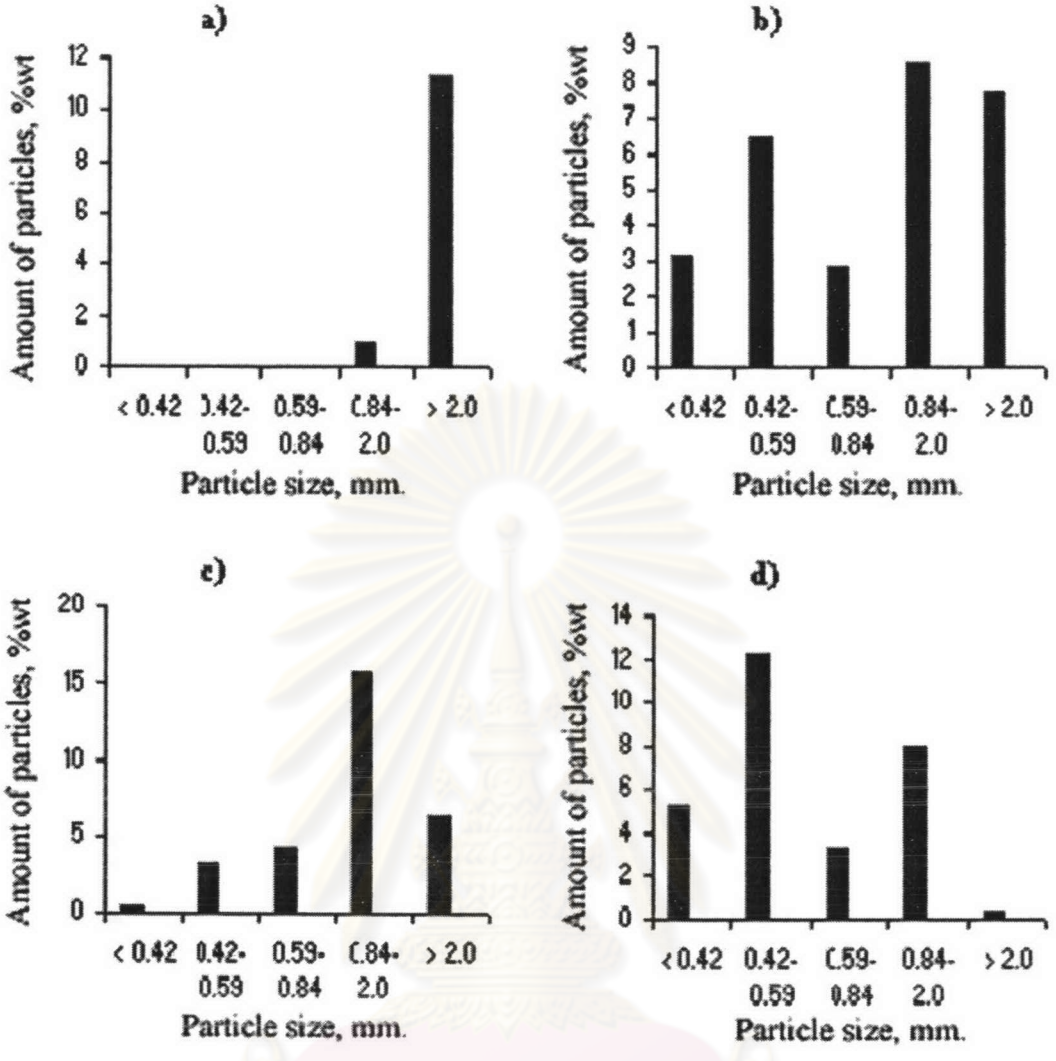

Figure 4.57 Effect of the crosslinking agent concentration of divinylbenzene on particle size distribution: a) 0%, b) 0.5%, c) 1.0, and d) 2.0% crosslinking agent based on the monomer phase.

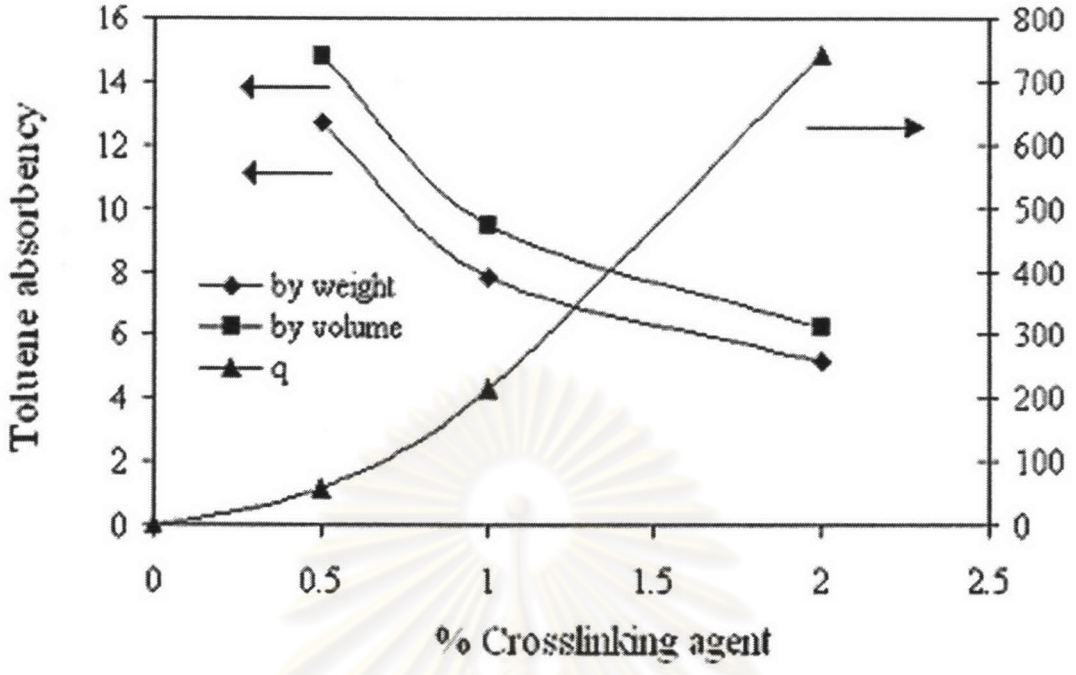

Figure 4.58 Effect of the concentration of crosslinking agent on toluene absorbency and crosslinking density.

4.2.2 Effect of diluent composition

The effects of the diluent composition on the conversion, the average particle size, the particle size distribution and swelling properties were investigated by varying the diluent compositions of 0, 20, 40, 60, and 80 wt % based on the monomer phase. The good and poor solvents are toluene and isoamyl alcohol, respectively. While the other parameters were kept constant as follows:

Monomer phase (0.14)	
- Butyl methacrylate-divinylbenzene ratio (94:6)	95 wt %
- Initiator concentration	0.5 wt %
- Crosslinking agent concentration	0.1 wt %
Aqueous phase (0.86)	
- Suspending agent concentration	0.2 wt %
- Reaction temperature	70 °C
- Reaction time	20 hours

- Agitation rate 140 rpm

(The unit of any chemical is used by weight % based on the monomer phase.) The resultant copolymer beads were confirmed by IR spectrum as shown in Figure 4.59.

The characterization of butyl methacrylate-divinylbenzene copolymer beads was performed with FTIR transmission spectroscopy. The peak interpretations are the same as in the effect of crosslinking agent concentration of butyl methacrylate-divinylbenzene copolymer as previous section. The peak at 1630 cm^{-1} was disappeared due to the conversion of monomer to polymer.

Table 4.15 shows the overall conversion, the average particle size, the particle size distribution, the average molecular weight between crosslink $(\overline{M}_c)$, the crosslinking density, the swelling ratio and density in the relation to the poor solvent of isoamyl alcohol composition. It was found the overall conversion in any batch was higher than 98 %. It also shows that the poor diluent composition dose not affect the conversion in this case. The average particle size increased with increasing the isoamyl alcohol content. The average particle size is higher than 2.0 mm in diameter.

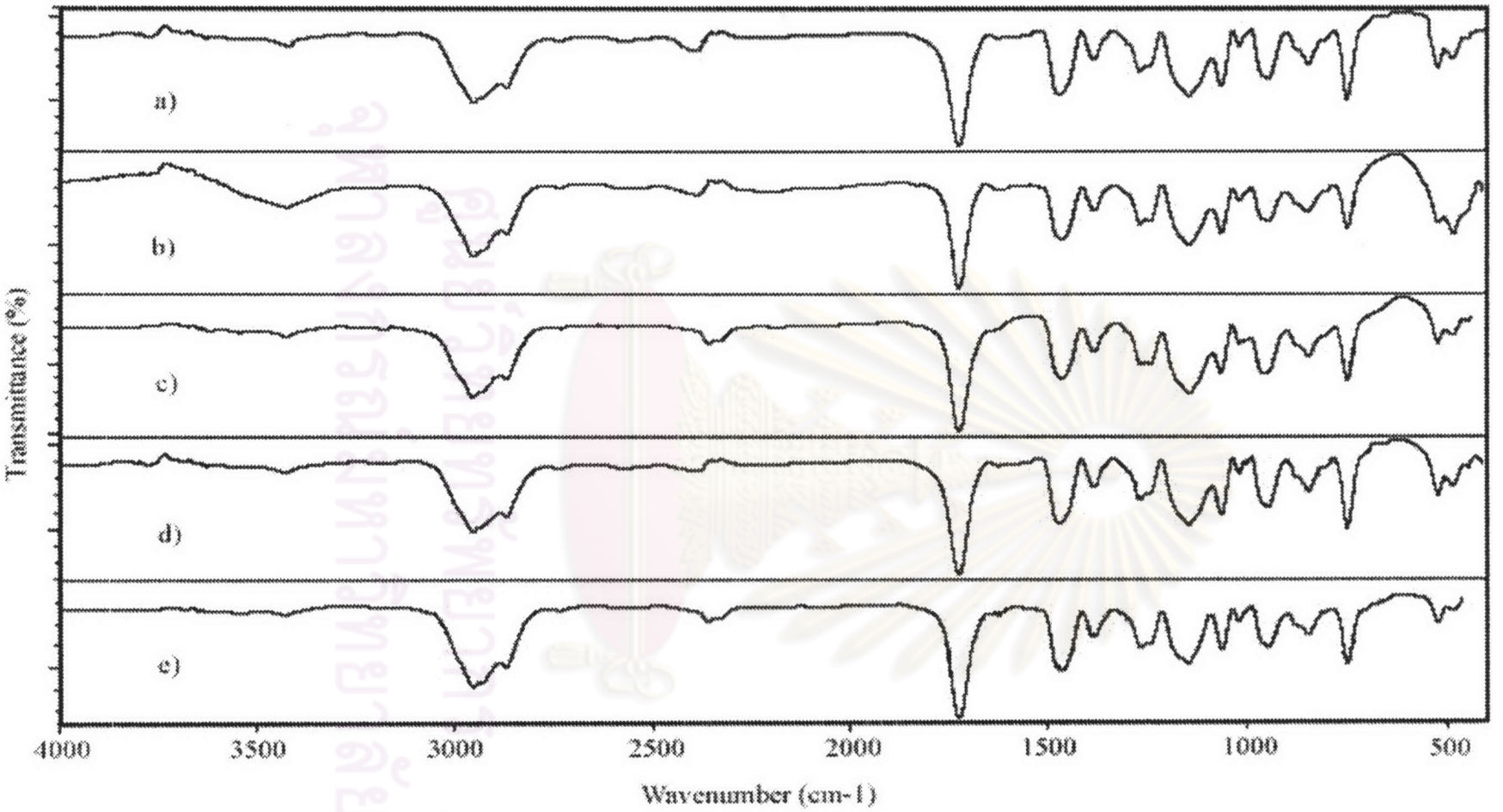

Figure 4.59 FTIR spectra of poly[(butyl methacrylate)-co-divinylbenzene] beads prepared by suspension copolymerization by various diluent composition: a) 0%, b) 20%, c) 40%, d) 60%, and e) 80% amyl alcohol based on the monomer phase.

It is well known that the diluent is a good solvent when $|\delta_1 - \delta_2| \leq 1$ $(MPa)^{1/2}$ and poor solvent when $|\delta_1 - \delta_2| \geq 3$ $(MPa)^{1/2}$, where δ is the solubility parameter, 1 denotes the particular solvent used for the specified substrate 2. The solubility parameter of BMA-DVB copolymer δ_2 is 17.7 $(MPa)^{1/2}$, from the swelling method tested in the present work, and 16.8 $(MPa)^{1/2}$ from the calculation in the present work, and 17.9 from literature, whereas those of δ_1 for toluene is 18.2 $(MPa)^{1/2}$ and for isoamyl alcohol is 20.5 $(MPa)^{1/2}$. The difference between the solubility parameter of MMA-DVB copolymer and toluene is 0.5 $(MPa)^{1/2}$. It shows that the toluene solvent is of course a good solvent for MMA-DVB copolymer. The difference between the solubility parameter of MMA-DVB copolymer and isoamyl alcohol is 2.8 $(MPa)^{1/2}$. It also shows that the isoamyl alcohol solvent is an intermediary poor solvent for MMA-DVB copolymer.

From Table 4.16 in the presence of monomers, the diluent phase is more compatible with its polymerizing beads, because the difference in the solubility parameter of the diluent and copolymer was smaller than that in the absence of monomers.

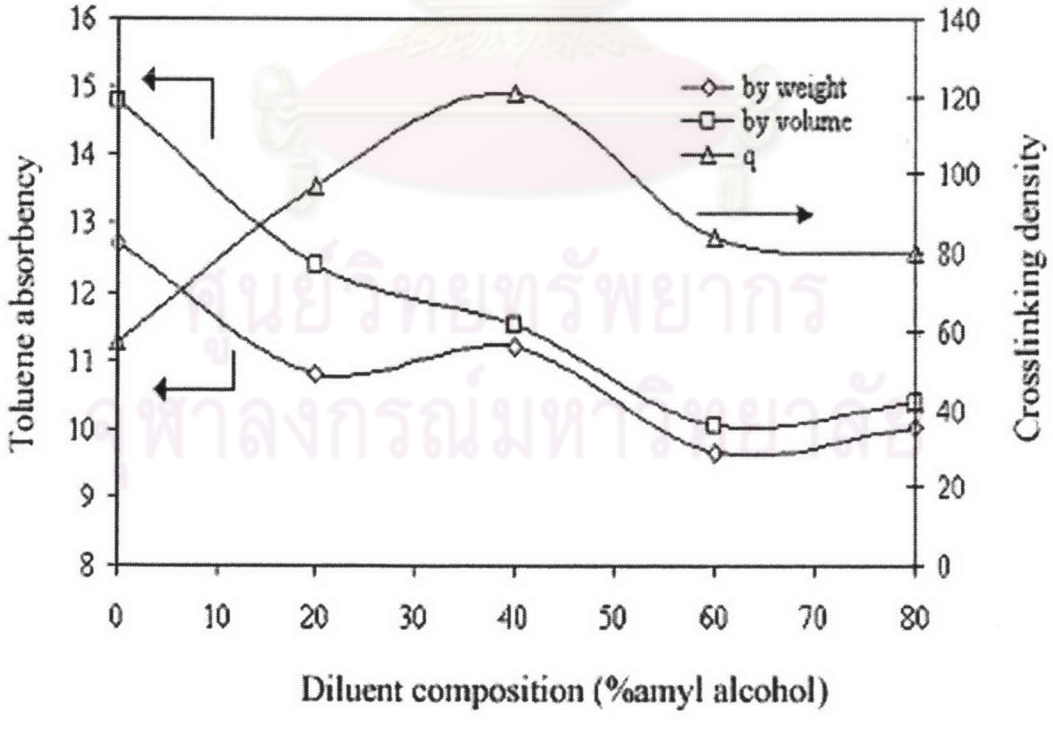

Figure 4.60 Effect of the diluent composition on toluene absorbency and crosslinking density.

Table 4.15 Effect of the diluent composition on bead properties

Parameter	Run				
	A00	A20	A40	A60	A80
Diluent composition (amyl alcohol)	0	20	40	60	80
% Yield	98	98	100	98	98
Bead size distribution, %wt					
<0.42 mm	3.17	-	-	-	-
0.42-0.59 mm	6.54	-	-	-	-
0.59-0.84 mm	2.85	-	-	-	-
0.84-2.0 mm	8.56	-	-	-	-
>2.0 mm	7.76	-	-	-	-
Average bead size, mm	1.19	>2.0	>2.0	>2.0	>2.0
$\overline{Mc}$	3200	1900	1500	2200	2300
Crosslinking density	57	97	121	84	80
Swelling ratio in toluene					
(by volume)	14.8	12.4	11.5	10.1	10.4
(by weight)	12.7	10.8	11.2	9.7	10.0
Bead density, kg m^{-3}	943	914	812	1082	1063

Toluene was used a diluent. M_0 = 186100.

Table 4.16 Solubility parameters of the diluents used with and without the polymerizing monomers.

Toluene/ Amyl alcohol	Solubility parameter, $(MPa)^{1/2}$	$\lvert \delta_1 - \delta_2 \rvert$	Surface appearance of the copolymer beads
100/0	18.2 (17.5)	0.5 (0.2)	Expanded gel
80/20	18.8 (17.8)	1.1 (0.1)	Expanded gel
60/40	19.3 (18.1)	1.6 (0.4)	Expanded gel
40/60	19.7 (18.4)	2.0 (0.7)	Expanded gel
20/80	20.1 (18.7)	2.4 (1.0)	Expanded gel

δ_{PBMA} = 17.9 $(MPa)^{1/2}$ [27], δ_{DVB} = 18.0 $(MPa)^{1/2}$ [19], $\delta_{PBMA/DVB}$ or δ_2 = 17.7 $(MPa)^{1/2}$ [from this work], δ_{BMA} = 16.8 $(MPa)^{1/2}$ [27], $\delta_{toluene}$ = 18.2 $(MPa)^{1/2}$ [27], $\delta_{isoamyl\ alcohol}$ = 20.5 $(MPa)^{1/2}$ [27] are calculated from the group molar attraction constant. [3] The numbers in parentheses are the solubility values with considering the presence of the polymerizing monomers.

The mechanism of porous bead formation is the same as in the previous section. Figure 4.60 and Table 4.15 show the decreasing toluene absorbency by volume when increasing the isoamyl alcohol content, but the toluene absorbency by weight was decreased until 20 % isoamyl alcohol content was reached and started to increase again until the isoamyl alcohol ratio was 40 % content. It was decreased afterwards when increasing the isoamyl alcohol. It shows that the beads from the experiment A00 can uptake solvents by chain displacement in the gel regions, causing the bead expansion. The beads from the experiment A20 can uptake solvents in two ways by chain displacement in the gel regions and filling the pores. The beads from the experiments A40-A80 could uptake the solvent by filling the pores. The crosslinking density increased to maximum at the isoamyl alcohol content of 40 % after which it decreased steadily. Because of the suitable condition, was divinylbenzene can dissolve best in the monomer phase system at 40% of the nonsolvent content. It is noted that the solubility parameter values in Table 4.16 and the solubility of divinylbenzene in butyl methacrylate are smaller than that of methyl

methacrylate, and the solubility of divinylbenzene in isoamyl alcohol is higher than heptane.

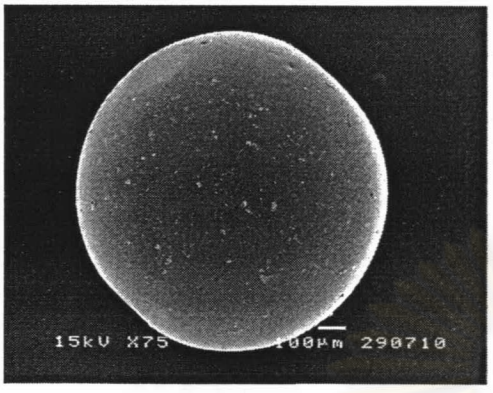

(a)

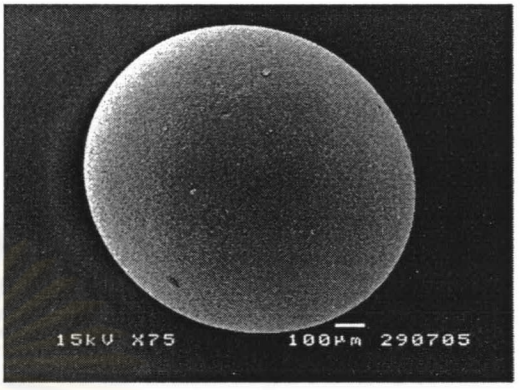

(b)

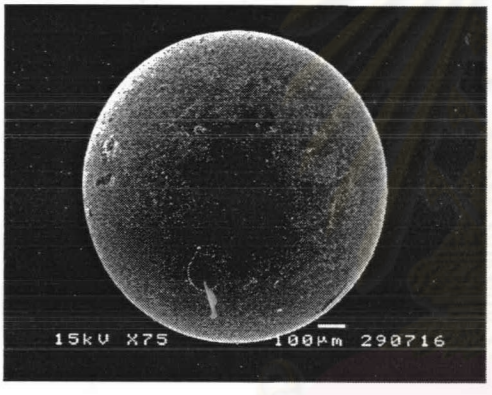

(c)

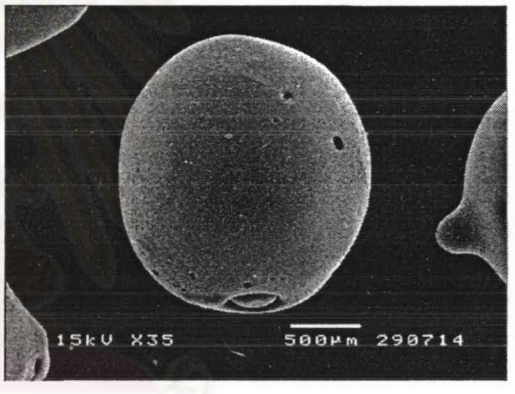

(d)

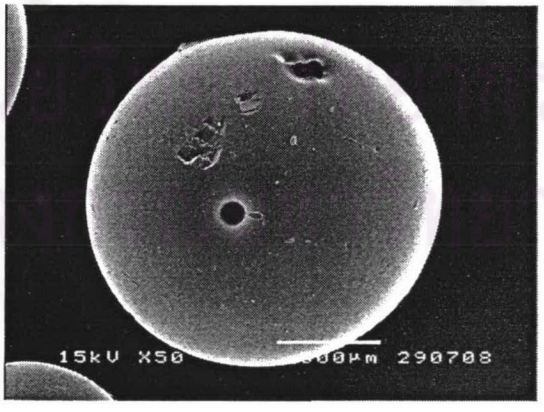

(e)

Figure 4.61 SEM photographs of the copolymers prepared at different toluene/isoamyl alcohol ratios: (a) A00 (×75), (b) A20 (×75), (c) A40 (×75), (d) A60 (×35), and (e) A80 (×50).

From Table 4.16, the difference of solubility parameter between the monomer phase and poly[(butyl methacrylate)-co-divinylbenzene] in all condition is not higher than 1, but the difference in the solubility parameter between the monomer phase and poly[(methyl methacrylate)-co-divinylbenzene] in all condition is higher than 1. It shows the permanent macroporous beads in the system of poly[(methyl methacrylate)-co-divinylbenzene] and microporous beads in the system of poly[(butyl methacrylate)-co-divinylbenzene].

Figure 4.61 shows the scanning electron micrographs of the surface morphology of BMA-DVB copolymer beads from the experiment (A00-A80) at the magnification range of 35-75 times. Figure 4.61 (a) shows the expanded gel and smooth surface when the good solvent (toluene) is used during the course of polymerization. From Figures 4.61 (b)-(e), when the diluent is a poor solvent for the polymer chains, a partial phase separation may eventually occur. As the polymerization progresses, the polymer chains are no longer extended, as in a good solvating system, and there is a tendency of the growing chains to become entangled inside the nuclei. Consequently, the nuclei of the final structure are large and connected by a relatively small number of coiled and crumpled internuclear chains. When the nonsolventing diluent is removed, the collapse of the system of interconnected nuclei can also occur. When mixtures of solvating and nonsolvating diluents are used, the copolymers produce porous structures with intermediary characteristics. The effects of synthetic conditions on the swelling properties are considerably more complex for copolymers obtained with diluent mixtures. [17]

In Figures 4.61 (d) and (e), we observed the large pores on the surface when the nonsolvent content was higher due to homopolymer of divinylbenzene. The decreasing crosslinking density was also evidenced. The reactivity ratios for MMA/DVB system are r_{12} and r_{21} for MMA (M_1) and p-DVB (M_2) are 0.62 and 1.3, respectively. Figure 4.62 shows the scanning electron micrographs of the surface morphology of the BMA-DVB copolymer beads from the experiment A00-A80 at the magnification of 500 times. Figure 4.63 shows the scanning electron micrographs of the crossection surface morphology of BMA-DVB copolymer beads from the experiment A00-A80 at the magnification of 5000 times. The pores so produced by the solvents are intermediary pores.

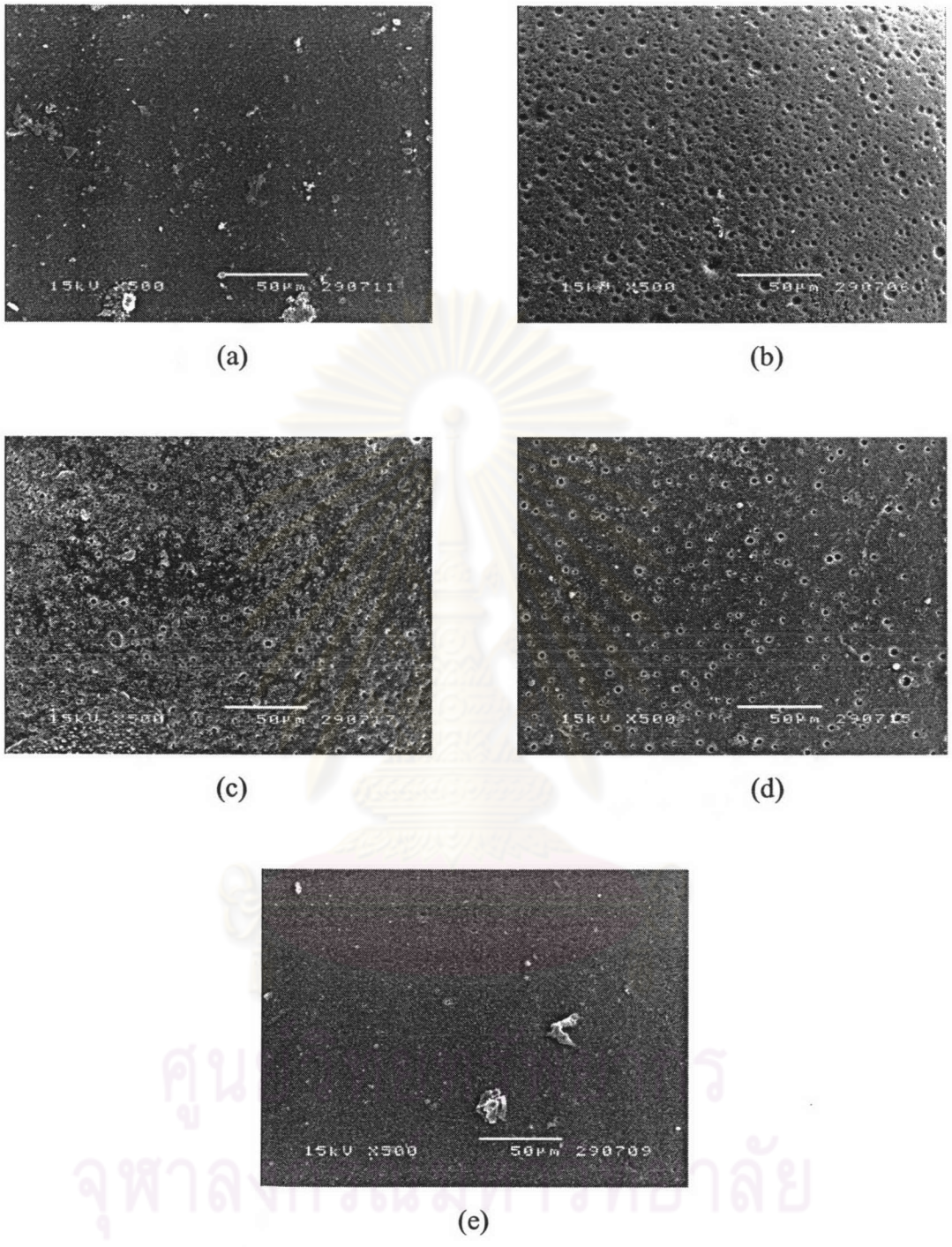

Figure 4.62 SEM photographs of the surface copolymers prepared at different toluene/isoamyl alcohol ratios: (a) A00, (b) A20, (c) A40, (d) A60, and (e) A80 (×500).

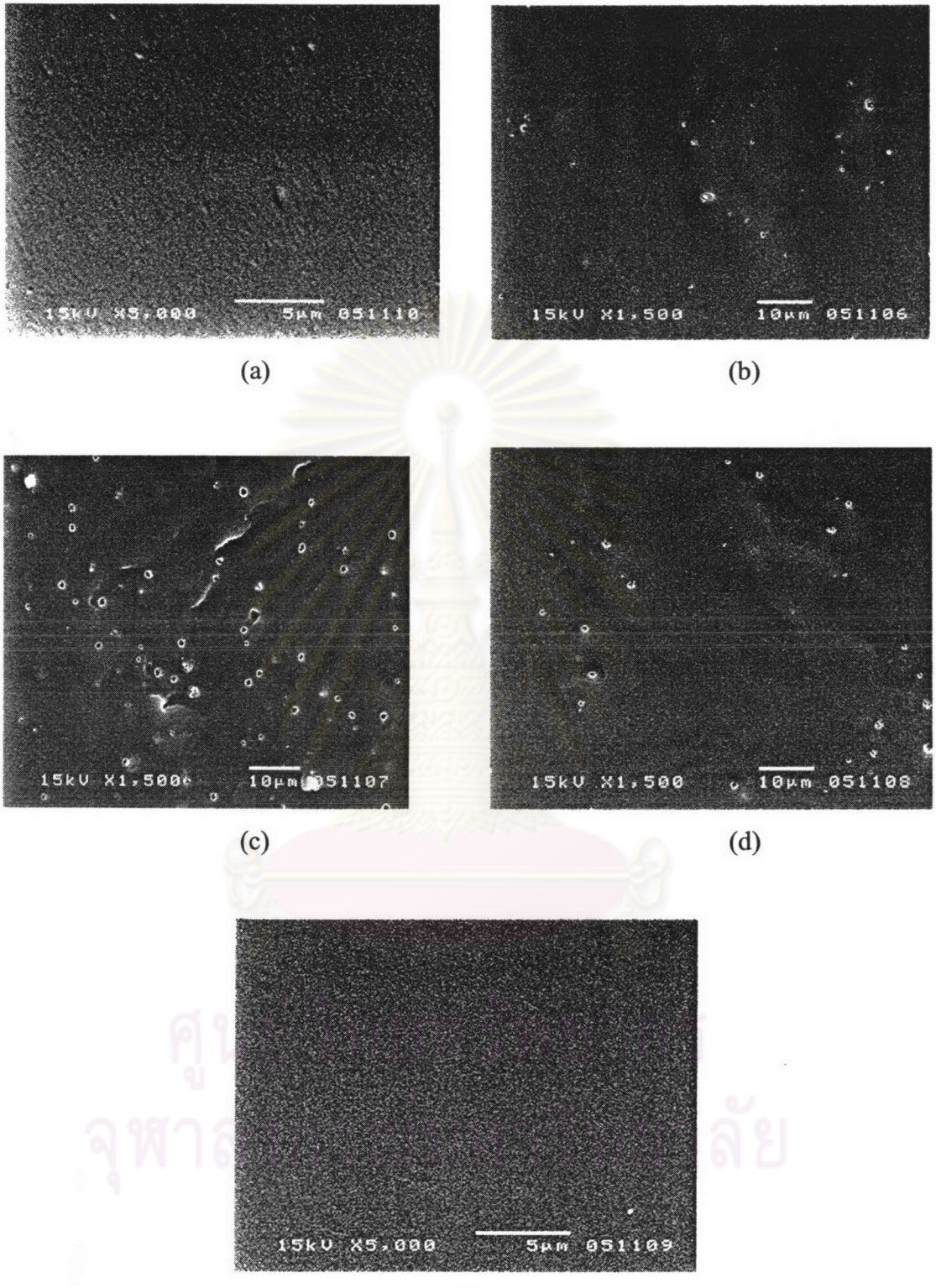

Figure 4.63 SEM photographs of the crossection surface copolymers prepared at different toluene/isoamyl alcohol ratios: (a) A00 (×5000), (b) A20 (×1500), (c) A40 (×1500), (d) A60 (×1500), and (e) A80 (×5000).

4.3 Effects of crosslinking agent concentration on lauryl methacrylate-divinylbenzene, stearyl acrylate-divinylbenzene, dodecyl acrylate-divinylbenzene copolymer beads

The effects of the crosslinking agent concentration on the conversion, average particle size, particle size distribution and swelling properties were investigated by varying the crosslinking agent concentration. Alkyl or (Meth)acrylates are lauryl methacrylate, stearyl acrylate, and dodecyl acrylate, while other parameters were kept constant as follows:

Monomer phase (0.14)	
- Alkyl (Meth)acrylate-divinylbenzene ratio	95 wt %
- Initiator concentration	0.5 wt %
Aqueous phase (0.86)	
- Suspending agent concentration	0.2 wt %
- Reaction temperature	70 °C
- Reaction time	20 hours
- Agitation rate	140 rpm
- Toluene: Heptane (100:0)	100 wt %

(The unit of any chemical is % weight based on the monomer phase.) The resultant lauryl methacrylate-divinylbenzene, stearyl acrylate-divinylbenzene, and dodecyl acrylate-divinylbenzene copolymer beads were confirmed by IR spectrum as shown in Figures 4.64, 4.65, and 4.66, respectively.

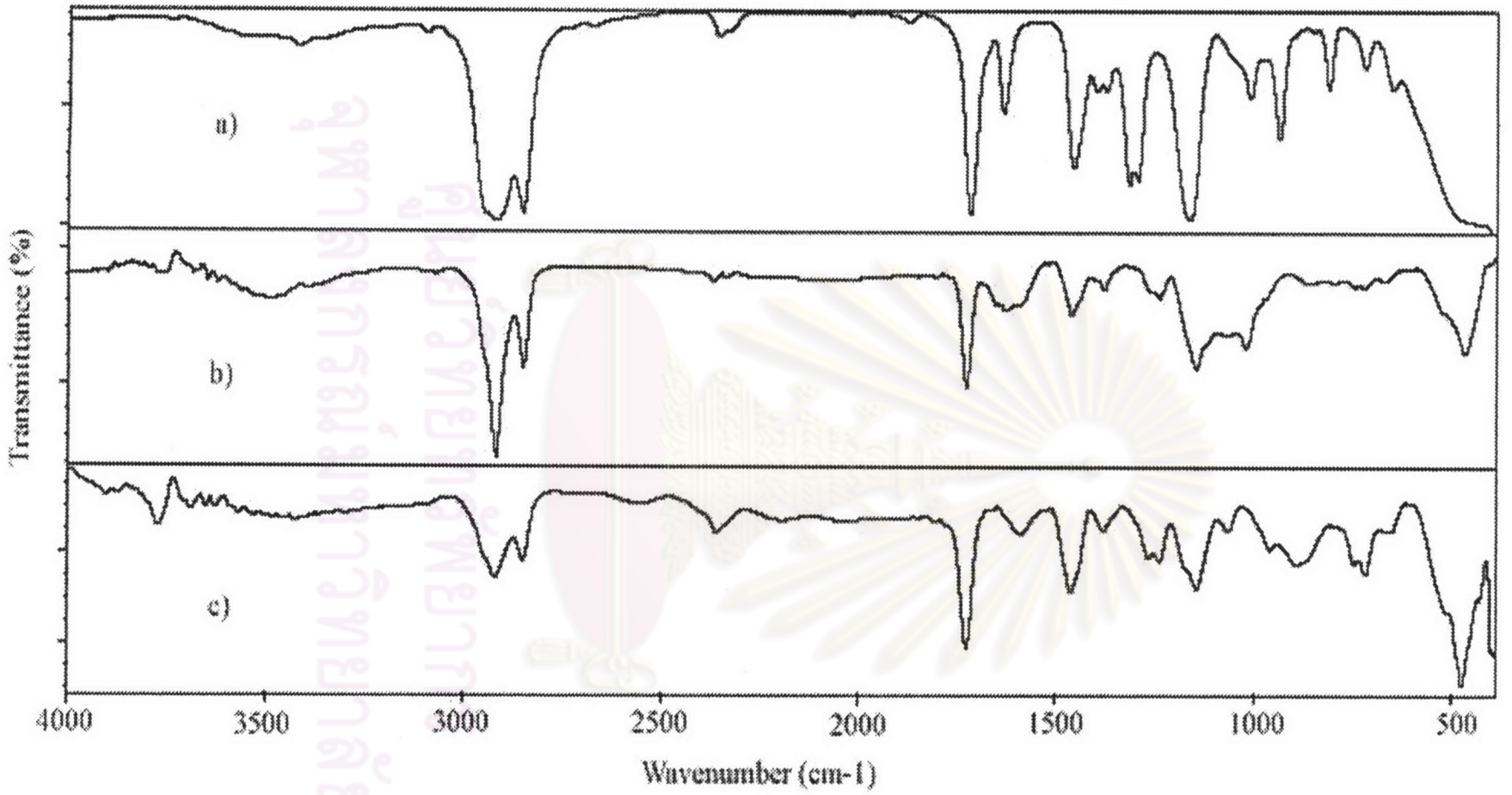

Figure 4.64 FTIR specta of poly[(lauryl methacrylate)-co-divinylbenzene] beads prepared by suspension copolymerization at various crosslinking agent concentrations: a) lauryl methacrylate monomer, b) 0.1%, and c) 0.3% crosslinking agent concentration based on the monomer phase.

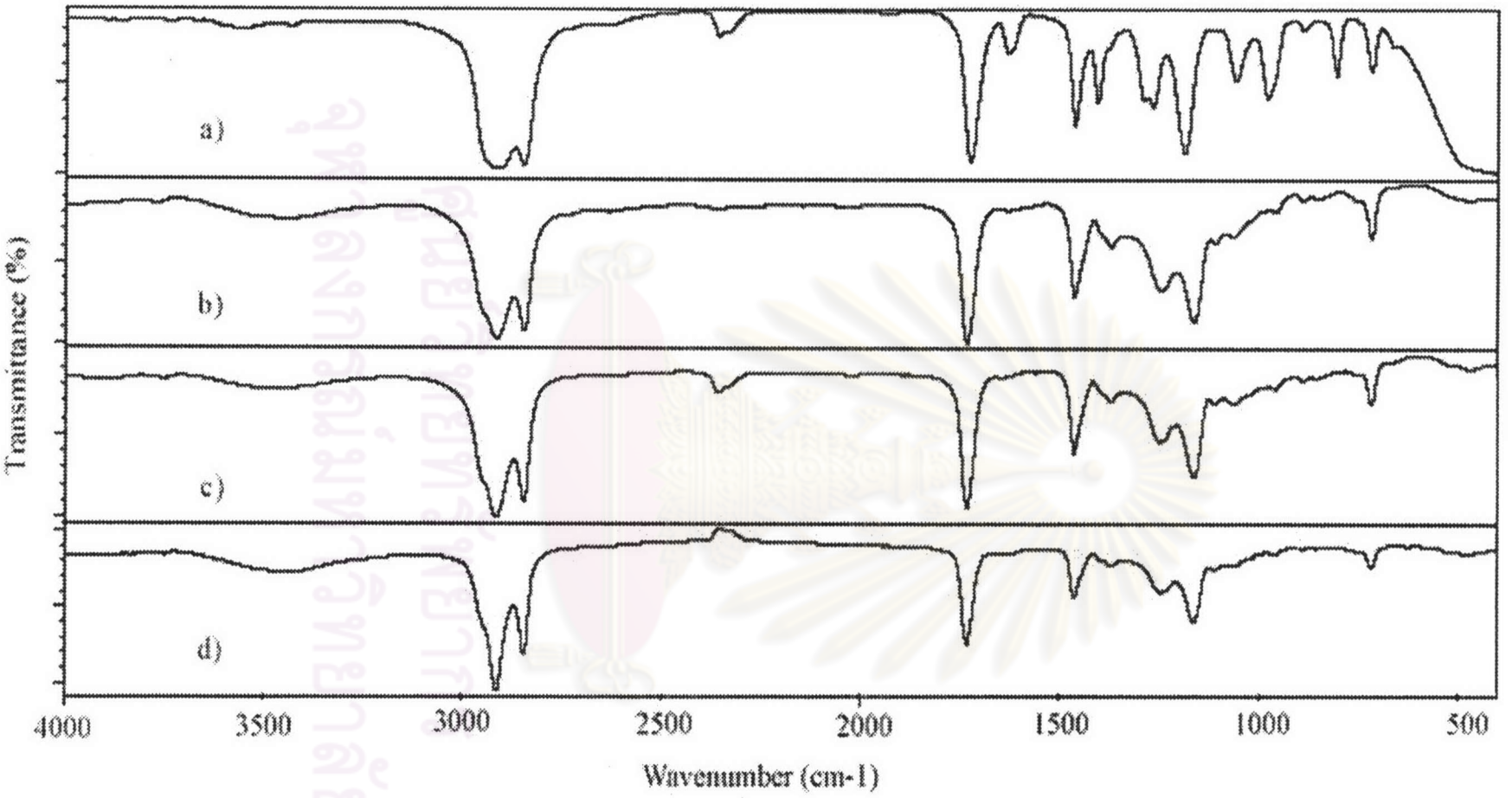

Figure 4.65 FTIR spectra of poly[(stearyl acrylate)-co-divinylbenzene] beads prepared by suspension copolymerization at various crosslinking agent concentrations: a) stearyl methacrylate monomer, b) 0.5% c) 1.0%, and d) 1.5% crosslinking agent concentration based on the monomer phase.

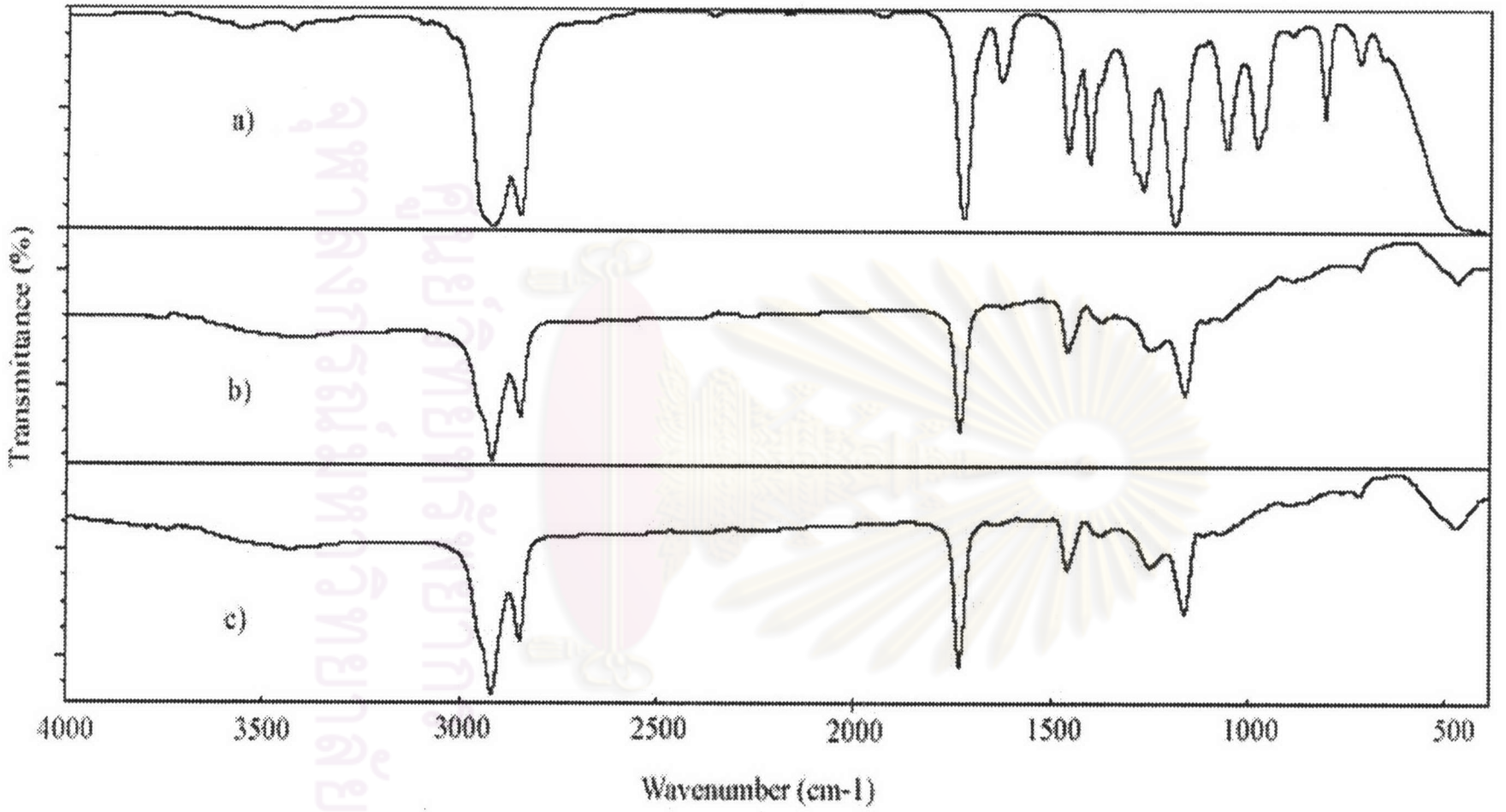

Figure 4.66 FTIR spectra of poly[(dodecyl acrylate)-co-divinylbenzene] beads prepared by suspension copolymerization at various crosslinking agent concentrations: a) dodecyl acrylate monomer, b) 1.0%, and c) 1.5% crossliking agent concentration based on the monomer phase.

The characterization of alkyl (meth)acrylate-divinylbenzene copolymer beads was performed with FTIR transmission spectroscopy. The peak interpretations are the same as in the previous section. The peak at 1630 cm^{-1} in Figure 4.64, 4.65, and 4.66 disappeared because the conversion of monomer to polymer (a double bond to a single bond) which is a proof of the polymerization.

Table 4.17 Effect of the crosslinking agent concentration on bead properties

Run	LMA00	LMA01	LMA03	LMA05	LMA10	LMA15
DVB concentration, wt %	0	0.1	0.3	0.5	1.0	1.5
% Yield	-	81	88	92	96	99
Average bead size, mm.	fused	fused	fused	0.56	0.57	0.54
Swelling ratio in toluene (by weight)	No bead formation	No bead formation	No bead formation	No bead formation	6.5	3.8

Table 4.18 Effect of the crosslinking agent concentration on bead properties

Run	DA05	DA10	DA15	DA20
DVB concentration, wt %	0.5	1.0	1.5	2.0
% Yield	-	94	89	90
Average bead size, mm.	No bead formation	No bead formation	1.02	0.07

Table 4.19 Effect of the crosslinking agent concentration on bead properties

Run	SA00	SA05	SA10	SA15	SA20
DVB concentration, wt %	0	0.5	1.0	1.5	2.0
% Yield	-	-	97	96	95
Average bead size, mm.	No bead formation	No bead formation	No bead formation	No bead formation	No bead formation

We cannot synthesize the lauryl methacrylate-divinylbenzene, stearyl acrylate-divinylbenzene, and dodecyl acrylate-divinylbenzene copolymers beads at the same

condition with methyl methacrylate-divinylbenzene and butyl methacrylate-divinylbenzene copolymer beads due to too little crosslinking agent concentration in the system to maintain the bead formation. The nature of lauryl methacrylate, stearyl acrylate, and dodecyl acrylate are highly sticky, i.e., it is not good for use as a porous bead by itself.

4.4 Effect of the third alkyl (meth)acrylate comonomer on absorption properties of methyl-methacrylate divinylbenzene copolymer beads

The effect of the third comonomer on the conversion, average particle size, particle size distribution and swelling properties were investigated. The alkyl(meth)acrylate comonomers were butyl methacrylate, lauryl methacrylate, stearyl acrylate, and dodecyl acrylate, while other parameters were kept constant as follows:

Monomer phase (0.14)	
- Alkyl (meth)acrylate-Divinylbenzene ratio (94:6)	95 wt %
- Initiator concentration	0.5 wt %
- Third comonomer	20 wt %
- Crosslinking agent concentration	0.375 wt %
Aqueous phase (0.86)	
- Suspending agent concentration	0.2 wt %
- Reaction temperature	70 °C
- Reaction time	20 hours
- Agitation rate	140 rpm
- Toluene: Heptane (100:0)	100 wt %

(The unit of any chemical is % weight based on the monomer phase.)

The resultant products of methyl methacrylate-lauryl methacrylate-divinylbenzene, methyl methacrylate-stearyl acrylate-divinylbenzene, and methyl methacrylate-dodecyl acrylate-divinylbenzene terpolymer beads were confirmed by IR spectrum as shown in Figure 4.67. The characterization of methyl methyacrylate-alkyl (meth)acrylate- divinylbenzene terpolymer beads was performed with FTIR transmission spectroscopy. The peak interpretations are the same as in the previous section. The peak at 1630 cm^{-1} in Figure 4.67 disappeared because the conversion of monomer to polymer (a double bond to a single bond), is a proof of the

polymerization. Figure 4.68 shows the increasing average particle size with increasing the hydrophobicity of the material, but the average particle size of MMA-SA copolymer was smaller than that of the MMA-DA copolymer because the MMA-DA copolymer has the highest sticky behavior. The stickiness of MMA-DA was higher than those MMA-LMA, MMA-SA, and MMA-BMA copolymer, respectively. The average particle size depends on the hydrophobicity and stickiness properties.

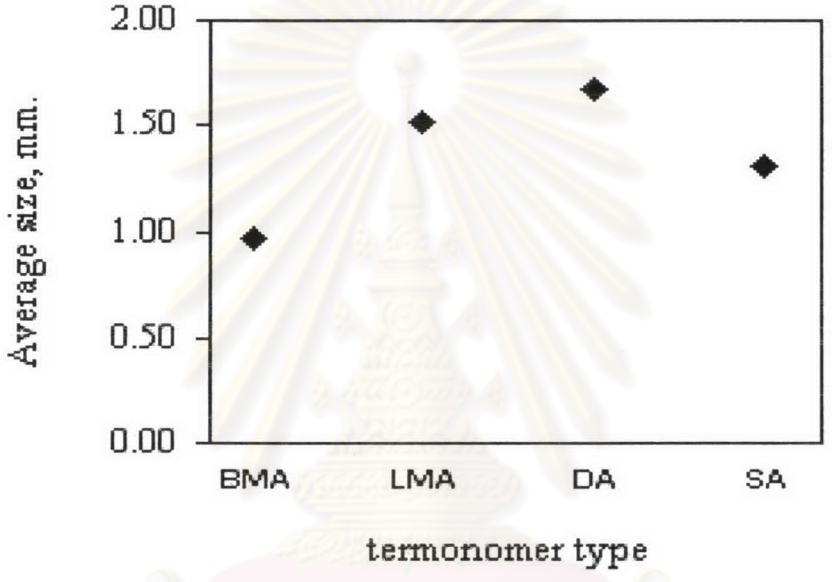

Figure 4.67 The average particle size in relation to the third comonomer type.

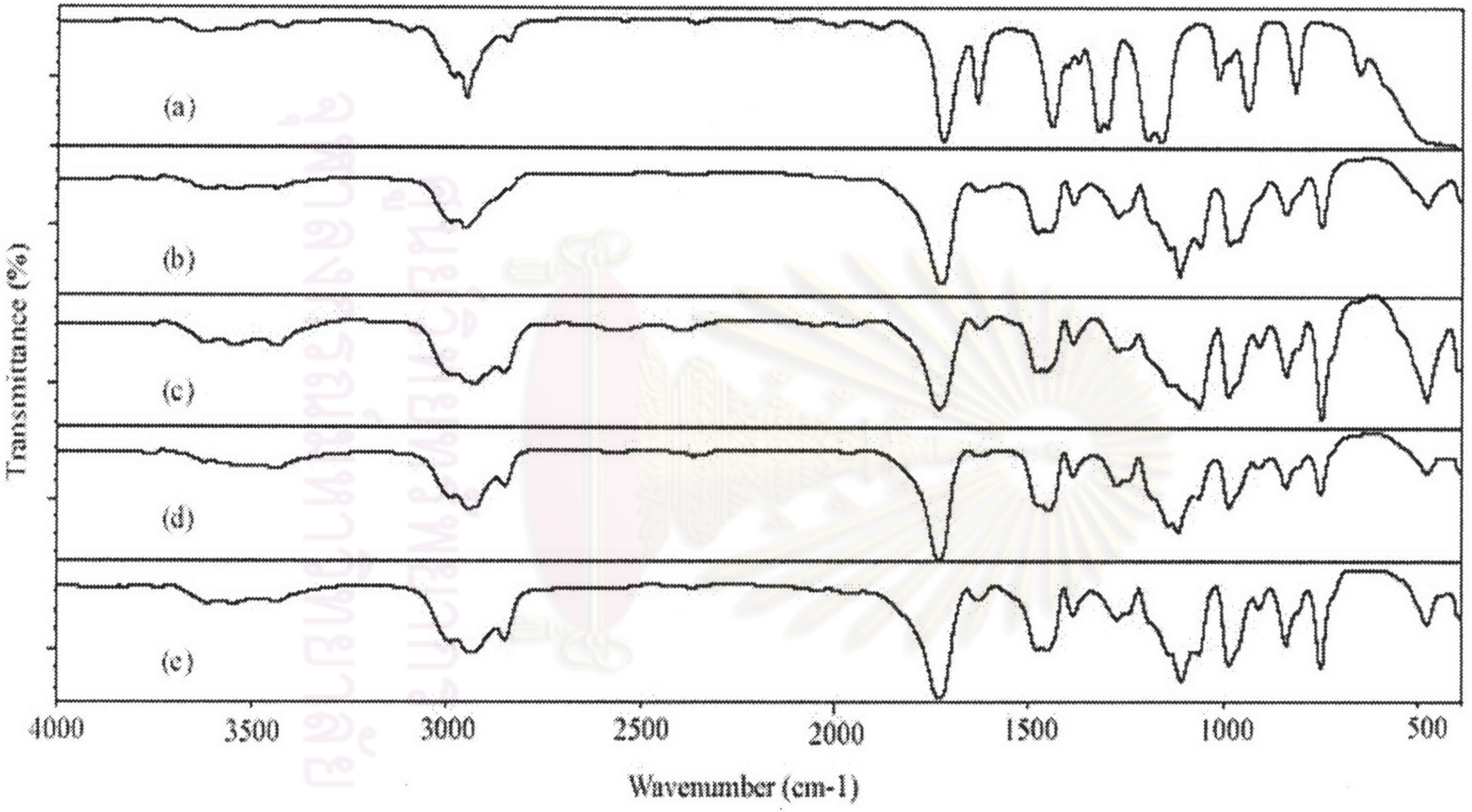

Figure 4.68 FTIR spectra of the terpolymer beads prepared by suspension copolymerization at various third copolymers: a) methyl methacrylate monomer, b) poly(MMA-BMA), c) poly(MMA-LMA), d) poly(MMA-DA), and e) poly(MMA-SA).

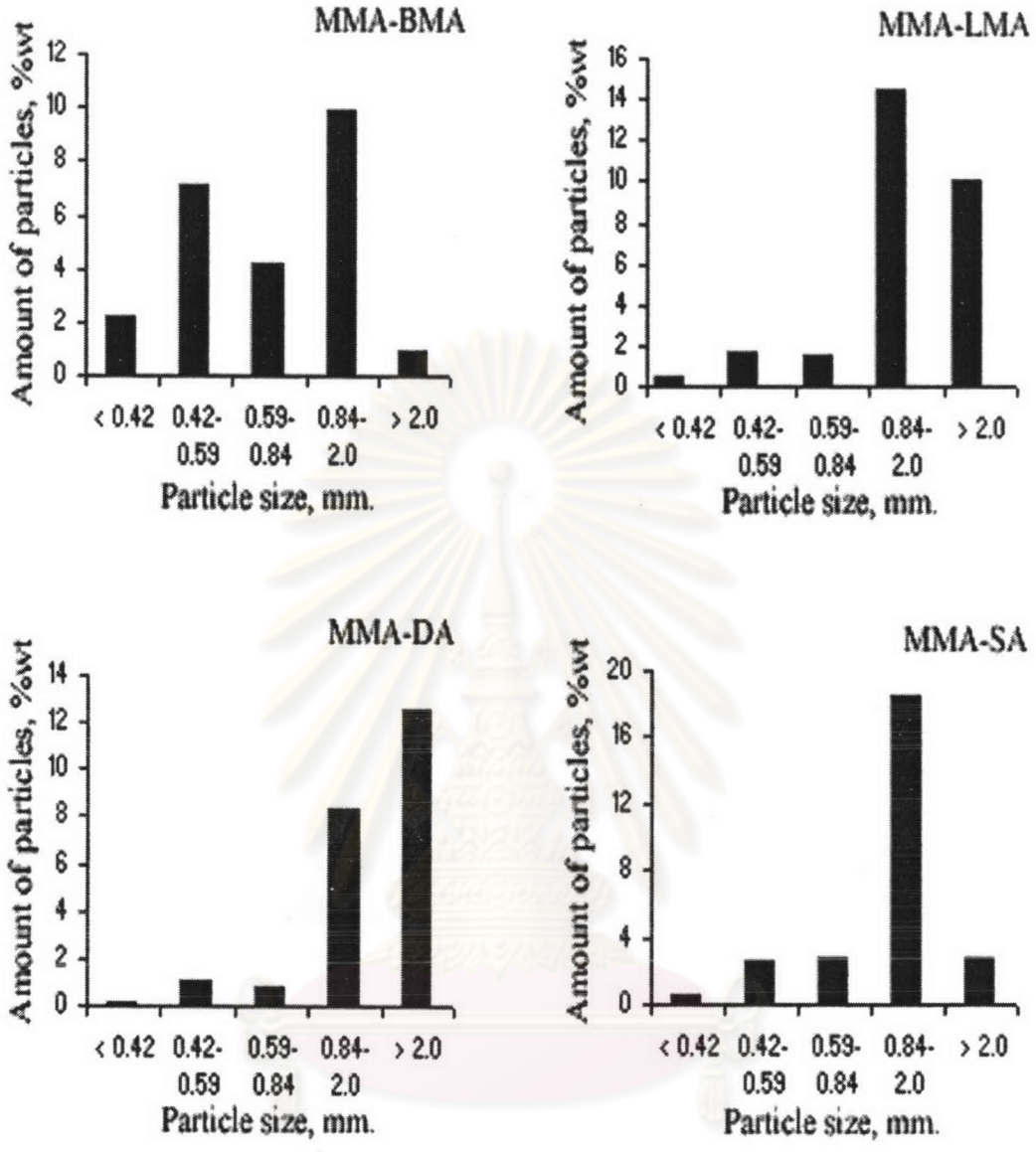

Figure 4.69 Effect of the third comonomer on particle size and particle size distribution: (a) MMA-BMA, (b) MMA-LMA, (c) MMA-DA, and (d) MMA-SA.

Table 4.20 Effect of the third comonomer type on bead properties

Parameter	Run			
	MMA-BMA	MMA-LMA	MMA-DA	MMA-SA
Third comonomer type	BMA	LMA	DA	SA
% Yield	83	94	87	90
Bead size distribution, %wt				
<0.42 mm	2.24	0.45	0.15	0.50
0.42-0.59 mm	7.15	1.61	1.03	2.55
0.59-0.84 mm	4.16	1.53	0.73	2.82
0.84-2.0 mm	9.93	14.45	8.31	18.51
>2.0 mm	0.91	10.13	12.51	2.73
Average bead size, mm	0.96	1.52	1.67	1.30
Swelling ratio in toluene				
(by volume)	25.3	19.3	22.1	19.9
(by weight)	19.2	15.4	18.0	16.2
Bead density, kg m^{-3}	1097	1020	1030	1014

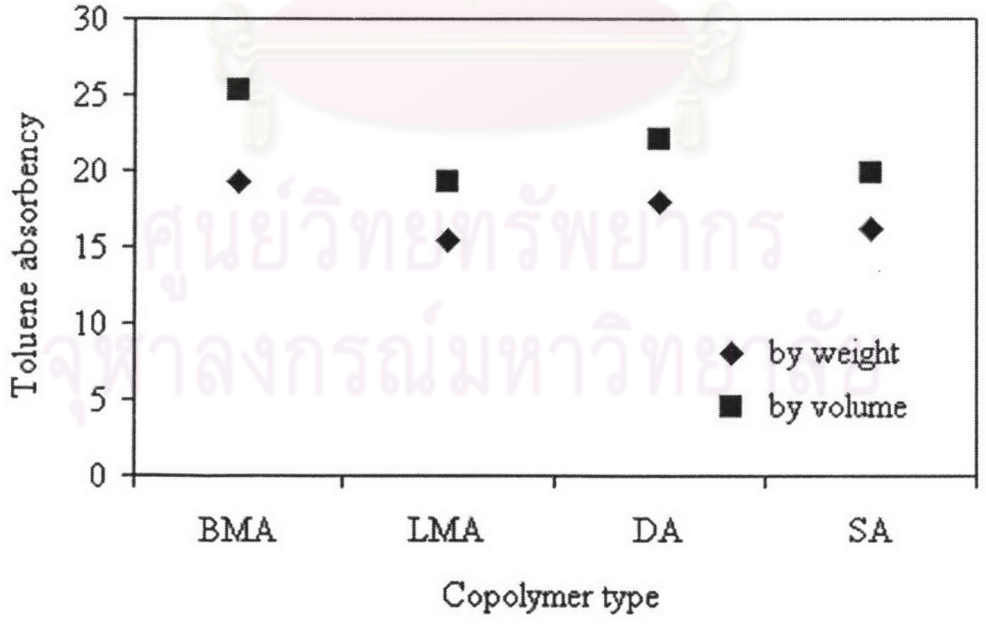

Figure 4.70 Effect of the third alkyl (meth)acrylate comonomer on toluene absorbency.

The particle size polydispersity shown in Figure 4.69 decreased with increasing the hydrophobic properties. We can specifically mention about the particle formation because it depended on the coalescence and breakage rate in the second stage of suspension polymerization kinetics and gel effect at high conversion. Table 4.19 shows the overall conversion, the average particle size, particle size distribution, swelling ratio and density in relation to alkyl(math)acrylate as a third comonomer type. Figure 4.64 shows the effect of the third alkyl(meth)acrylate comonomer on the toluene absorbency. From Table 4.19 and Figure 4.70, the toluene absorbency decreased when decreasing the polarity of copolymer. The toluene absorbency in a sequential order is as follows: MMA-BMA, MMA-DA, MMA-LMA, and MMA-SA.

4.5 Effect of the third alkyl (meth)Acrylate comonomer on oil adsorption properties of methyl-methacrylate divinylbenzene copolymer beads

The oil absorbency has been widely used to absorb oil-like solvent. In this study we propose various acrylates functionalities to help methyl methacrylate-divinylbenzene copolymer improve its lube oil swelling property characteristic. The capacity of oil absorbent of methyl methacrylate-divinylbenzene copolymer was affected by the reaction condition as shown in Figure 4.71 to 4.78.

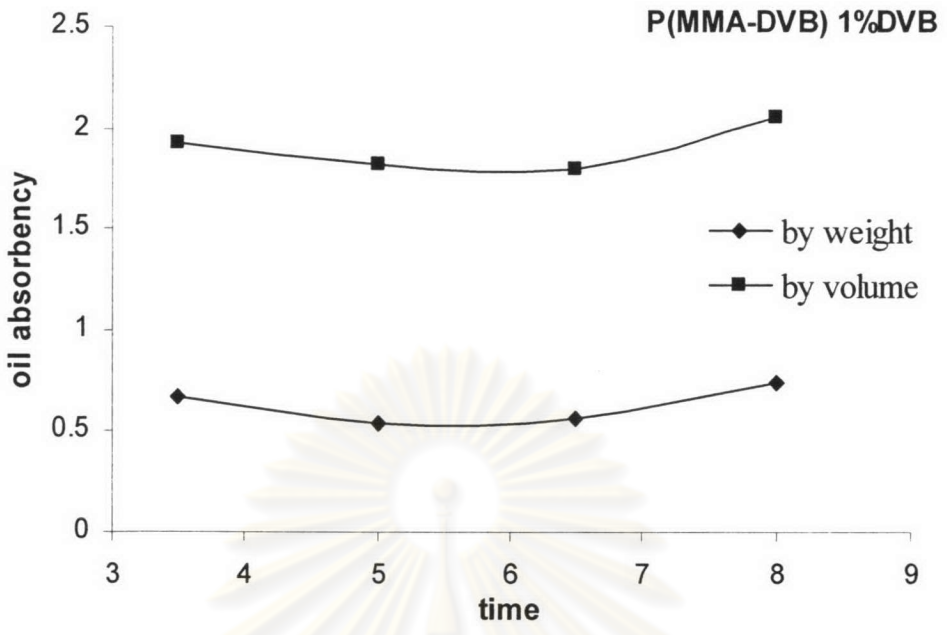

Figure 4.71 The oil absorbency versus reaction time of methyl methacrylate-divinylbenzene copolymer: ■ by volume and ♦ by weight.

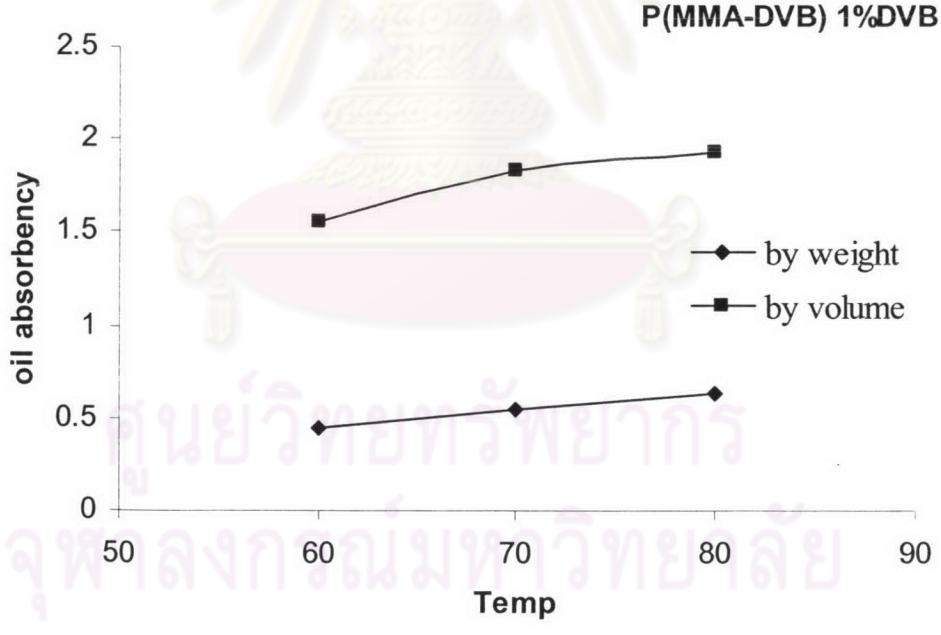

Figure 4.72 The oil absorbency versus reaction temperature of methyl methacrylate-divinylbenzene copolymer; ■ by volume and ♦ by weight.

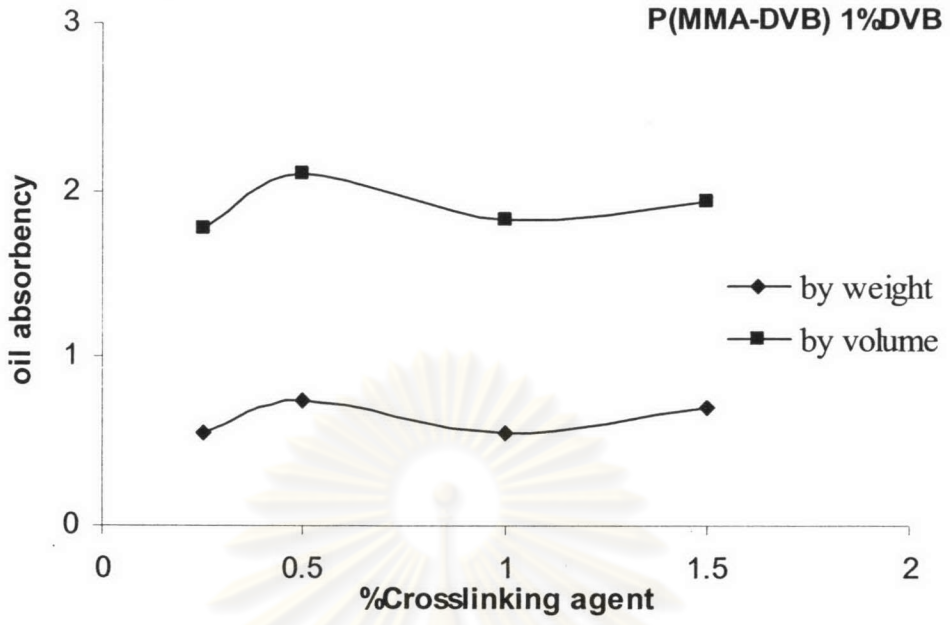

Figure 4.73 The oil absorbency versus crosslinking agent concentration of methyl methacrylate-divinylbenzene copolymer: ■ by volume and ♦ by weight.

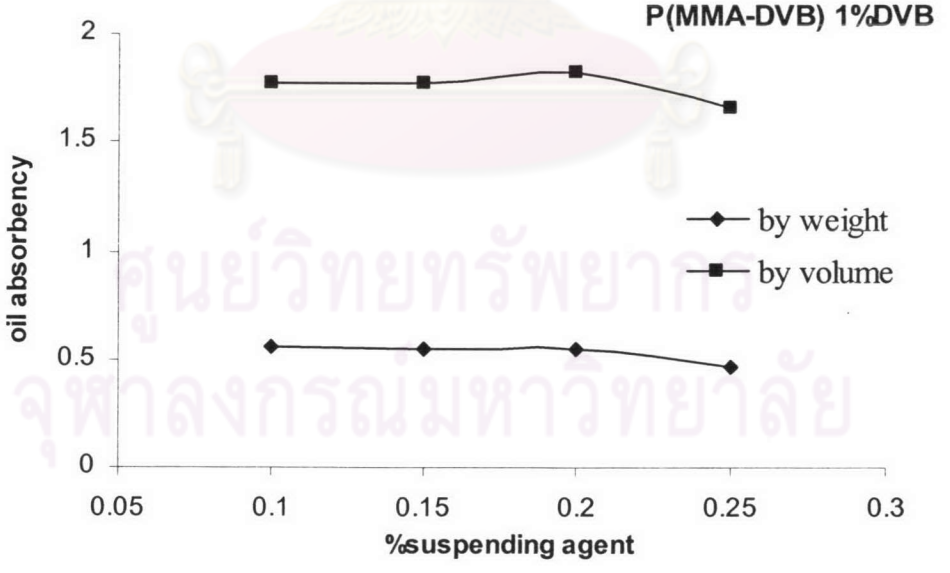

Figure 4.74 The oil absorbency versus suspending agent concentration of methyl methacrylate-divinylbenzene copolymer: ■ by volume and ♦ by weight.

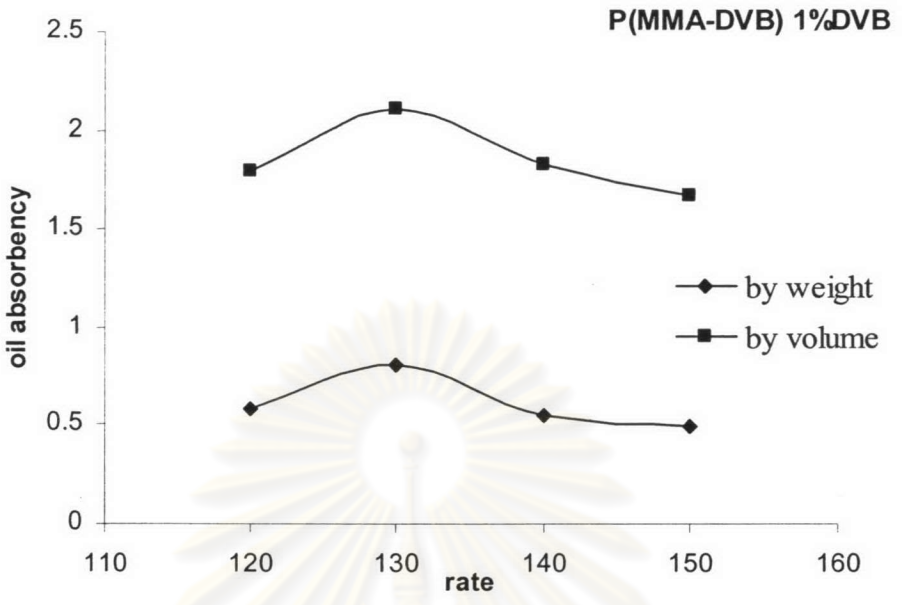

Figure 4.75 The oil absorbency versus agitation rate of methyl methacrylate-divinylbenzene copolymer: ■ by volume and ♦ by weight.

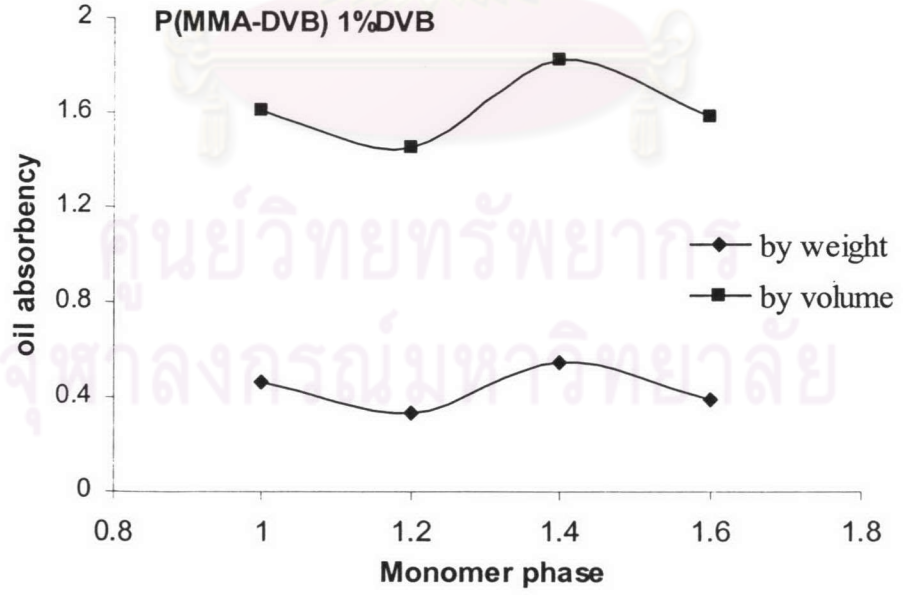

Figure 4.76 The oil absorbency versus monomer phase ratio of methyl methacrylate-divinylbenzene copolymer: ■ by volume and ♦ by weight.

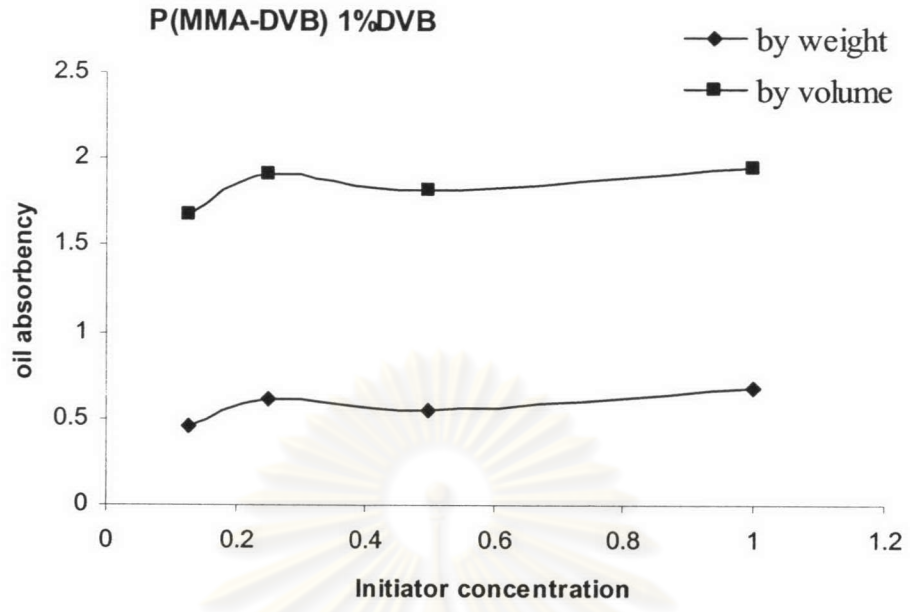

Figure 4.77 The oil absorbency versus initiator concentration of methyl methacrylate-divinylbenzene copolymer: ■ by volume and ♦ by weight.

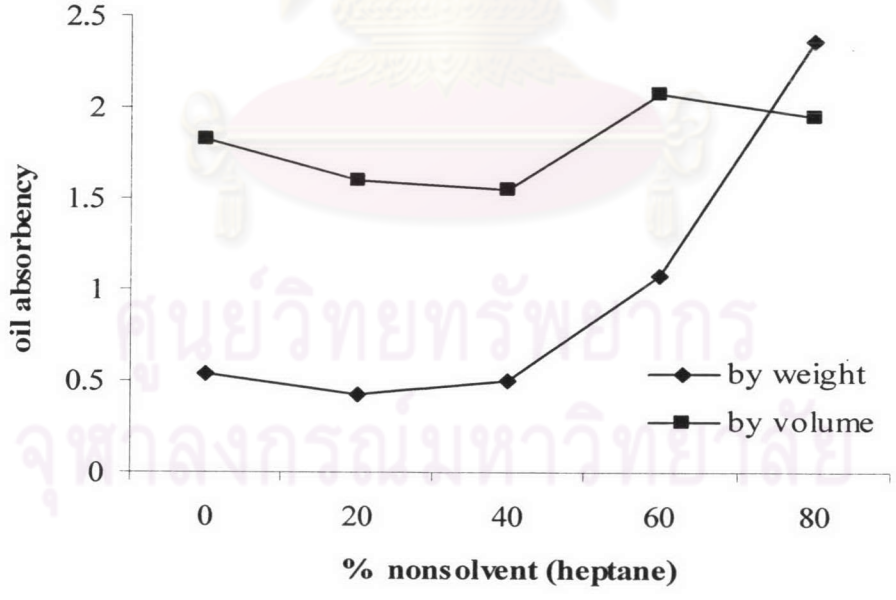

Figure 4.78 The oil absorbency versus nonsolvent (heptane) ratio of methyl methacrylate-divinylbenzene copolymer: ■ by volume and ♦ by weight.

Figure 4.71 to Figure 4.78 show that the oil absorbency was affected by the reaction conditions such as reaction time, reaction temperature, crosslinking agent concentration, suspending agent concentration, agitation rate, monomer to aqueous phase, initiator concentration, and nonsolvent ratio on methyl methacrylate-divinylbenzene copolymer. All of the results did not show any specific but most of them gave some degree of steady trend. However, the oil absorbency tends to increase with increasing the nonsolvent ratio. The increasing oil absorbency was influenced by the amount of pores in beads as shown in the previous part. The amount of pores increased when the nonsolvent ratio increased. The capacity of oil absorbent thus increased when the increasing amount of pores in the beads. The effect of nonsolvent ratio is not so important on the capacity of oil absorption on butyl methacrylate-divinylbenzene copolymer as well. Figure 4.79 show the oil absorbency of butyl methacrylate-divinylbenzene copolymer in amyl alcohol nonsolvent during copolymerization.

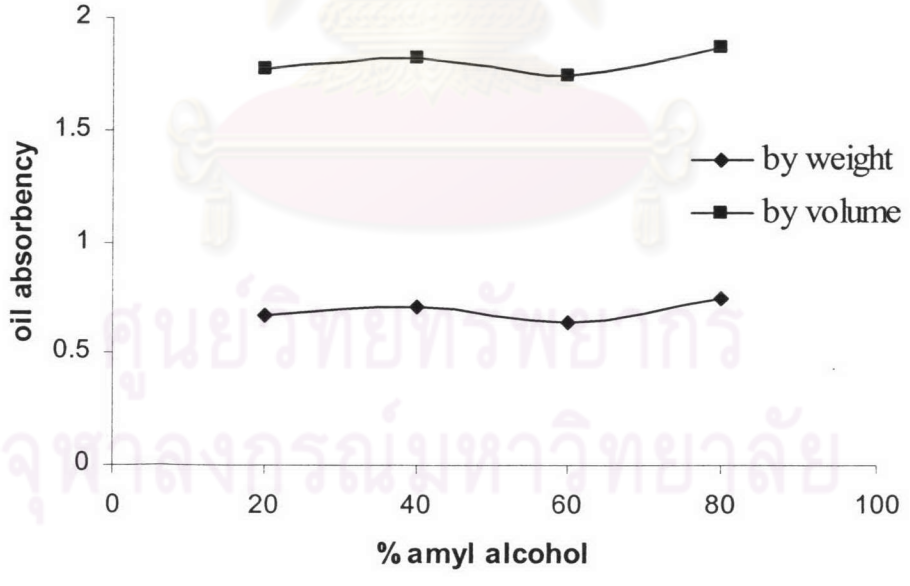

Figure 4.79 The oil absorbency versus nonsolvent (amyl alcohol) ratio of butyl methacrylate-divinylbenzene copolymer: ■ by volume and ♦ by weight.

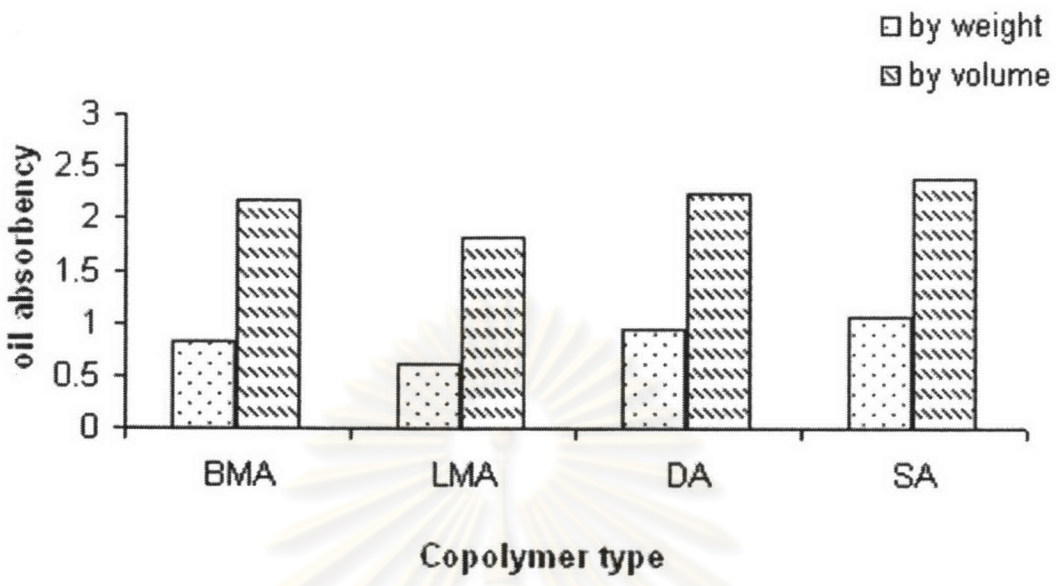

Figure 4.80 The oil absorbency versus the type of third-monomer on methyl methacrylate-divinylbenzene copolymer: ■ by volume and ♦ by weight.

The effect of the third-copolymer on oil absorbency of methyl methacrylate-divinylbenzene copolymer (terpolymer) was shown in Figure 4.80. The oil absorption capacity increases when increasing the hydrophobic type of the third monomer. All of them could not be used as good oil absorbent because the highest oil absorption capacity is about 2 times their original amount, which is not significant.

4.6 Determination of solubility parameter of MMA-DVB, BMA-DVB, methyl methacrylate-divinylbenzene-alkyl (meth)acrylate terpolymers.

There are many techniques to determine solubility parameter of a new polymer. In case of a crosslinked polymer, the solubility parameter can be determined by swelling experiments. The solubility parameter describes the enthalpy change on mixing of nonpolar solvents well but it does not give uniform results when extended to polar system. Complete miscibility is expected to occur if the solubility parameters are similar and the degree of hydrogen bonding is similar between the components.

In this experiment several solvents with known solubility parameter are selected, and the crosslinked polymer is swollen to equilibrium in each solvent. After that the swelling ratio was plotted against the solvent solubility parameter. The solvent that gives the maximum swelling ratio is defined as the solubility parameter of the polymer.

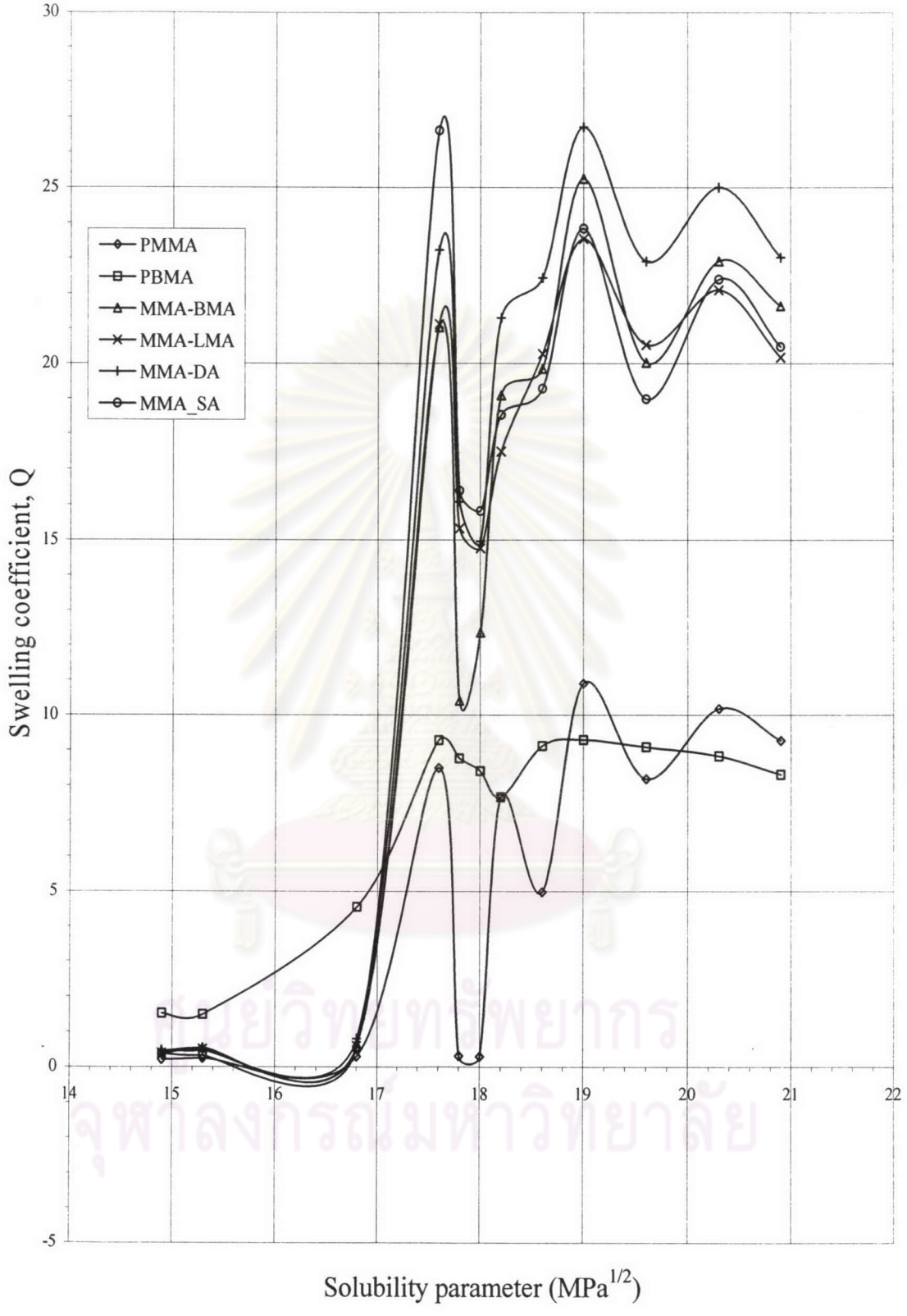

Figure 4.81 Comparison of solubility parameters of synthetic copolymer beads by swelling experiments.

Table 4.21 Swelling ratio of the synthetic copolymer beads in various solvents.

Solvent	Solubility parameter $(MPa)^{1/2}$				Swelling ratio of the copolymer					
	δ_D	δ_P	δ_H	δ_T	MMA10	BMA10	MMA-BMA10	MMA-LMA10	MMA-DA10	MMA-SA10
Hexane	14.9	0	0	14.9	0.1	1.0	0.3	0.3	0.3	0.3
Heptane	15.3	0	0	15.3	0.2	1.0	0.4	0.3	0.3	0.2
Cyclohexane	16.8	0	0.2	16.8	0.2	3.5	0.4	0.5	0.6	0.4
Trichloroethane	17.0	4.3	2.0	17.6	12.4	13.4	30.8	30.9	34.0	38.9
Carbon tetrachloride	17.8	0	0.6	17.8	0.5	14.0	16.6	24.4	25.6	26.1
Xylene	17.8	1.0	3.1	18.0	0.3	7.3	10.7	12.8	12.9	13.7
Toluene	18.0	1.4	2.0	18.2	6.6	6.6	16.6	15.2	18.5	16.1
Benzene	18.4	0	2.0	18.6	4.4	8.0	17.4	17.8	19.7	17.0
Chlorofrom	17.8	3.1	5.7	19.0	16.1	13.8	37.4	34.9	39.6	35.3
Chlorobenzene	19.0	4.3	2.0	19.6	9.1	10.1	22.2	22.7	25.3	21.0
Methyllene chloride	18.2	6.3	6.1	20.3	13.5	11.7	30.4	29.3	33.1	29.7
Ethylene chloride	19.0	7.4	4.1	20.9	11.6	10.4	27.1	25.3	28.8	25.7

Figure 4.71 and Table 4.20 indicate that the solubility parameters of the synthetic copolymers for MMA10, BMA10, MMA-BMA10, MMA-LMA10, MMA-DA10 and MMA-SA10 are about 19.0, 17.8, 19.0, 19.0, 19.0, and 17.6 $(MPa)^{1/2}$, respectively. Three kinds of solvent were used in this study. The first kind is aliphatic hydrocarbons, namely hexane, heptane and cyclohexane; the second is aromatic hydrocarbons, namely xylene, toluene and benzene; the third is halogenated

hydrocarbons, namely trichloroethane, carbon tetrachloride, chloroform, chlorobenzene, methylene chloride, and ethylene chloride. Hydrocarbons and chlorinated hydrocarbons are considered to be poor hydrogen-bonding solvents. Hansen and coworker [27] assumed that the cohesive energy arosen from dispersive, permanent dipole-dipole interactions and hydrogen bonding forces.

$$\delta^2 = \delta_d^2 + \delta_p^2 + \delta_h^2 \qquad (4.8)$$

where δ_d = dispersive term, δ_p = polar term, and δ_h = hydrogen bonding term. δ_h probably accounts for a variety of association bonds, including permanent dipole-induced dipole. The acrylate group is somewhat polarity even if it represents the nonpolar characteristic as we can observe from this experiment that it shows two high peaks from the solubility parameter curve (Figure 4.65). All of acrylate polymers in this study show the high peaks for chloroform and trichloroethane solvents, as they are the chlorinated hydrocarbon. Furthermore, the copolymer structure should be considered as well. The difference between poly[(methyl methcrylate)-co-divinylbenzene] and poly[(butyl methcrylate)-co-divinylbenzene] is that the polarity and the molar volume as methyl methacrylate are more polar than butyl methacrylate because the latter have higher the number of carbon atoms in the side chain and the former has a lower molar volume than butyl methycrylate. That is why methyl methacrylate prefers to swell in the chloroform solvent as it has a smaller molecule than trichloroethane. In case of the terpolymer when we added another acrylate molecule for the addition number of carbon atoms in the side chain while the ratio between methyl methacrylate and other acrylate is similar. We can observe from this experiment that the solubility parameters of MMA-BMA, MMA-LMA, and MMA-DA terpolymer are similar with MMA-DVB copolymer and the solubility parameter of MMA-SA copolymer is similar with BMA-DVB copolymer.